

Purdue University

TPF-5(238) Design and Fabrication Standards to Eliminate Fracture Critical
Concerns in Two Girder Bridge Systems

2015

Fracture Characterization of High Performance Steel

William N. Collins,
University of Kansas, william.collins@ku.edu

Ryan J. Sherman
Purdue University, rjsherma@purdue.edu

Robert J. Connor,
Purdue University, rconnor@purdue.edu

RECOMMENDED CITATION

Collins, W. N., Sherman, and R. J. Connor: *Fracture Characterization of High Performance Steel*. Purdue University, West Lafayette, Indiana, 2015.

AUTHORS

William N. Collins, Ph.D

Assistant Professor
University of Kansas
(785) 864-0672
william.collins@ku.edu
Corresponding Author

Ryan J. Sherman

Ph.D. Candidate
Purdue University

Robert J. Connor, Ph.D.

Associate Professor of Civil Engineering
Director of S-BRITE Center
Purdue University

ACKNOWLEDGEMENTS

This project was funded through Transportation Pooled Fund 5(238). Special thanks are extended to Dr. Rick Link and Dr. Jim Joyce of the Naval Academy for their advice and expertise concerning fracture toughness testing and analysis. Additionally, we offer a thank you to Dr. Bill Wright for his involvement with this project. And finally, we acknowledge the essential contributions from staff professionals and graduate students at Virginia Tech and Purdue University throughout this research.

EXECUTIVE SUMMARY

Fracture Characterization of High Performance Steel

Introduction

FHWA Transportation Pooled Fund (TPF) Project 5-238, Design and Fabrication Standards to Eliminate Fracture Critical Concerns in Steel Members Traditionally Classified as Fracture Critical, was initiated with the objective of taking advantage of the inherent fracture performance benefits of High Performance Steel (HPS). The project includes the examination of material characteristics, fatigue, fracture design and detailing specifications, fabrication methodology, and shop and field inspections to be used for bridges designed and built with HPS.

The experimental program of this TPF includes the behavior characterization of multiple grades of HPS, as well as fracture testing of full scale girders. Researchers at Purdue University and Virginia Tech are collaborating in these efforts. The end goal of this research is to create specifications for a new class of bridges which will take advantage of the improved performance of HPS. This will eliminate or greatly reduce the extensive inspection requirements of bridges currently classified as fracture critical, thus making two and three girder steel bridge systems more competitive in the marketplace.

Summary of Findings

The main conclusions from this portion of TPF-5(238) study can be summarized as follows.

- The HPS 690W (100W) and 485W (70W) tested displayed CVN impact energies significantly higher than that required in ASTM A709-13 for fracture critical components.
- Although this is a small sample size, it is apparent that HPS is being produced that readily and substantially surpasses current impact energy requirements.
- Static reference temperatures for HPS are extremely low, significantly below bridge service temperatures.
- Dynamic reference temperatures for HPS are more difficult to obtain due to loss of specimen constraint at high test rates. However, data indicates that dynamic reference temperature values are still consistently at or below service temperatures for all grades examined.

- The effect of loading rate is clearly evident when examining the results of static and dynamic fracture initiation testing. As seen in the difference in reference temperature values, this effect can be represented by a temperature shift.
- Crack arrest toughness testing proved to be extremely difficult, resulting in very little usable data. The state of testing standards and low validity success rate makes more arrest testing unfeasible at this point in time.

Contents

Executive Summary	i
1. Introduction	1
1.1 Scope and Objectives of This Study	1
2. Experimental Procedure	2
2.1 Plate Designations and Sampling Procedure	2
2.2 Test Specimen Geometry	3
2.2.1 Tension Test Specimens	4
2.2.2 Charpy V-Notch Specimens	4
2.2.3 Single Edge Bend Specimens	4
2.2.4 Crack Arrest Specimens	6
2.3 Material Characterization Testing Procedures	7
2.3.1 Tensile Testing	7
2.3.2 Charpy V-Notch Impact Testing	8
2.3.3 Fracture Toughness Testing	11
2.3.4 Crack Arrest Toughness Testing	17
2.3.5 Specimen Cooling Chamber	21
2.4 Data Analysis	23
2.4.1 Charpy V-Notch Temperature Transition Characterization	23
2.4.2 Fracture Toughness Master Curve Characterization	24
3. Experimental Test Results	28
3.1 Tensile Test Results	28
3.2 Charpy V-Notch Impact Test Results	28
3.2.1 Charpy V-Notch Impact Toughness of HPS 690W (100W)	29
3.2.2 Charpy V-Notch Impact Toughness of HPS 485W (70W)	31
3.3 Static Fracture Toughness Test Results	35

3.3.1 Static Fracture Toughness of HPS 690W (100W)	35
3.3.2 Static Fracture Toughness of HPS 485W (70W)	37
3.4 Dynamic Fracture Toughness Test Results	41
3.4.1 Dynamic Fracture Toughness of HPS 690W (100W)	41
3.4.2 Dynamic Fracture Toughness of HPS 485W (70W)	43
3.5 Crack Arrest Toughness Test Results	50
3.5.1 Crack Arrest Toughness of HPS 690W (100W)	51
3.5.2 Crack Arrest Toughness of HPS 485W (70W)	52
4. Summary and Conclusions	54
4.1 Summary	54
4.2 Conclusions	56
References	58
Appendix A: Tabulated CVN Data	59
Appendix B: Tabulated Static Fracture Toughness	64
Appendix C: Tabulated Dynamic Fracture Toughness	72
Appendix D: Tabulated Crack Arrest Toughness	82

List of Figures

Figure 2-1. Specimen Orientation Designations-----	3
Figure 2-2. Tension Specimen Geometry -----	4
Figure 2-3. CVN Specimen Geometry -----	4
Figure 2-4. SE(B) Specimen Notch Details -----	5
Figure 2-5. SE(B) Specimen Dimensions-----	5
Figure 2-6. SE(B) Side Groove Location and Dimensions-----	6
Figure 2-7. Crack Arrest Specimen Geometry -----	7
Figure 2-8. Tensile Test Specimen with Extensometer -----	8
Figure 2-9. Impact Test Machine-----	9
Figure 2-10. CVN Specimen Reaching Desired Test Temperature -----	10
Figure 2-11. SE(B) Cracking and Testing Apparatus -----	11
Figure 2-12. Typical Load-CMOD Plot with Elastic Compliance Unloadings -----	13
Figure 2-13. Typical Load-CMOD Plot without Elastic Compliance Unloadings -----	14
Figure 2-14. Measured Fracture Surface of Typical SE(B) Specimen -----	15
Figure 2-15. Plastic and Elastic Portions of Test Record-----	17
Figure 2-16. Crack Arrest Specimen Prior to Testing-----	18
Figure 2-17. Measured Fracture Surface of Typical Crack Arrest Specimen-----	20
Figure 2-18. Typical Crack Arrest Test Record -----	21
Figure 2-19. Environmental Chamber on Crack Arrest Apparatus-----	22
Figure 2-20. Typical CVN Behavior for HPS Steel-----	23
Figure 2-21. Typical Master Curve with Tolerance Bounds-----	26
Figure 3-1. CVN Data for Plate C, HPS 690W, 19 mm -----	29
Figure 3-2. CVN Data for Plate E, HPS 690W, 38.1 mm-----	30
Figure 3-3. CVN Data for Plate F, HPS 690W, 50.8 mm-----	30
Figure 3-4. CVN Data for Plate A, HPS 485W, 25.4 mm -----	32
Figure 3-5. CVN Data for Plate D, HPS 485W, 63.5 mm -----	32
Figure 3-6. CVN Data for Plate H, HPS 485W, 31.8 mm -----	33
Figure 3-7. CVN Data for Plate I, HPS 485W, 31.8 mm -----	34
Figure 3-8. CVN Data for Plate J, HPS 485W, 38.1 mm -----	34
Figure 3-9. Fracture Toughness Data and Master Curve for Plate C, HPS 690W, 19 mm -----	36
Figure 3-10. Fracture Toughness Data and Master Curve for Plate E, HPS 690W, 38.1 mm -----	36

Figure 3-11. Fracture Toughness Data and Master Curve for Plate F, HPS 690W, 50.8 mm -----37

Figure 3-12. Fracture Toughness Data and Master Curve for Plate A, HPS 485W, 25.4 mm -----38

Figure 3-13. Fracture Toughness Data and Master Curve for Plate D, HPS 485W, 63.5 mm-----39

Figure 3-14. Fracture Toughness Data and Master Curve for Plate H, HPS 485W, 31.8 mm-----39

Figure 3-15. Fracture Toughness Data and Master Curve for Plate I, HPS 485W, 31.8 mm-----40

Figure 3-16. Fracture Toughness Data and Master Curve for Plate J, HPS 485W, 38.1 mm-----40

Figure 3-17. Dynamic Fracture Toughness Data and Master Curve for Plate C -----42

Figure 3-18. Dynamic Fracture Toughness Data and Master Curve for Plate E-----42

Figure 3-19. Dynamic Fracture Toughness Data and Master Curve for Plate F-----43

Figure 3-20. Dynamic Fracture Toughness Data and Master Curve for Plate A -----44

Figure 3-21. Dynamic Fracture Toughness Data and Master Curve for Plate D -----45

Figure 3-22. Dynamic Fracture Toughness Data and Alternate Master Curve for Plate D-----46

Figure 3-23. Dynamic Fracture Toughness Data and Master Curve for Plate H -----47

Figure 3-24. Dynamic Fracture Toughness Data and Alternate Master Curve for Plate H-----47

Figure 3-25. Dynamic Fracture Toughness Data and Master Curve for Plate I -----48

Figure 3-26. Dynamic Fracture Toughness Data and Alternate Master Curve for Plate I -----49

Figure 3-27. Dynamic Fracture Toughness Data and Master Curve for Plate J -----50

Figure 3-28. Crack Arrest Toughness Data and Master Curve for Plate E-----51

Figure 3-29. Crack Arrest Toughness Data and Master Curve for Plate F-----52

Figure 3-30. Crack Arrest Toughness Data and Master Curve for Plate D -----53

List of Tables

Table 2-1. Designations and Details of HPS Plates.....	2
Table 2-2. ASTM E1921 Weighting Factors for Multi-Temperature Analysis	27
Table 3-1. Tensile Test Results, Room Temperature, Quasi-Static Load Rate	28
Table 4-1. Summary of Static, Dynamic, and Arrest Reference Temperatures	56
Table A-0-1. CVN Data for Plate A, HPS 485W, 25.4 mm	59
Table A-0-2. CVN Data for Plate C, HPS 690W, 19 mm.....	60
Table A-0-3. CVN Data for Plate D, HPS 485W, 63.5 mm	61
Table A-0-4. CVN Data for Plate E, HPS 690W, 38.1 mm.....	62
Table A-0-5. CVN Data for Plate F, HPS 690W, 50.8 mm	63
Table B-0-6. Static Specimen Information for Plate A, HPS 485W, 25.4 mm	64
Table B-0-7. Static Test Information for Plate A, HPS 485W, 25.4 mm	64
Table B-0-8. Static Specimen Information for Plate C, HPS 690W, 19 mm	65
Table B-0-9. Static Test Information for Plate C, HPS 690W, 19 mm	65
Table B-0-10. Static Specimen Information for Plate D, HPS 485W, 63.5 mm	66
Table B-0-11. Static Test Information for Plate D, HPS 485W, 63.5 mm	66
Table B-0-12. Static Specimen Information for Plate E, HPS 690W, 38.1 mm.....	67
Table B-0-13. Static Test Information for Plate E, HPS 690W, 38.1 mm	67
Table B-0-14. Static Specimen Information for Plate F, HPS 690W, 50.8 mm.....	68
Table B-0-15. Static Test Information for Plate F, HPS 690W, 50.8 mm.....	68
Table B-0-16. Static Specimen Information for Plate H, HPS 485W, 31.8 mm	69
Table B-0-17. Static Test Information for Plate H, HPS 485W, 31.8 mm	69
Table B-0-18. Static Specimen Information for Plate I, HPS 485W, 31.8 mm	70
Table B-0-19. Static Test Information for Plate I, HPS 485W, 31.8 mm	70
Table B-0-20. Static Specimen Information for Plate J, HPS 485W, 38.1 mm	71
Table B-0-21. Static Test Information for Plate J, HPS 485W, 38.1 mm	71
Table C-0-22. Dynamic Specimen Information for Plate A, HPS 485W, 25.4 mm	72
Table C-0-23. Dynamic Test Information for Plate A, HPS 485W, 25.4 mm	72
Table C-0-24. Dynamic Specimen Information for Plate C, HPS 690W, 19 mm	73
Table C-0-25. Dynamic Test Information for Plate C, HPS 690W, 19 mm	73
Table C-0-26. Dynamic Specimen Information for Plate D, HPS 485W, 63.5 mm.....	74
Table C-0-27. Dynamic Test Information for Plate D, HPS 485W, 63.5 mm	75

Table C-0-28. Dynamic Specimen Information for Plate E, HPS 690W, 38.1 mm.....	76
Table C-0-29. Dynamic Test Information for Plate E, HPS 690W, 38.1 mm	77
Table C-0-30. Dynamic Specimen Information for Plate F, HPS 690W, 50.8 mm.....	78
Table C-0-31. Dynamic Test Information for Plate F, HPS 690W, 50.8 mm.....	78
Table C-0-32. Dynamic Specimen Information for Plate H, HPS 485W, 31.8 mm	79
Table C-0-33. Dynamic Test Information for Plate H, HPS 485W, 31.8 mm	79
Table C-0-34. Dynamic Specimen Information for Plate I, HPS 485W, 31.8 mm	80
Table C-0-35. Dynamic Test Information for Plate I, HPS 485W, 31.8 mm	80
Table C-0-36. Dynamic Specimen Information for Plate J, HPS 485W, 38.1 mm	81
Table C-0-37. Dynamic Test Information for Plate J, HPS 485W, 38.1 mm	81
Table D-0-1. Valid Arrest Specimen Information.....	82
Table D-0-2. Valid Arrest Test Record Information.....	83
Table D-0-3. Invalid Arrest Specimen Information	84
Table D-0-4. Invalid Arrest Test Record Information.....	84

1. INTRODUCTION

FHWA Transportation Pooled Fund (TPF) Project 5-238, Design and Fabrication Standards to Eliminate Fracture Critical Concerns in Steel Members Traditionally Classified as Fracture Critical, was initiated with the objective of taking advantage of the inherent fracture performance benefits of High Performance Steel (HPS). The project includes the examination of material characteristics, fatigue, fracture design and detailing specifications, fabrication methodology, and shop and field inspections to be used for bridges designed and built with HPS.

The experimental program of this TPF includes the behavior characterization of multiple grades of HPS, as well as fracture testing of full scale girders. Researchers at Purdue University and Virginia Tech are collaborating in these efforts. The end goal of this research is to create specifications for a new class of bridges which will take advantage of the improved performance of HPS. This will eliminate or greatly reduce the extensive inspection requirements of bridges currently classified as fracture critical, thus making two and three girder steel bridge systems more competitive in the marketplace.

1.1 Scope and Objectives of This Study

TPF 5-238 will use results from material characterization tests and full scale fracture tests to set specifications for a new category of bridges using HPS steel. The main objectives of this study are to fully characterize the fracture behavior of multiple heats, plates, and grades of HPS. Specifically, HPS material testing includes:

- Yield and Tensile Strength
- Charpy V-Notch Impact Toughness
- Fracture Toughness at Static and Dynamic Rates
- Crack Arrest Toughness

Analysis of this data may result in the determination of appropriate correlations between Charpy V-Notch (CVN) tests and quantifiable fracture and performance parameters. Development of appropriate specifications and material requirements would be based on these correlations, enabling producers and designers to easily verify the fracture characteristics of plate steel being produced for bridge applications.

2. EXPERIMENTAL PROCEDURE

Characterization of HPS was accomplished through the utilization of numerous experimental tests. Described herein are the sources of steel examined, as well as the different specimens used in the material characterization. Additionally, this section presents the test methods utilized, as well as the analysis techniques used to describe the results.

2.1 Plate Designations and Sampling Procedure

Test specimens were fabricated from eight different HPS plates of varying grade and thickness. Each plate was designated a letter for specimen and testing numbering purposes. Details of each tested HPS plate, including letter designation, grade, thickness, and heat number can be found in Table 2-1.

Table 2-1. Designations and Details of HPS Plates

Letter Designation	Grade, MPa (ksi)	Thickness, mm. (in.)	Heat/ID Number
A	485 (70)	25.4 (1.0)	801W10170
C	690 (100)	19 (0.75)	W24549 55 W4
D	485 (70)	63.5 (2.5)	U5191-6A
E	690 (100)	38.1 (1.5)	P60017 W24549
F	690 (100)	50.8 (2.0)	T1W24594
H	485 (70)	31.8 (1.25)	HT813C7220
I	485 (70)	31.8 (1.25)	HT822H34790
J	485 (70)	38.1 (1.5)	821T06770

Specimens were fabricated from the plates at specific locations and in specific orientations. All tension specimens were sampled at mid-thickness and oriented with the longitudinal axis in the direction of rolling. As specified in ASTM A673-07, CVN specimens are to be centered at one-quarter plate thickness (ASTM 2007). All CVN and single edge bend (SE(B)) specimens tested as part of this study were located at this depth. The only exceptions to this are in plate C, where plate thickness prohibited this practice. For plate C specimens were centered at one-third plate thickness. In addition, a limited number of CVN tests were performed for each HPS plate sampled at mid-thickness.

The majority of CVN specimens and all of the SE(B) and crack arrest specimens were oriented such that the crack propagates perpendicular to the rolling direction of the plate. This is referred to as L-T orientation, as seen in Figure 2-1. For comparison purposes a limited number of CVN tests were performed on specimens from the T-L orientation. Crack arrest specimens were fabricated at plate thickness unless the plate was greater than 50.8 mm. (2 in.), in which case the specimens were centered at mid-thickness and cut down to 50.8 mm. (2 in.). Like CVN and SE(B) specimens, crack arrest specimens were machined in the L-T orientation.

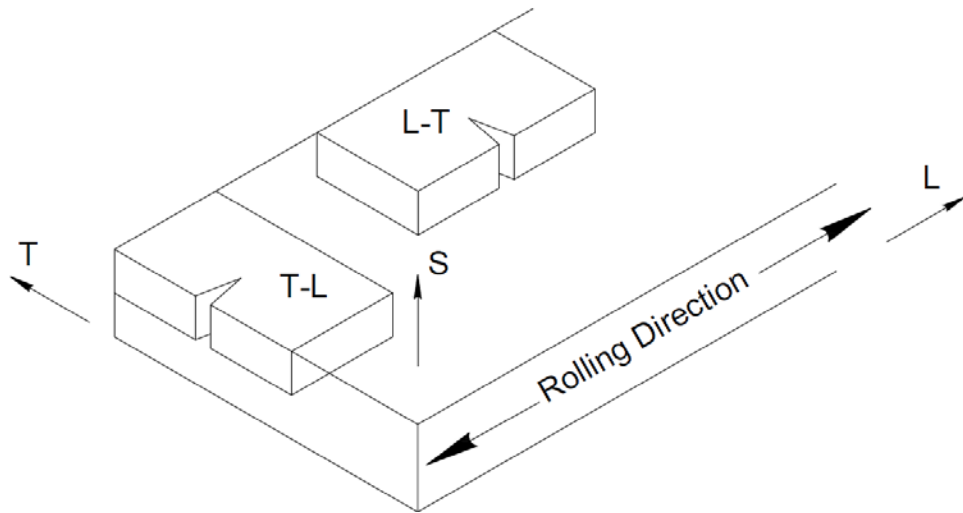


Figure 2-1. Specimen Orientation Designations

Specimen identification marking included the plate letter as well as a unique identifying number. CVN specimens were designated with only these two markings. SE(B) specimens were identified with a prime following the letter and number designation, while arrest and tension specimens were labeled with an a and t following the number designations, respectively. Following this pattern, specimen labels A1, A1', A1a, and A1t would indicate the first CVN, SE(B), arrest, and tension specimens removed from plate A, respectively.

2.2 Test Specimen Geometry

Various test specimens were used in an array of test methods. Presented herein are the different specimens used in this study.

2.2.1 Tension Test Specimens

Round tensile specimens in accordance with ASTM E8-08 were fabricated with a diameter of 9 mm. (0.35 in.) and a total reduced section length of 75 mm. (3 in.), as seen in Figure 2-2 (ASTM 2008).

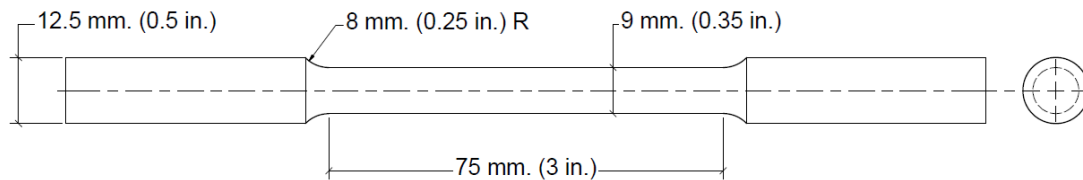


Figure 2-2. Tension Specimen Geometry

2.2.2 Charpy V-Notch Specimens

Typical CVN specimens used in impact testing are described in ASTM E23-07 (ASTM 2007). Specimens are 10 mm. (0.394 in.) square by 55 mm. (2.165 in.) in length. A 2 mm. (0.079 in.) deep notch with a 0.25 mm. (0.01 in.) radius is broached into the center of the specimen, as seen in Figure 2-3.

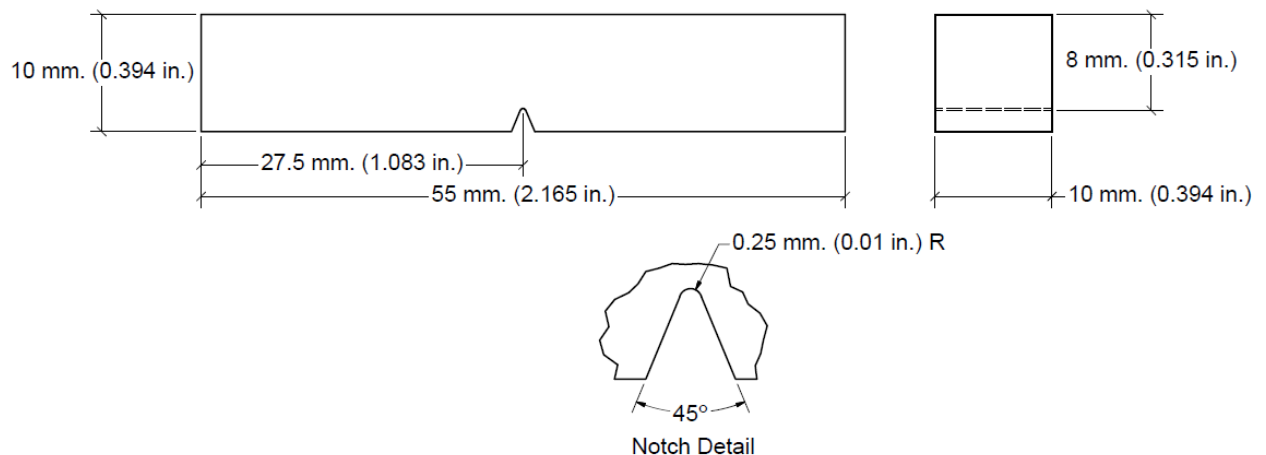


Figure 2-3. CVN Specimen Geometry

2.2.3 Single Edge Bend Specimens

Geometry requirements for SE(B) fracture toughness specimens can be found in ASTM E1921-13 and E1820-08 (ASTM 2013, 2008). The chosen specimen for use in this study is sometimes referred to as a pre-cracked Charpy-sized SE(B). This style of specimen was used for both static and dynamic fracture

toughness testing. The specimen blank geometry is the same as described above for the CVN specimen. The specimen is different at the notch however, as fracture toughness testing requires a sharp crack front. To ease fatigue pre-cracking, an EDM notch is cut into the center of the SE(B) blank, as seen in Figure 2-4. The notch width and end radius corresponds with the diameter and radius of EDM wire, while the shoulders cut into the face of the specimen facilitate the use of a clip gage during testing.

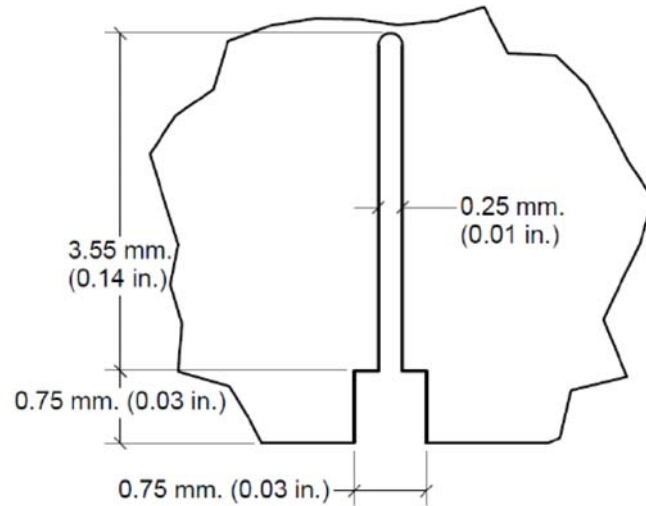


Figure 2-4. SE(B) Specimen Notch Details

Typically fracture toughness specimens are defined by dimensions B and W, which represent the thickness and height of the specimen, respectively. Also used to define specimen geometry is dimension a, which is the length of the crack. These dimensions can be seen on an SE(B) specimen in Figure 2-5. As mentioned above, all SE(B) specimens used in this study use CVN specimen geometry with dimensions B and W both equal to 10 mm. (0.394 in.).

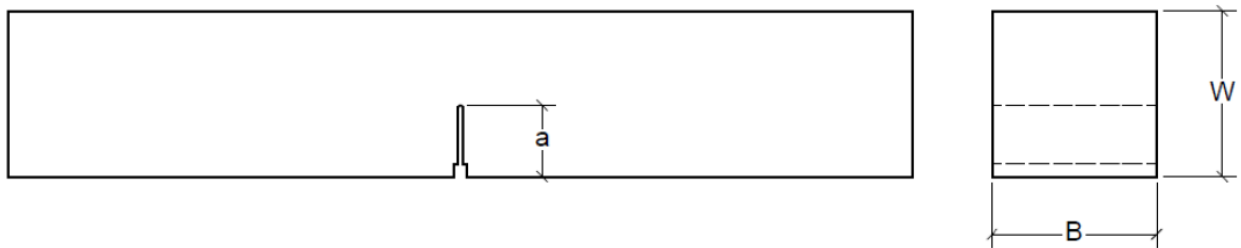


Figure 2-5. SE(B) Specimen Dimensions

To ensure a straight crack front during testing, side grooves are machined on the specimen sides after the completion of fatigue pre-cracking. Side grooves used in this study have a depth of 1 mm. (0.0394 in.) and an included angle of 45 degrees, and are centered on the specimen in line with the fatigue crack. Side grooves are located on two opposite sides of the specimen, perpendicular to the notched face, as can be seen in Figure 2-6. In this figure, the previously discussed notch has been machined into the bottom of the specimen.

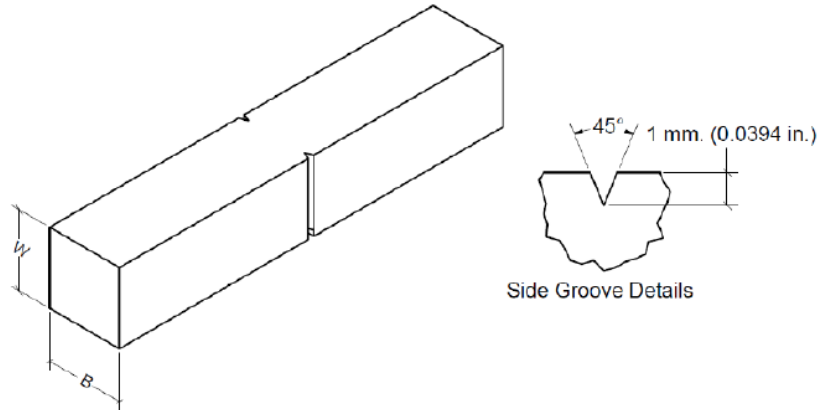


Figure 2-6. SE(B) Side Groove Location and Dimensions

2.2.4 Crack Arrest Specimens

Specimens used for crack arrest testing are modified compact tension (C(T)) specimens with geometry requirements described in ASTM E1221-12 (ASTM 2012). C(T) specimen geometry is defined in a similar manner to SE(B) specimens, with dimensions B and W defining thickness and width, respectively. Crack arrest testing is typically performed at plate thickness, so in this study B varied from plate to plate. Specimen width W , however, measured from the load line to the end of the specimen, was held constant at 102 mm. (4 in.) for all specimens. Wedge loading is applied through a 25.4 mm. (1.0 in.) diameter hole, centered on a 10.2 mm. (0.4 in.) slot that is machined to extend from the load line 30 mm. (1.2 in.) into the specimen. Initial machining geometry as described above can be seen in Figure 2-7. Additionally, 19 mm. (0.75 in.) diameter holes are also included in fabrication to accommodate clevis grips.

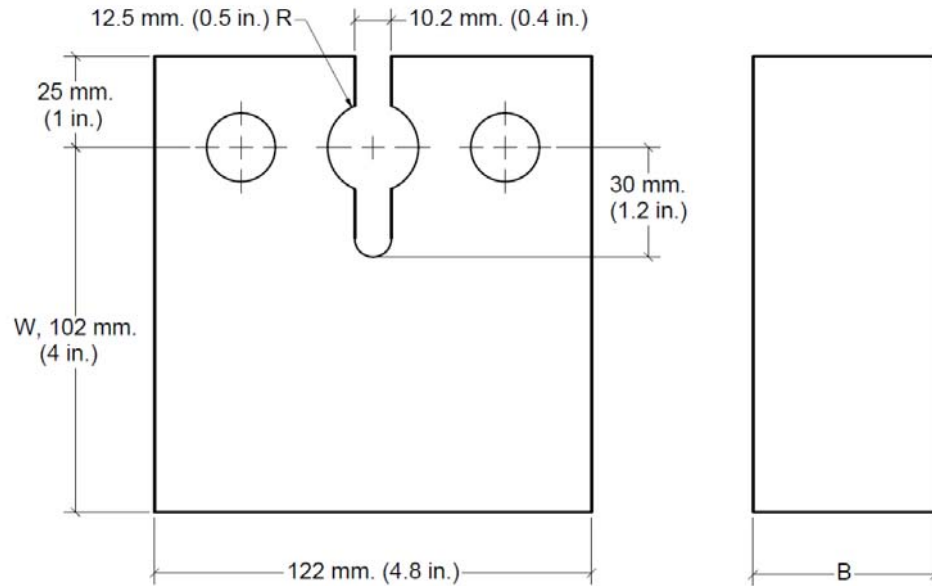


Figure 2-7. Crack Arrest Specimen Geometry

Following initial machining a brittle weld is deposited at the bottom of the slot, and then an EDM cut notch is machined into this deposit. The distance from the load line to the end of the notch, the initial crack length, a_0 , is 28 mm. (1.1 in.). This places the end of the initial crack within the weld deposit, approximately 2.5 mm. (0.1 in.) from the base metal. Similar to the SE(B) specimens, side grooves are also employed on crack arrest specimens. The two side grooves on crack arrest specimens are machined to a total depth of 25% specimen thickness with an included angle of 45 degrees.

2.3 Material Characterization Testing Procedures

2.3.1 Tensile Testing

Tensile testing was performed on a 100 kN (22 kip) Instron electro-mechanical test machine. Tests were performed in accordance with ASTM E8-08 (ASTM 2008). An Instron 5982 Type 1 extensometer was attached to each specimen prior to testing in order to measure elongation, as seen in Figure 2-8. Measurements were made until specimens reached 5 per cent elongation, at which point the gages were removed. After extensometer removal, elongation was measured by the movement of the load frame crosshead.



Figure 2-8. Tensile Test Specimen with Extensometer

Upon completion of the test, the records of both the extensometer and the crosshead were combined to form the final stress-strain curve of the specimen. Yield strength of each specimen was evaluated using the 0.2 per cent offset method. Tensile strength evaluation was made by dividing the maximum attained load by the original cross-sectional area of the specimen. All tensile testing was performed at room temperature and at a quasi-static loading rate.

2.3.2 Charpy V-Notch Impact Testing

CVN tests of HPS were performed on a friction compensated Tinius Olsen impact test machine with a maximum capacity of 400 J (300 ft-lb), seen in Figure 2-9. Prior to the beginning of testing this impact test machine was verified using NIST low and high energy specimens and was found to be in calibration.



Figure 2-9. Impact Test Machine

This impact machine uses an analog scale to indicate absorbed energy at fracture. Prior to testing the pendulum arm is raised and locked into place with a safety latch. Once the dial indicator is turned to full scale reading, a test specimen is placed on the anvil with the notch centered, oriented vertically, and facing away from the striking surface of the impact hammer. The safety latch is then removed and the hammer is released, allowing the arm to swing and causing the hammer to strike the back face of the specimen. The height of the swinging pendulum after fracture is then related to energy absorption, and is indicated on the dial. Energy values below 80 per cent of machine capacity are considered valid. Indicated values above this limit are considered invalid due to pendulum speed validity requirements.

Because full temperature transition curves were desired, CVN specimens were cooled using a methanol cooling bath capable of temperatures as low as $-80\text{ }^{\circ}\text{C}$ ($-112\text{ }^{\circ}\text{F}$). Specimens were deposited in the bath once the desired temperature was obtained, and left to cool prior to testing. Temperatures

were monitored using a sample CVN specimen with an embedded thermo-couple. Specimens were removed from the cooling bath and placed on the anvils with the use of Charpy centering tongs, which had also been placed in the cooling bath. Measures were taken to ensure that the time between removal from temperature bath and impact was less than five seconds. If an error occurred and specimens were removed from the cooling bath for longer than five seconds prior to testing, they were again placed in the methanol bath for re-cooling.

When lower-shelf behavior could not be obtained at $-80\text{ }^{\circ}\text{C}$ ($-112\text{ }^{\circ}\text{F}$), liquid nitrogen was used to cool specimens to lower test temperatures. Specimens were placed in an insulated container with the thermo-couple embedded specimen, and liquid nitrogen was introduced. Temperatures were allowed to drop below the desired test temperature, and then specimens were removed from the container and placed on a metal plate along with the thermo-couple embedded specimen, as seen in Figure 2-10. The temperature of the embedded CVN was monitored as the specimens gradually warmed up, and tests were completed as the desired temperature was reached.



Figure 2-10. CVN Specimen Reaching Desired Test Temperature

2.3.3 Fracture Toughness Testing

Fracture toughness tests were performed on specimens prepared with specialized machining as described above, as well as fatigue pre-cracking, prior to testing. All pre-cracking and testing of fracture toughness specimens was performed on an MTS Landmark servo-hydraulic test machine. Software used for pre-cracking and testing was developed by researchers at the Naval Academy (Joyce and Link 2012).

2.3.2.1 Fatigue Pre-Cracking Procedure

Fatigue pre-cracking is performed on the same three point bend test apparatus that is used for fracture toughness testing, as seen in Figure 2-11. For both pre-cracking and testing, CMOD is measured using the Tension Measurement SFDG-08 clip gage, also shown in Figure 2-11. The span of the test setup is equal to four times the specimen width, or 40 mm. (1.575 in.) as required in ASTM E1820-08 (ASTM 2008).

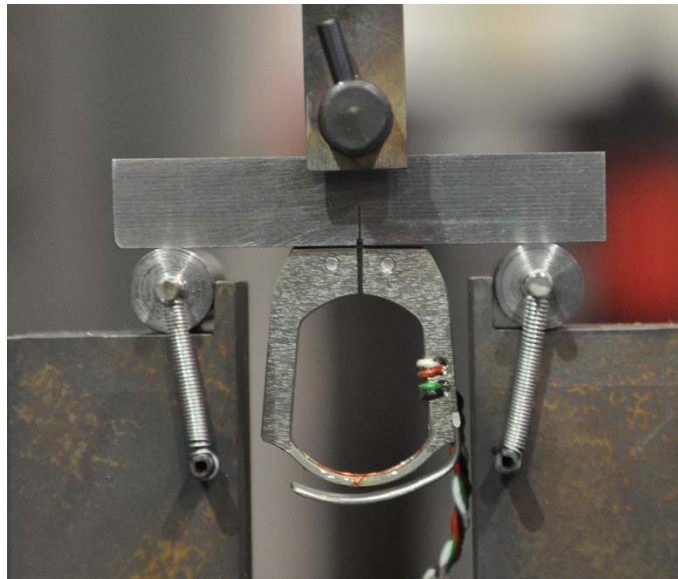


Figure 2-11. SE(B) Cracking and Testing Apparatus

Original EDM specimen notches are machined to a depth of 4.3 mm. (0.17 in.). This depth was chosen to minimize fatigue pre-cracking time. An initial crack length, a_0 , of $W/2$ is desirable for reference temperature testing. Because ASTM E1921-13 requires a minimum of 0.6 mm. (0.024 in.) of

crack extension beyond the machined notch, an initial notch depth of 4.3 mm. (0.17 in.) produces an acceptable fatigue pre-crack at an a_0/W ratio equal to 0.5.

Pre-cracking is performed at room temperature, which is recorded as part of the test record. Because test temperatures are much colder than pre-cracking temperatures, there are stringent rules in place to avoid warm prestressing during the pre-crack process. Limits on stress intensity values during the last segment of pre-cracking are prescribed in ASTM E1921-13. The first half of the pre-crack is run in a load shedding approach, as described in ASTM E647-13 (ASTM 2013). In this process, the stress intensity is stepped down from a start of 17.5 MPa√m (16 ksi√in) to 14.3 MPa√m (13 ksi√in) during the first half of crack growth. Once the crack has reached 0.3 mm. (0.012 in.) beyond the initial notch, the specimen is turned around to complete pre-cracking at a constant stress intensity of 14.3 MPa√m (13 ksi√in). Turning the specimen helps to ensure a straight crack front by eliminating small errors that may occur due to mis-alignment.

Once the fatigue pre-crack has reached the desired length, each specimen is re-machined with side grooves, as previously described. Side grooves eliminate any crack curvature that often occurs at the ends of specimen. Eliminating this tunneling effect provides a straight fatigue crack front for fracture toughness testing.

2.3.2.2 Fracture Toughness Testing Procedure

Fracture toughness testing of SE(B) specimens is performed on the same testing apparatus shown in Figure 2-11 above. Testing standards ASTM E1921-13 and E1820-08 were followed (ASTM 2013, 2008). Test specimens are centered on the apparatus using a jig that enables proper alignment. A clip gage connected to the front face of the specimen measures crack mouth opening displacement (CMOD).

A small amount of pre-load is applied to the specimen to hold the specimen in place on the fixture while the environmental chamber is reaching the desired test temperature. More information on the environmental cooling chamber can be found in Section 2.3.5. Once the desired test temperature has stabilized, testing can begin. Three to five elastic loading-unloading cycles are performed to check specimen alignment. Once proper alignment is verified, testing begins.

Load is applied to the specimen in displacement control mode. Static tests are performed at a rate that is equivalent to approximately 0.1 MPa√m/sec (0.091 ksi√in) in the elastic regime of the test.

Dynamic tests are performed at the highest rate attainable by the servo-hydraulic test machine. Depending on toughness, this resulted in dynamic test rates ranging from 1000 to 5000 MPa√m/sec (910 to 4550 ksi√in/sec).

For reference temperature determination no elastic compliance unloadings are necessary, as the master curve method does not correct for slow stable crack growth. If testing at temperatures well beyond temperature ranges where cleavage fracture is expected to occur, it is necessary to perform unloadings in order to generate a resistance curve. However, the majority of testing is focused on evaluating cleavage fracture initiation toughness, so unloadings are typically not used. Graphical examples of typical test records both with and without unloadings are presented in Figure 2-12 and Figure 2-13. Both of these figures display plots of load versus CMOD.

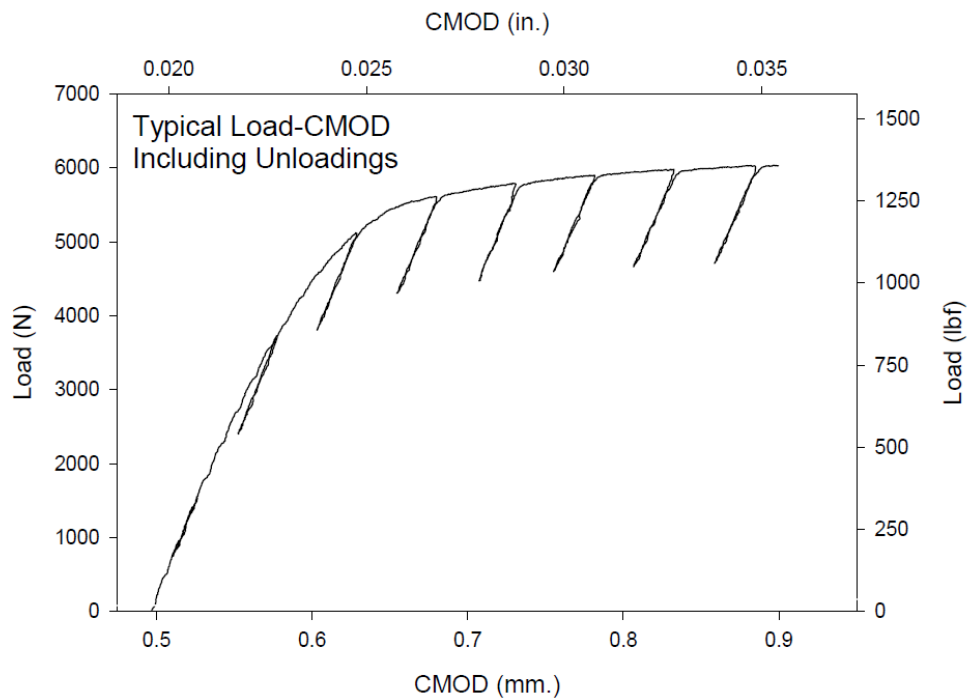


Figure 2-12. Typical Load-CMOD Plot with Elastic Compliance Unloadings

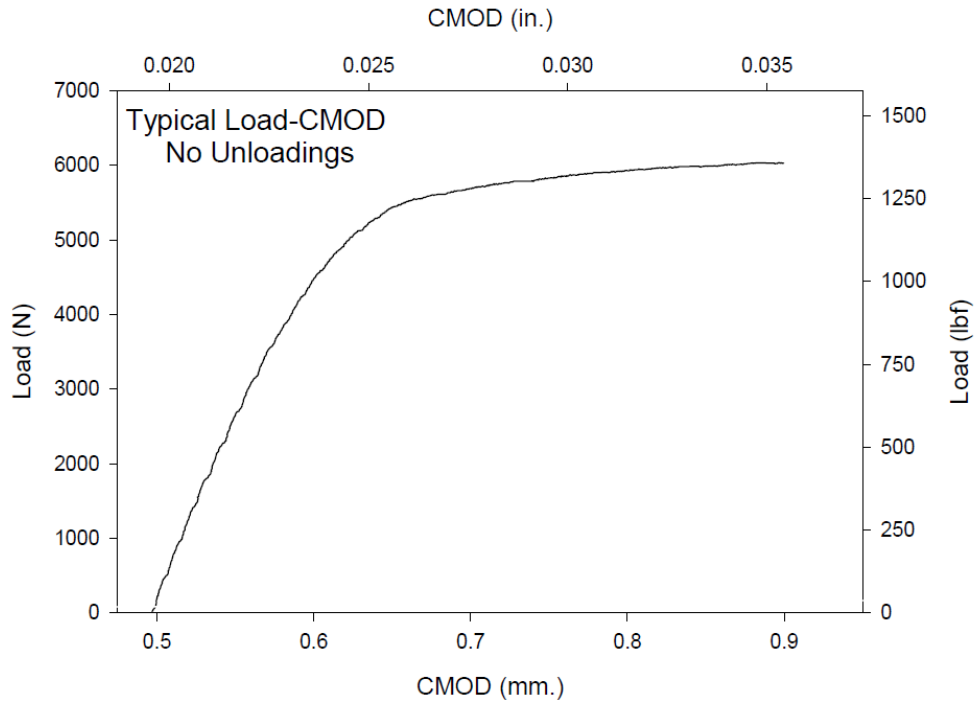


Figure 2-13. Typical Load-CMOD Plot without Elastic Compliance Unloadings

2.3.2.3 Fracture Toughness Data Analysis

Once fracture has occurred, specimens are removed from the cooling chamber and are placed on a hot plate for heat tinting. This changes the color of the fatigue crack and fracture surfaces, allowing for accurate measurement of initial crack size. Digital photographs of crack surfaces are scaled in AutoCAD, and nine-point measurements of initial crack size are made in accordance with ASTM E1820-08. An example of a measured crack is shown in Figure 2-14. The light blue section of this specimen is the fatigue crack, while the golden is the fractured surface. The silver surface is the remaining ligament of the specimen that was broken after heat tinting.

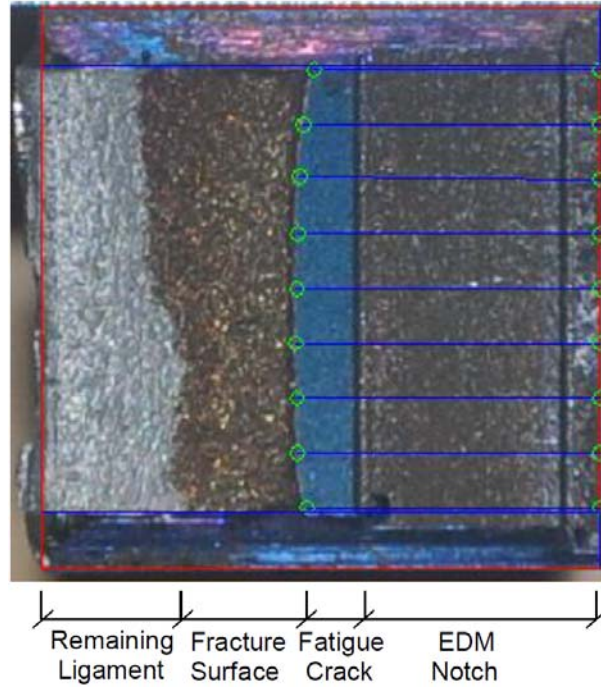


Figure 2-14. Measured Fracture Surface of Typical SE(B) Specimen

Calculation of the J-Integral is then made using the measured initial crack size, specimen geometry, and load-CMOD test record. It is also possible to use the load line displacement (LLD) rather than CMOD. However, for this study CMOD measurements are used because the clip gage resolution and stability are better than that of the load line displacement test record.

Adjustments to the modulus of elasticity are made until the elastic compliance method predicts an initial crack size corresponding to the optically measured fatigue crack. Testing specifications allow for up to 10 per cent deviation from expected elastic modulus in this calculation. Any test record requiring more than a 10 per cent adjustment is considered to be invalid due to specimen misalignment.

The J-Integral at the onset of cleavage fracture, J_c , is the parameter used for identification of fracture initiation. This is experimentally calculated by separating the elastic and plastic components of the J-Integral, signified by J_e and J_p . These two values are given in Equations 2.1 and 2.2.

$$J_e = \frac{(1 - \nu^2)K_e^2}{E} \quad \text{Eq. 2.1}$$

$$J_p = \frac{\eta A_p}{B_N b_o} \quad \text{Eq. 2.2}$$

In Equation 2.1, J_e is the elastic component of the J-Integral, ν is Poisson's ratio, E is the material modulus of elasticity, and K_e is an elastic fracture toughness value, calculated as shown in Equation 2.3.

$$K_e = \frac{PS}{(BB_N)^{1/2}W^{3/2}} f(a_o/W) \quad \text{Eq. 2.3}$$

For calculating the elastic fracture toughness, P is the load at fracture, S is the span length of the test apparatus, B is the gross specimen thickness, B_N is the nominal specimen thickness, W is specimen width, and $f(a_o/W)$ is a function related to initial crack size, a_o , and specimen width, W . This function is presented in Equation 2.4.

$$f(a_o/W) = \frac{3(a_o/W)^{1/2}}{2[1 + 2(a_o/W)]} \frac{1.99 - (a_o/W)(1 - a_o/W) [2.15 - 3.93(a_o/W) + 2.7(a_o/W)^2]}{(1 - a_o/W)^{3/2}} \quad \text{Eq. 2.4}$$

In Equation 2.2, J_p is the plastic component of the J-Integral, η is a dimensionless parameter relating plastic work to crack growth resistance, A_p is the plastic area under the Load-CMOD or Load-LLD curve, BN is the nominal specimen thickness, and b_o is the initial remaining ligament. The plastic eta factor, η , varies upon the type of test record being examined. For LLD, η is taken to be 1.9. When CMOD is used, η varies as a function of specimen geometry, as shown in Equation 2.5.

$$\eta = 3.784 - 3.101(a_o/W) + 2.018(a_o/W)^2 \quad \text{Eq. 2.5}$$

The plastic area under the Load-CMOD or Load-LLD curve, A_p , is graphically shown in Figure 2-15. This area is calculated using an unloading line from the point of fracture. This unloading line is parallel to the initial elastic slope, $1/C_o$.

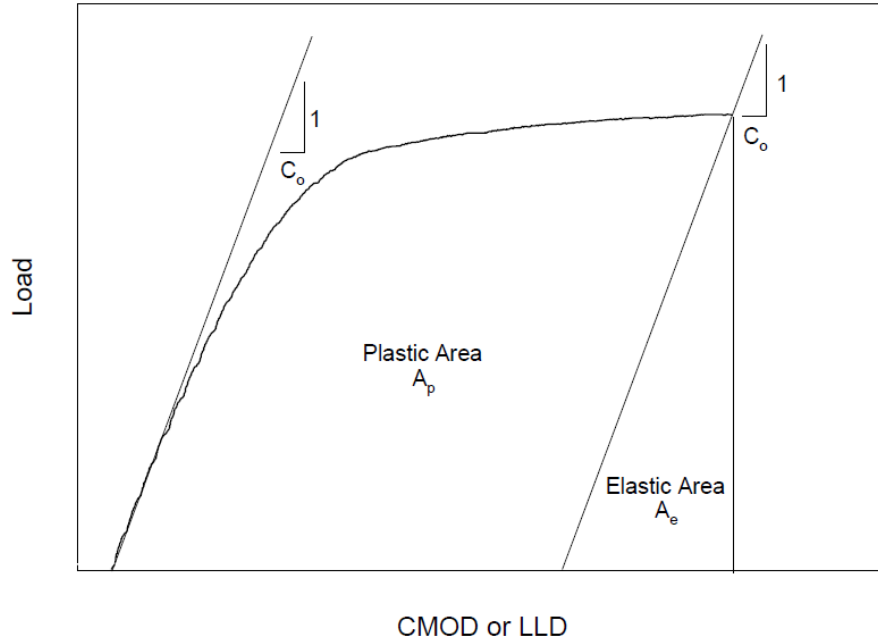


Figure 2-15. Plastic and Elastic Portions of Test Record

These two components, J_e and J_p , are combined to arrive at the critical J-Integral value at the onset of cleavage fracture, J_c . This critical J-Integral value is then converted into an equivalent elastic plastic stress intensity value, K_J , through the use of Equation 2.6. It should be noted that J_c values are only considered to be conditional until a multitude of validity requirements are met.

$$K_J = \sqrt{J \frac{E}{1 - \nu^2}} \quad \text{Eq. 2.6}$$

2.3.4 Crack Arrest Toughness Testing

2.3.4.1 Crack Arrest Toughness Testing Procedure

Crack arrest testing was performed on an MTS Insight 150 kN (33 kip) electro-mechanical machine, in accordance with ASTM E1221-12 (ASTM 2012). Load is applied cyclically to the specimen through a wedge and split pin apparatus, as shown in Figure 2-16. Various configurations are allowed for crack arrest testing. For this study the specimens rest on the shoulders of the split pin and are not in contact with the base plate.



Figure 2-16. Crack Arrest Specimen Prior to Testing

A Tension Measurement DG-25 clip gage is used to record CMOD as the test is performed. Common nomenclature for crack arrest testing uses δ to represent CMOD. Load is applied in displacement control at a rate of approximately 8 mm/min (0.3 in/min) until δ reaches a maximum value calculated by Equation 2.7. If fracture occurs prior to any unloading cycles, this limit should be reduced when testing subsequent specimens.

$$\delta_{1_{max}} = \frac{0.69\sigma_{ys}W\sqrt{B_N/B}}{Ef(a_o/W)} \quad \text{Eq. 2.7}$$

For Equation 2.7, subscript one signifies the first loading cycle, $f(a_o/W)$ is a specimen geometry related function as defined in Equation 2.8, and all other variables are as previously defined.

$$f(a_o/W) = (1 - a_o/W)^{0.5} (0.748 - 2.176(a_o/W) + 3.56(a_o/W)^2 - 2.55(a_o/W)^3 + 0.62(a_o/W)^4) \quad \text{Eq. 2.8}$$

When this limit is reached, the wedge is extracted from the specimen. This wedge extraction is the reason for the hold-down plate seen in Figure 2-16. The wedge is extracted completely from the specimen with the clip gage constantly recording CMOD. This allows for a record of displacement offset that occurs at zero force. It is common for load readings to reverse into tension during wedge

extraction. To counter this, thread tape is applied to the wedge to reduce friction with split pins, although this does not eliminate the load reversal. This is not thought to influence test results.

Once wedge extraction is complete, the next cycle of loading begins. The wedge is again introduced into the specimen, applying load to the specimen until a fracture event occurs, or the next CMOD limit is reached. CMOD loading limits for all cycles following the first are given by Equation 2.9.

$$\delta_{n_{max}} = [1 + 0.25(n - 1)] \left[\frac{0.69\sigma_{ys}W\sqrt{B_N/B}}{Ef(a_o/W)} \right] \quad \text{Eq. 2.9}$$

The variable n signifies the cycle number in this equation, and all other variables are as previously defined. This process continues until fracture occurs, or the maximum CMOD limit is reached. This displacement limit, beyond which point the specimen is not likely to yield a successful result, is presented in Equation 2.10.

$$\delta_{o_{limit}} = \frac{1.5\sigma_{ys}W\sqrt{B_N/B}}{Ef(a_o/W)} \quad \text{Eq. 2.10}$$

If this limit is reached without fracture initiation, the test is stopped and the specimen re-machined to remove the material in the area of the plastic zone around the started notch. Specimens are then tested again at a lower temperature, where fracture initiation may occur.

Similar to SE(B) fracture toughness specimens, crack arrest specimens are heat tinted and photographed to allow for accurate measurements of the fracture surface. The nine point measurement process used for fracture toughness testing is not used on crack arrest specimens. Crack arrest point measurements are made with a visual average along three lines of measurement, as seen in Figure 2-17. This allows more room for judgment, as arrested cracks rarely form perfectly straight or flat. Limits on crack straightness are greatly relaxed in comparison to those in place for fracture toughness testing. The photograph presented as Figure 2-17 shows the arrested crack surface measured from the end of the started notch. Additional measurements are also taken from the starter notch to the load line. The distance from the load line to the arrested surface represents the starter notch is the initial crack length, a_o . The final arrested crack length, a_a , is measured from the load line to the visual average discussed above.

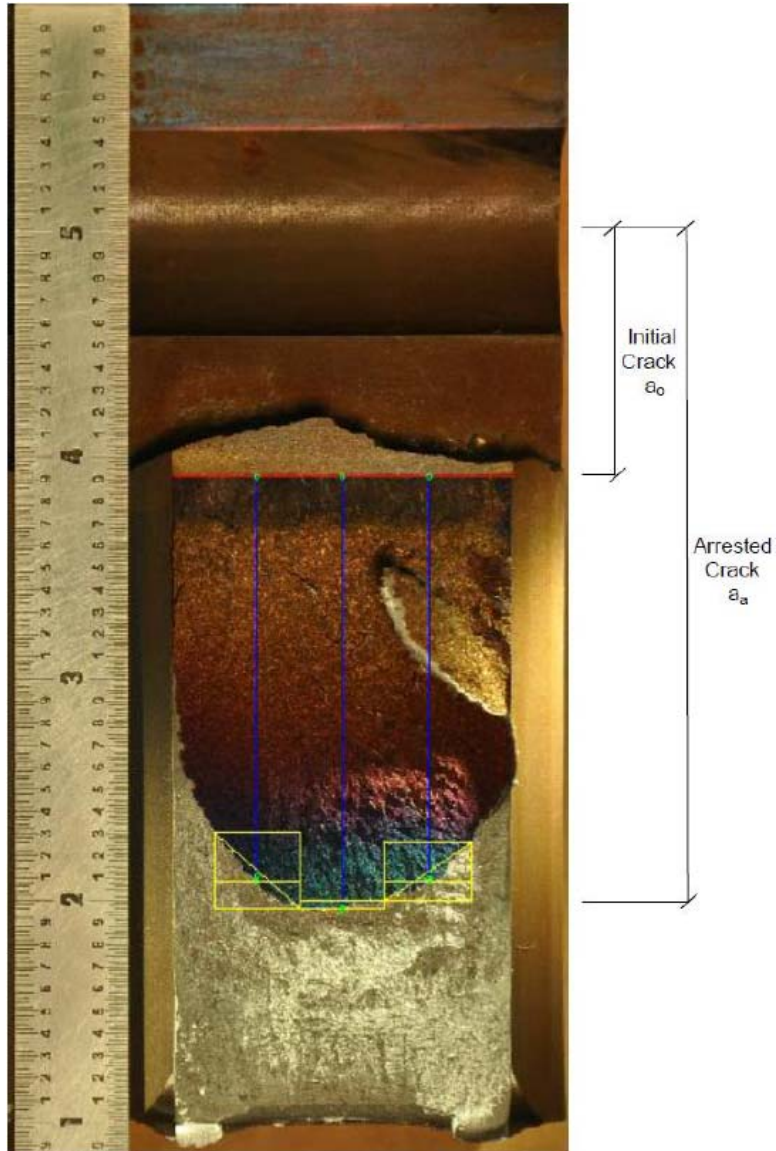


Figure 2-17. Measured Fracture Surface of Typical Crack Arrest Specimen

2.3.4.2 Crack Arrest Data Analysis

Crack arrest toughness values for each specimen are determined from the final arrested crack length and data taken from the Load-CMOD test record. The calculation of crack arrest toughness is done with the use of Equation 2.11.

$$K_{Qa} = Edf(a/W) \frac{\sqrt{B_N/B}}{\sqrt{W}} \quad \text{Eq. 2.11}$$

In this equation for a conditional value of crack arrest toughness, d is a function related to multiple CMOD values as defined by Equation 2.12. All other variables are as previously defined with a_o used in place of a_o in the geometry function defined by Equation 2.8.

$$d = 0.5 \left[\delta_o + \delta_a - (\delta_p)_1 - (\delta_p)_{n-1} \right] \quad \text{Eq. 2.12}$$

In this equation, δ_o represents the CMOD at the onset of unstable crack growth, δ_a represents the displacement just after crack arrest, $(\delta_p)_1$ represents the displacement offset at the end of the first loading cycle, and $(\delta_p)_{n-1}$ represents the CMOD offset at the start of the last loading cycle. These points are all indicated graphically on the typical test record plot shown in Figure 2-18.

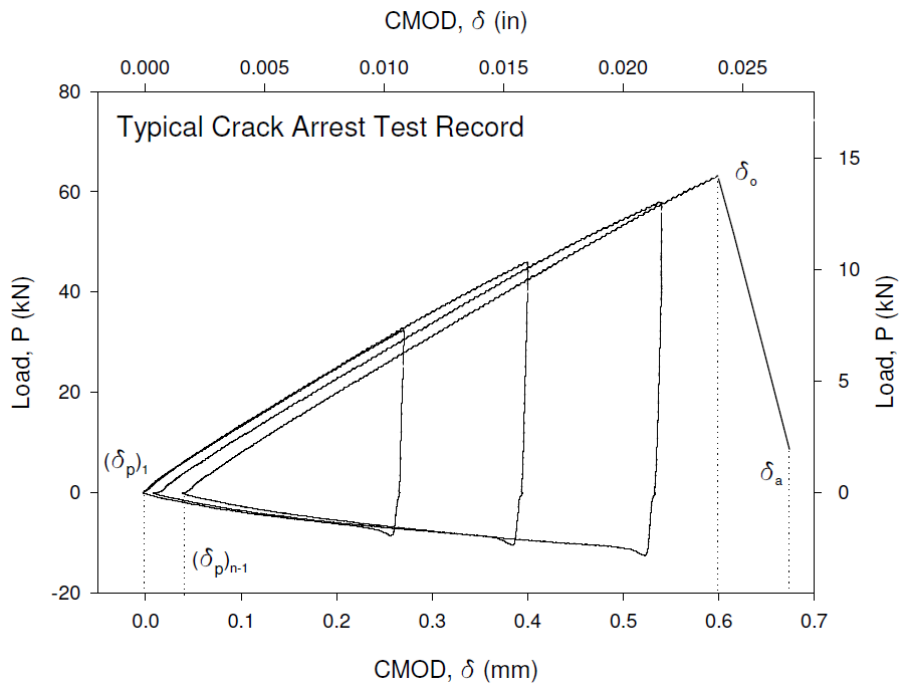


Figure 2-18. Typical Crack Arrest Test Record

As with fracture toughness testing, crack arrest toughness values are considered to be conditional until it can be shown that all validity requirements have been met.

2.3.5 Specimen Cooling Chamber

For both fracture toughness and crack arrest testing, extremely low test temperature are required. These temperatures are obtained and consistently maintained through the use of a liquid nitrogen

delivery system. An adjustable environmental chamber was fabricated out of foam and plywood. The chamber was designed to be easily adaptable to either of the two test setups it was needed for, as shown on the crack arrest apparatus in Figure 2-19.



Figure 2-19. Environmental Chamber on Crack Arrest Apparatus

A cryogenic hose connects a tank of liquid nitrogen to an electronically controlled solenoid valve, which in turn leads to a copper pipe with multiple perforations inside of the cooling chamber. The operation of the normally-closed valve is performed by a programmable digital controller connected to a thermocouple inside the chamber. For fracture toughness testing, the thermocouple is embedded in a dummy SE(B) specimen that is placed near the actual test specimen during testing. As previously stated, during crack arrest testing the thermocouple wire is embedded in the crack arrest specimen.

Once a set point temperature is entered, the controller signals for the valve to open if the thermocouple reading was greater than the set point. The controller then measures the rate of change of the temperature, closing and opening the valve as necessary to regulate the temperature. The ability of the controller to regulate valve opening, combined with the insulation provided by the chamber,

allow for extremely stable test temperatures. Once set point temperatures are given time to stabilize, test temperatures do not fluctuate by more than ± 1 °C.

2.4 Data Analysis

Fracture behavior of all metals, including structural steels, is highly dependent upon test temperature. Failure modes change throughout a range of test temperatures, resulting in changing of fracture toughness and impact energy. The following section serves as a brief introduction to how the data of this study were characterized over the range of test temperatures.

2.4.1 Charpy V-Notch Temperature Transition Characterization

Typical behavior exhibited by steel CVN impact specimens includes brittle, cleavage fracture at low temperatures, termed lower shelf behavior. As test temperature is increased, the toughness also increases in what is known as the brittle to ductile transition region. Finally, at high temperatures, steels exhibit ductile behavior and high CVN impact toughness values, and their behavior is said to be on the upper shelf. These behavior regimes are presented for a typical HPS 485W (70W) steel in Figure 2-20.

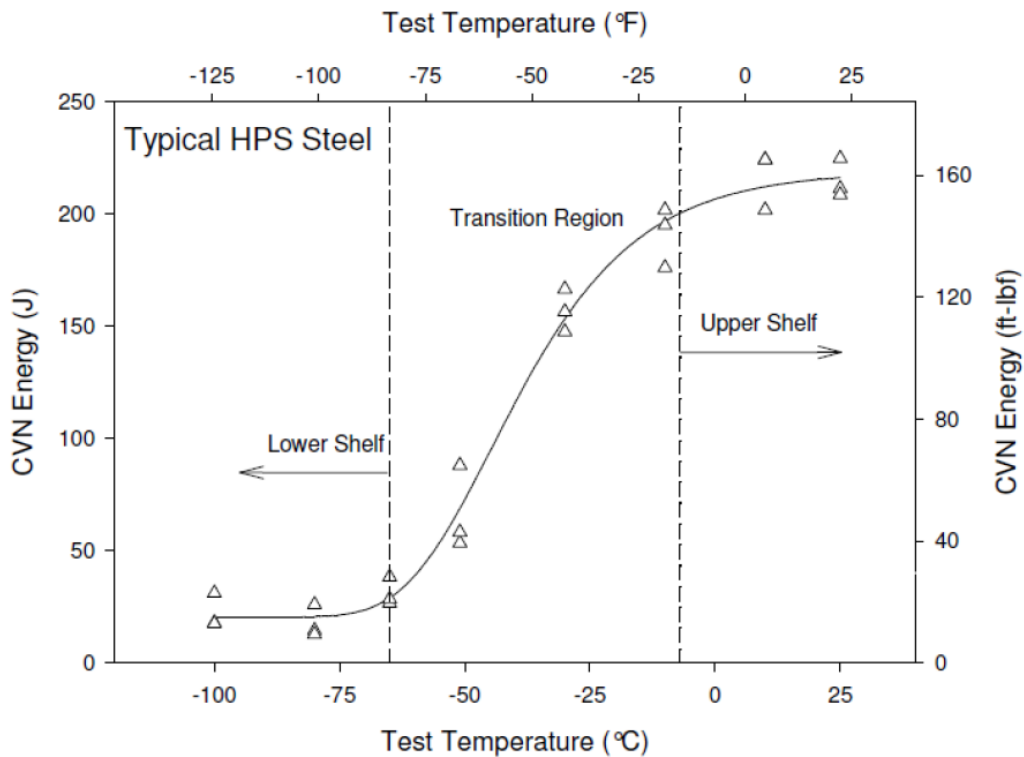


Figure 2-20. Typical CVN Behavior for HPS Steel

Characterization of this behavior is done through the use of a five parameter exponential sigmoid function, provided in Equation 2.13. In this function CVN and T are CVN energy and temperature, respectively, and a , b , c , d , and f are five fitted parameters. Fitting a function of this form allows the CVN data to be characterized through all three behavior regimes.

$$CVN(T) = a + \frac{b}{\left[1 + e^{-\frac{(T-c)}{d}}\right]^f} \quad \text{Eq. 2.13}$$

2.4.2 Fracture Toughness Master Curve Characterization

As the emphasis of this study was placed on the brittle fracture behavior of HPS grade bridge steels, testing focused on fracture caused by cleavage mechanisms. Thus, characterization of fracture toughness was necessary through the lower shelf and transition behavior regimes. Also needed in the characterization of fracture behavior is the inclusion of the statistical nature of cleavage fracture. For these reasons the master curve approach was used to describe fracture toughness of both quasi-static and dynamic initiation, as well as arrest toughness.

The master curve refers to the exponential function, empirically derived from fracture toughness data of ferritic steels and weld metals, shown to characterize the relationship between fracture toughness and temperature. Typically the master curve is used to represent median fracture toughness, which is the toughness value at a given temperature for which a specimen has a 50 per cent probability of failure. As the exponential shape applies to all ferritic steels, the curve can be defined by a single temperature which corresponds to a specific toughness value. This temperature is known as the reference temperature, T_o , and is rooted to the median toughness curve at a value of 100 MPa√m (91 ksi√in). The median fracture toughness with respect to temperature is given in Equation 2.14.

$$K_{Jc(\text{med})} = 30 + 70e^{(0.019(T-T_o))} \quad \text{Eq. 2.14}$$

In this equation, $K_{Jc(\text{med})}$ is the median elastic-plastic critical fracture toughness in MPa√m, T is test temperature in degrees Celsius, and T_o is the reference temperature in degrees Celsius.

Size effects are normalized prior to application of the master curve methodology to account for distribution of initiation sites throughout the material matrix. Thickness is designated using xT

nomenclature, where 'x' is the specimen thickness in inches. Thus, a 25.4 mm (1 in) thick specimen is said to be of thickness 1T. Master curve data is typically normalized to a 1T specimen thickness, although any thickness may be chosen. Thickness normalization is performed by using Equation 2.15, where $K_{Jc(x)}$ is the elastic-plastic critical fracture toughness adjusted to a desired thickness, B_x , absolute minimum toughness, $K_{min} = 20 \text{ MPa}\sqrt{\text{m}}$ (18 ksi $\sqrt{\text{in}}$), $K_{Jc(o)}$ is the fracture toughness at a known thickness, B_o .

$$K_{Jc(x)} = K_{min} + [K_{Jc(o)} - K_{min}] \left(\frac{B_o}{B_x} \right)^{1/4} \quad \text{Eq. 2.15}$$

Scatter in test data is accounted for using a three-parameter Weibull distribution, for which two of the parameters have been empirically determined. The three parameters used include absolute minimum toughness, Weibull slope set equal to 4, and a scale parameter. The scale parameter is determined based upon the number of valid data in a sample, and is included in the master curve methodology. Applying the probability of failure from the Weibull distribution, tolerance bounds can be determined in units of MPa $\sqrt{\text{m}}$ with Equation 2.16, where 0.xx represents the desired probability of failure, and temperature values are given in degrees Celsius.

$$K_{Jc(0.xx)} = 20 + \left[\ln \left(\frac{1}{1 - 0.xx} \right) \right]^{(1/4)} \{ 11 + 77e^{(0.019(T-T_o))} \} \quad \text{Eq. 2.16}$$

A typical Master Curve with T_o equal to -30 °C (-22 °F) and tolerance bounds of 5 and 95 per cent is shown in Figure 2-21.

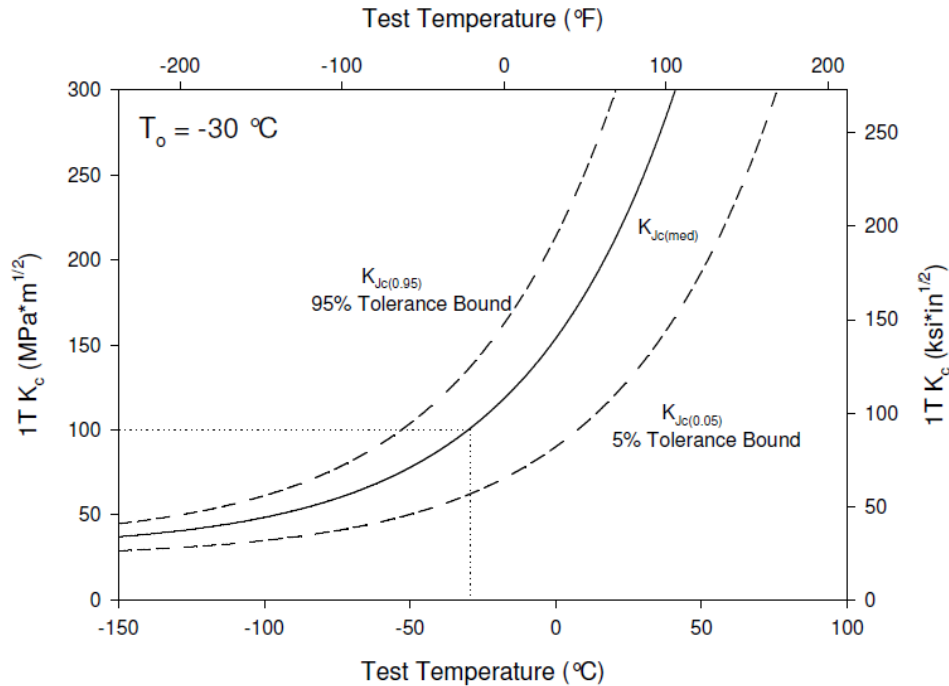


Figure 2-21. Typical Master Curve with Tolerance Bounds

ASTM E1921 (2013) places two validity limits on K_{Jc} data for use with the master curve methodology. The first is an actual toughness limit, $K_{Jc(limit)}$, defined by Equation 2.17. The limit equation is defined using the initial remaining ligament of the specimen, b_o in millimeters, which is the difference between the specimen width, W , and the initial crack, a_o . Also included in this equation is the material 0.2 per cent offset yield stress, σ_{ys} , in MPa, and modulus of elasticity in GPa. The purpose of the limit is to ensure adequate crack tip constraint in the specimen.

$$K_{Jc(limit)} = \sqrt{\frac{E b_o \sigma_{ys}}{30(1 - \nu^2)}} \quad \text{Eq. 2.17}$$

Any toughness value exceeding this limit is censored in the ASTM E1921 master curve analysis. The second limit is placed on slow stable crack growth preceding cleavage fracture. Any data obtained from a specimen with crack growth beyond the initial fatigue crack exceeding the smaller of 1 mm (0.04 in.) or 5 per cent of the original ligament length, b_o , is also censored. In both cases, censored values may be used in place of the original datum for master curve analysis. If the limit is violated, $K_{Jc(limit)}$ is the censored value for master curve purposes. When the crack growth limit is violated, the corresponding

toughness at that amount of crack growth is used. In the case of both limits being exceeded, the smaller of the two is used as the censoring value.

To obtain the reference temperature for a dataset of size N, fracture toughness and test temperature data are entered into Equation 2.18. Accounting for censored data values, δ_i is equal to one if the “ith” datum is valid, and zero if it is censored. Using Equation 2.18, a provisional value of the reference temperature, T_{oQ} , is determined through iteration. This calculation is limited to data experimentally obtained at temperatures within a range of $\pm 50^\circ\text{C}$ from the provisional reference temperature.

$$\sum_{i=1}^N \delta_i \frac{e^{[0.019(T_i - T_{oQ})]}}{11 + 76.7e^{[0.019(T_i - T_{oQ})]}} - \sum_{i=1}^N \frac{(K_{Jc(i)} - 20)^4 e^{[0.019(T_i - T_{oQ})]}}{\{11 + 76.7e^{[0.019(T_i - T_{oQ})]}\}^5} = 0 \quad \text{Eq. 2.18}$$

The provisional value of the reference temperature is considered to be the true reference temperature, T_o , only if the size of the data set meets validity requirements. Data collected at temperatures well below the reference temperature are considered to make reduced accuracy contributions towards T_o determination. For this reason, each valid datum is assigned a weighting factor, n_i , determined by the test temperature. These weighting factors are given in Table 2-2. Summing all weighting factors must result in a value greater than one for the provisional value of the reference temperature, T_{oQ} , to be considered a valid reference temperature, T_o .

Table 2-2. ASTM E1921 Weighting Factors for Multi-Temperature Analysis

(T-T _o) Range, °C	1T K _{Jc(med)} Range, MPa√m	Weighting Factor, n _i
50 to -14	212 to 84	1/6
-15 to -35	83 to 66	1/7
-36 to -50	65 to 58	1/8

3. EXPERIMENTAL TEST RESULTS

3.1 Tensile Test Results

As previously discussed, tensile specimens were tested for each plate of steel in this study. The exception to this is plates D, E, and F, which were tested as part of a previous FHWA research project (Wright, unpublished). This unpublished report examined the effects of rate and temperature on both yield and tensile strength, and results showed that these are well accounted for using the correction developed by Madison and Irwin (1974). For this reason, tensile testing as part of this project was only performed at room temperature and under quasi-static loading rates. Average yield and tensile values for each plate are presented in Table 3-1, including those from the unpublished FHWA study. Test records for each tensile specimen examined in this study can be found in the dissertation corresponding to this research (Collins 2014).

Table 3-1. Tensile Test Results, Room Temperature, Quasi-Static Load Rate

Letter Designation	Average Yield Strength, MPa (ksi)	Average Tensile Strength, MPa (ksi)
A	593 (86)	682 (99)
C	792 (115)	831 (120)
D	519 (76)	618 (90)
E	758 (111)	800 (117)
F	756 (110)	800 (117)
H	512 (74)	638 (92)
I	483 (70)	614 (89)
J	514 (74)	639 (93)

3.2 Charpy V-Notch Impact Test Results

A total of 246 CVN impact tests were performed for the eight different plates of HPS. Impact energy values of 1/4T L-T CVN specimens from each plate were plotted with respect to test temperature in order to develop a transition curve. The exception to this is plate C, which had specimens sampled at 1/3T due to thickness limitations.

3.2.1 Charpy V-Notch Impact Toughness of HPS 690W (100W)

Displayed in Figure 3-1 through Figure 3-3 are results for the three 690W (100W) plates. The three AASHTO temperature zones of -18, -34, and -51 °C (0, -30, and -60 °F) are represented by vertical dotted lines in each of these plots. The mandated fracture critical CVN test temperature of -34 °C (-30 °F) is shown with a vertical dashed line, and the specified minimum average energy value of 48 J (35 ft-lbf) is designated with an X. These requirements were easily achieved by all steels, with sigmoid fit values of 139, 147, and 144 J (102, 108, and 106 ft-lbf) for plates C, E, and F, respectively. The examined plates even displayed behavior well above the toughness requirements of ASTM A709-13 at the AASHTO Zone III temperature of -51 °C (-60 °F), with average test values of 66.5, 89.5, and 98 J (49, 66, and 72 ft-lbf). It should also be noted for these three plates of HPS 690W (100W), there was little difference in toughness due to changes in specimen orientation or through thickness sampling location.

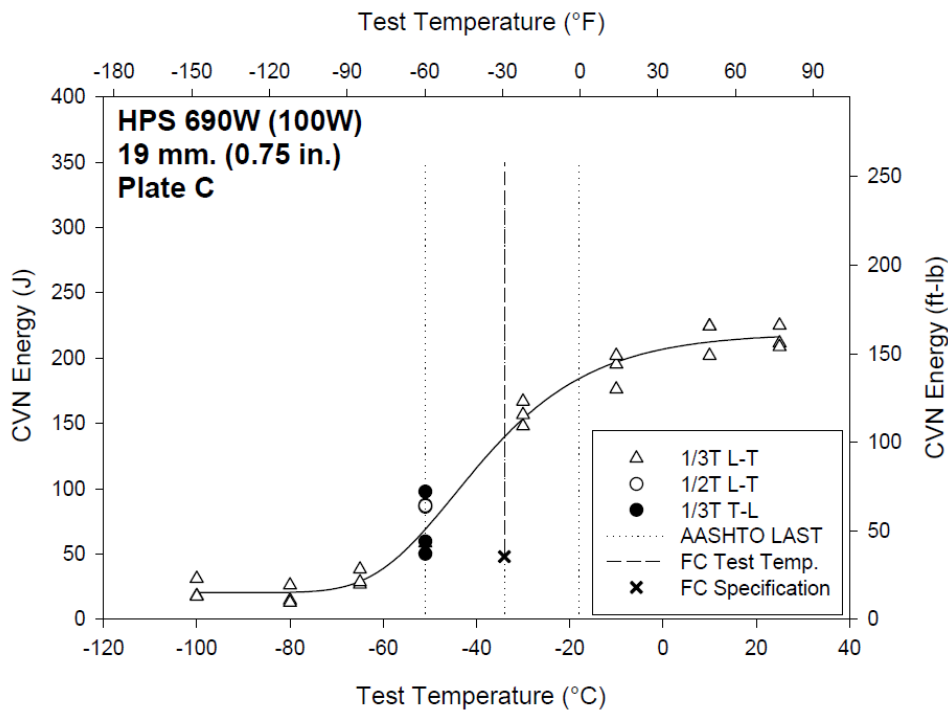


Figure 3-1. CVN Data for Plate C, HPS 690W, 19 mm

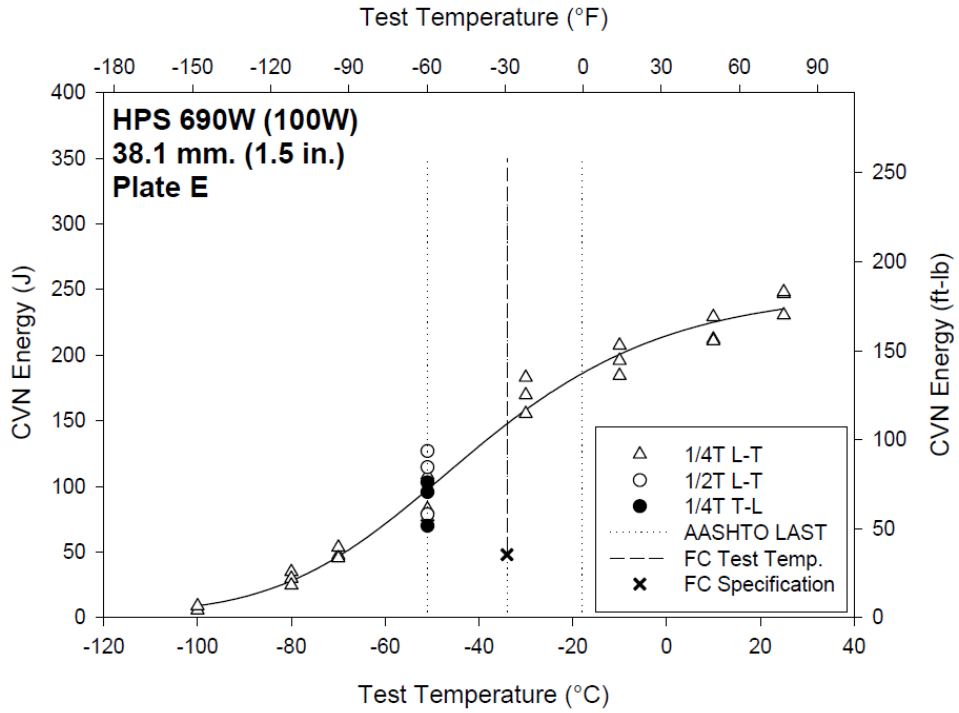


Figure 3-2. CVN Data for Plate E, HPS 690W, 38.1 mm

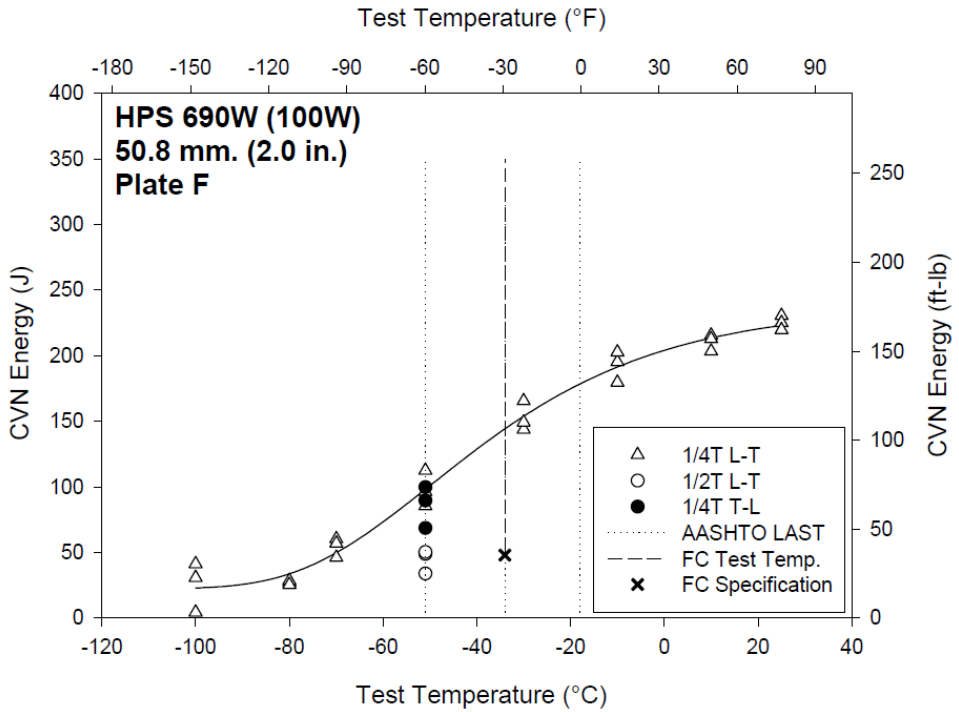


Figure 3-3. CVN Data for Plate F, HPS 690W, 50.8 mm

3.2.2 Charpy V-Notch Impact Toughness of HPS 485W (70W)

The CVN test results of HPS 485W (70W) are presented in Figure 3-4 through Figure 3-8. Specimens machined from 485W (70W) also exhibited toughness much greater than that required in the current fracture critical specification. However, plates A and J did not display typical temperature transition behavior, with no well-defined upper or lower toughness shelves. The lack of clearly defined upper and lower shelf behavior may be due to the fact that specimens were not tested at more extreme temperatures. More testing at both colder and warmer temperatures may have produced data that would allow for the sigmoid fit to exhibit more typical behavior. As the behavior of the steel within service temperature ranges was desired, it was determined further testing at extreme temperatures was not necessary.

The fracture critical toughness test temperature of HPS 485W (70W) is $-23\text{ }^{\circ}\text{C}$ ($-10\text{ }^{\circ}\text{F}$), shown as a vertical dashed line. The required minimum average energy remains at a value of 48 J (35 ft-lbf), represented again by an X. Although more scatter exists in the 485W (70W) data than in the 690W (100W) data, it is clear the toughness at $-23\text{ }^{\circ}\text{C}$ ($-10\text{ }^{\circ}\text{F}$) greatly exceeds the specification requirement. Sigmoidal fit values at the specification test temperature range from 213.5 J (157.5 ft-lbf) for plate A, to 342 J (252 ft-lbf) for plate I, with an average of 278.5 J (205 ft-lbf) for all five plates. Zone III CVN toughness values also greatly exceed the required minimum energy, with average values ranging from 161.5 J (119 ft-lbf) for plate A to 288.5 J (213 ft-lbf) for plate H, and an average of 209 J (154 ft-lbf) across the five plates.

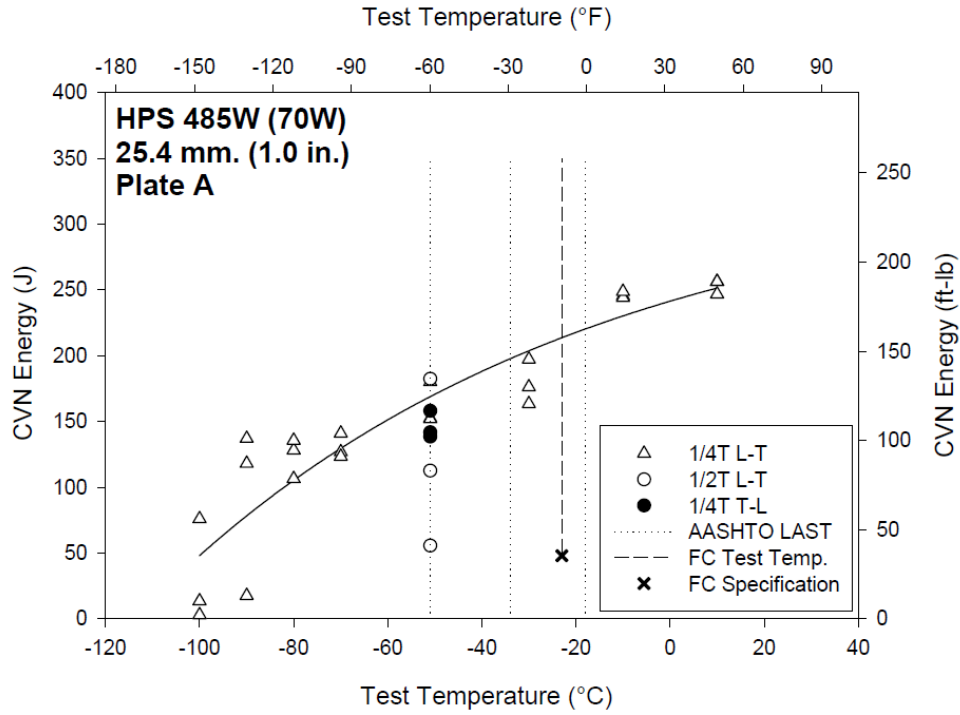


Figure 3-4. CVN Data for Plate A, HPS 485W, 25.4 mm

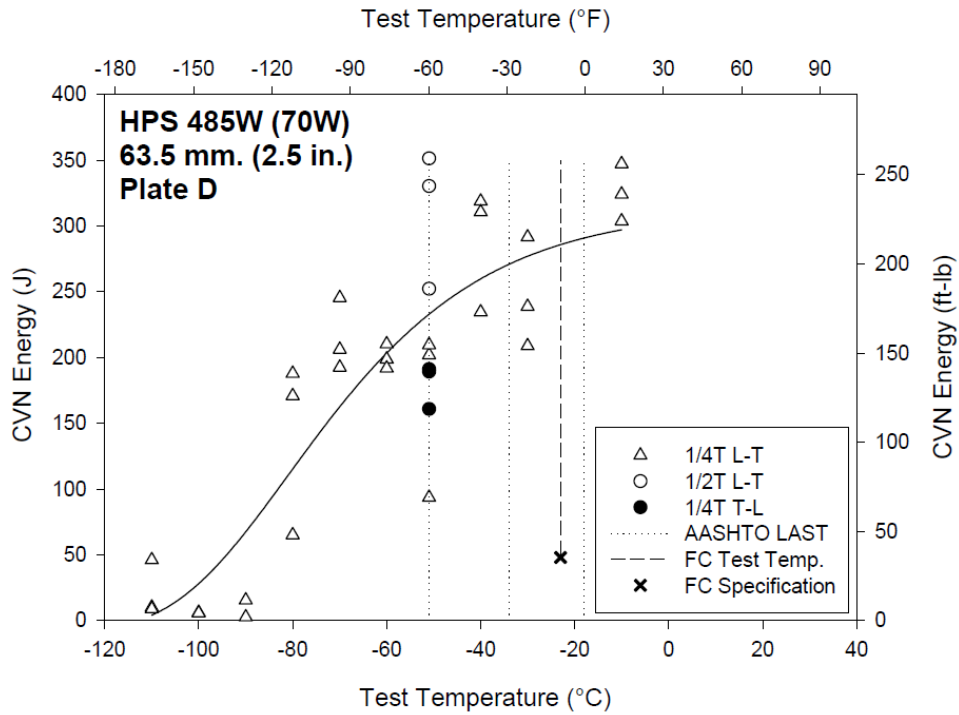


Figure 3-5. CVN Data for Plate D, HPS 485W, 63.5 mm

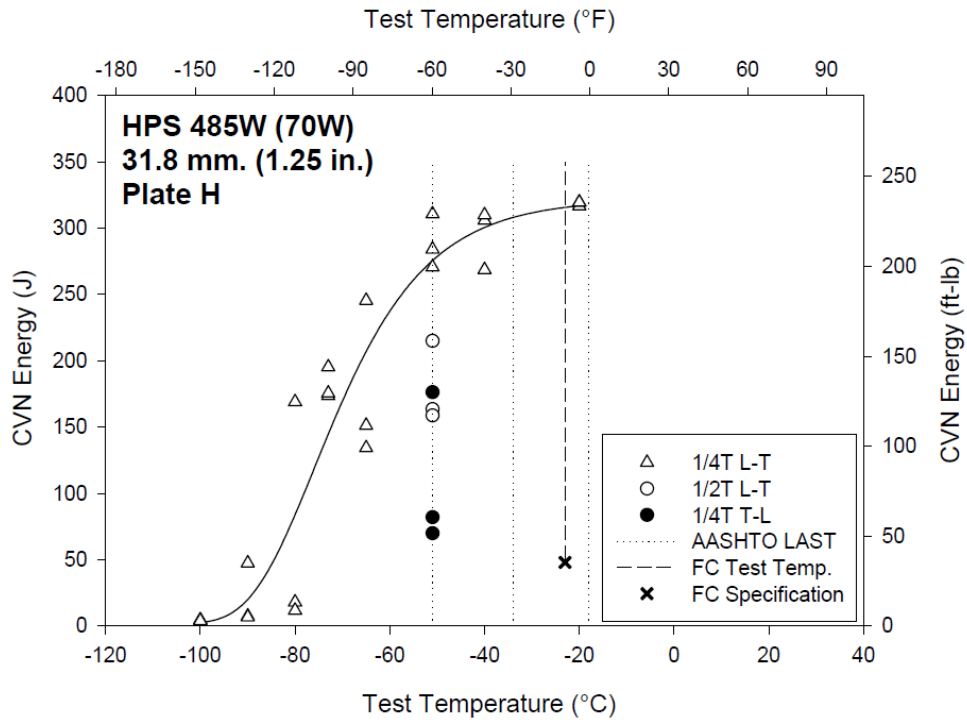


Figure 3-6. CVN Data for Plate H, HPS 485W, 31.8 mm

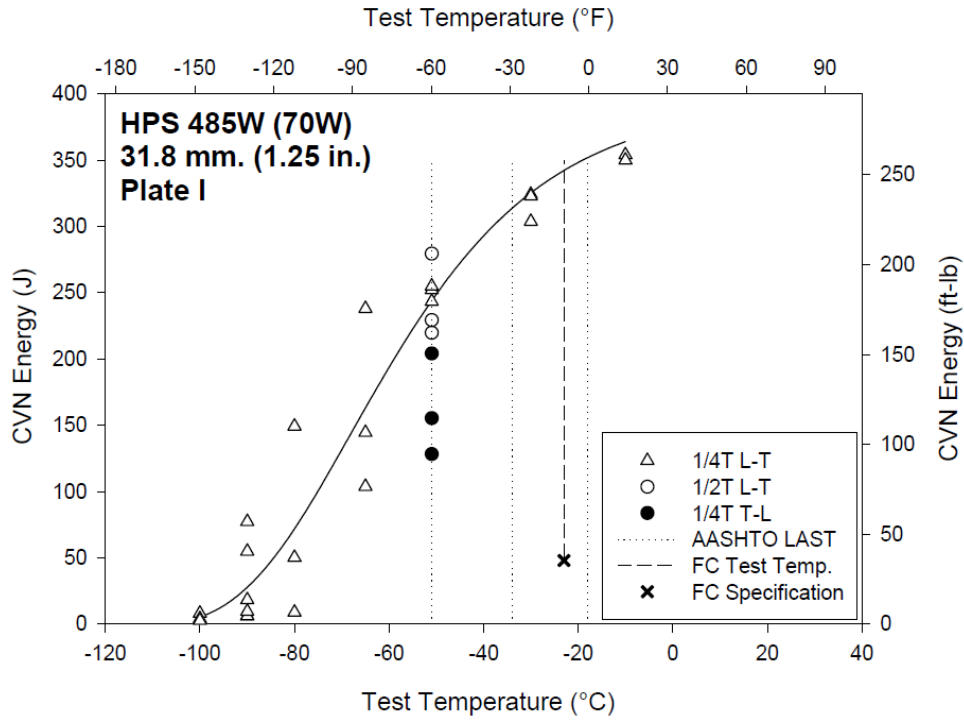


Figure 3-7. CVN Data for Plate I, HPS 485W, 31.8 mm

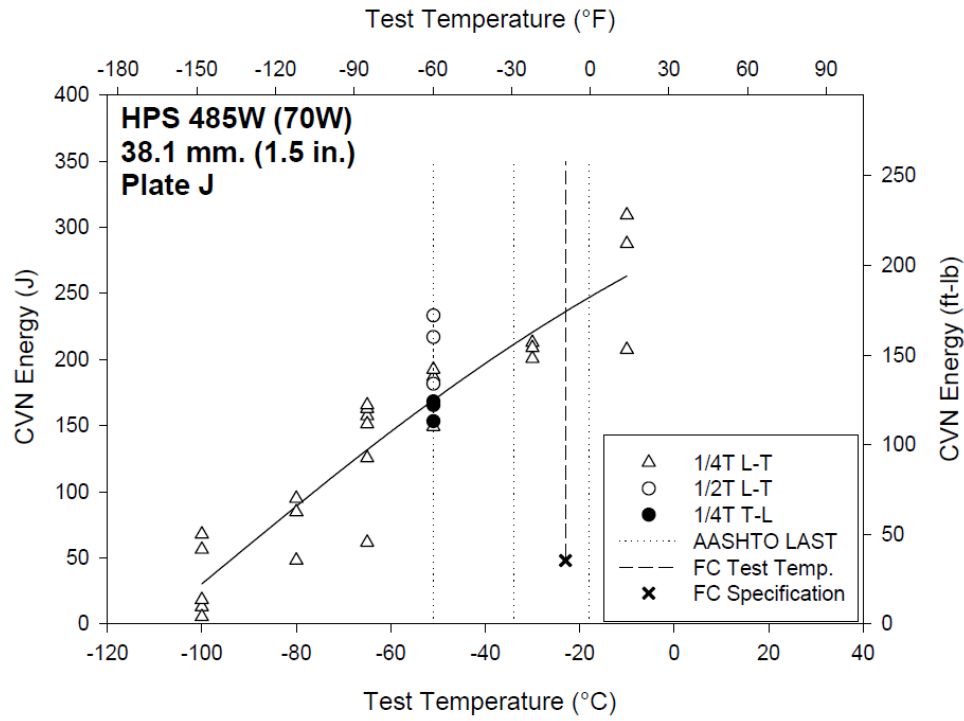


Figure 3-8. CVN Data for Plate J, HPS 485W, 38.1 mm

Examination of HPS 485W (70W) CVN data reveals differences in specimen orientation and through thickness sampling do have an effect on impact energy values when compared with 1/4T L-T specimens; however, the effect is not consistent between plates.

Tabulated results of CVN impact testing for both HPS 690W (100W) and 485W (70W) can be found in Appendix A.

3.3 Static Fracture Toughness Test Results

A total of 114 pre-cracked Charpy-sized SE(B) specimens were prepared from the eight plates of HPS for static fracture toughness testing. The master curve methodology was applied to each data set in order to determine the 1T reference temperature, T_o , of each plate of HPS. Results of these tests are presented in this section, with tabulated data and individual specimen information in Appendix B. Test records and fracture surfaces, although not included in this report, can be found in the dissertation corresponding with this research (Collins 2014).

3.3.1 Static Fracture Toughness of HPS 690W (100W)

The three plates of HPS 690W (100W) have reference temperatures of -80, -102, and -95 °C, for plates C, E, and F, respectively. The average reference temperature is -92 °C (-134 °F), which corresponds to a median 1T fracture toughness of 183 MPa√m (166 ksi√in) at -51 °C (-60 °F). Examination of the master curve tolerance bounds at service temperatures presents expected toughness values with a provided amount of statistical confidence. Material exhibiting a T_o of -92 °C (-134 °F) has 1T toughness values of 105 and 77 MPa√m (96 and 70 ksi√in) at the 5 and 1 per cent tolerance bounds, respectively.

Analysis of all three HPS 690W (100W) data sets resulted in valid reference temperatures with weighting factors greater than 1.0. Size corrected 1T fracture toughness data for HPS 690W (100W) plates C, E, and F are presented in Figure 3-9 through Figure 3-11, along with their median toughness master curve and associated 5 and 95 per cent tolerance bounds. Although presented in these plots, neither uncensored data exceeding the specimen constraint limit or invalid data were used in the calculation of the reference temperature.

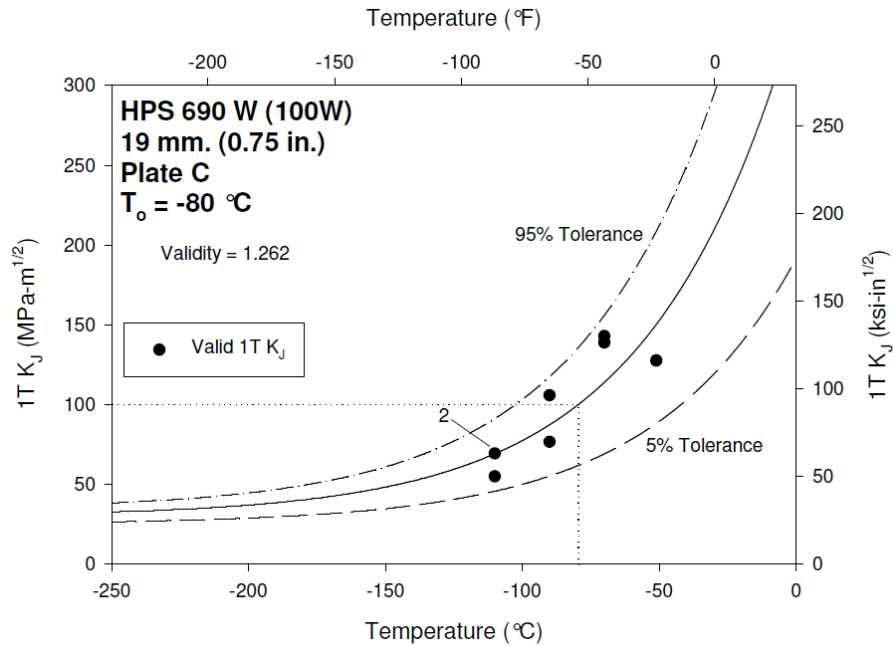


Figure 3-9. Fracture Toughness Data and Master Curve for Plate C, HPS 690W, 19 mm

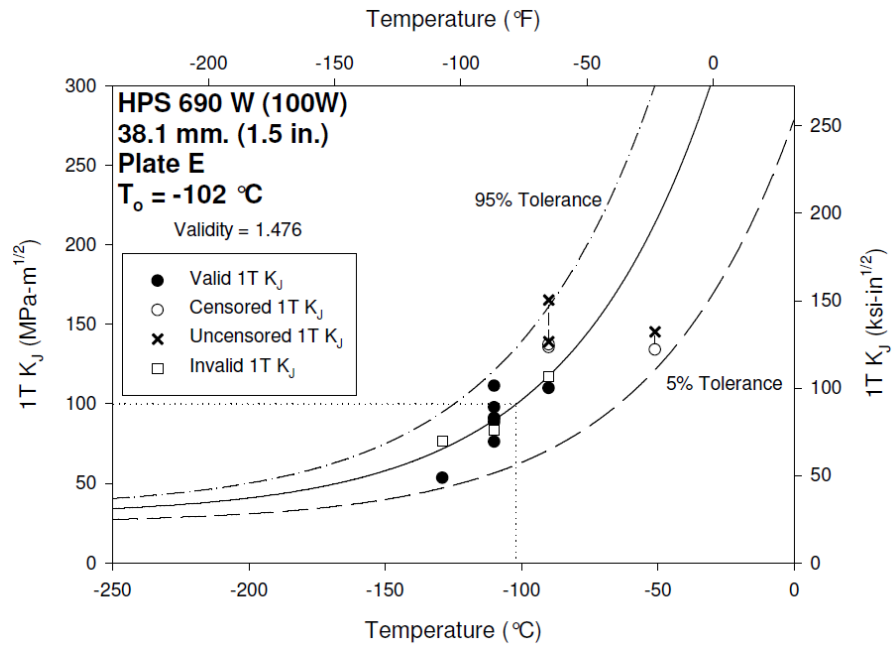


Figure 3-10. Fracture Toughness Data and Master Curve for Plate E, HPS 690W, 38.1 mm

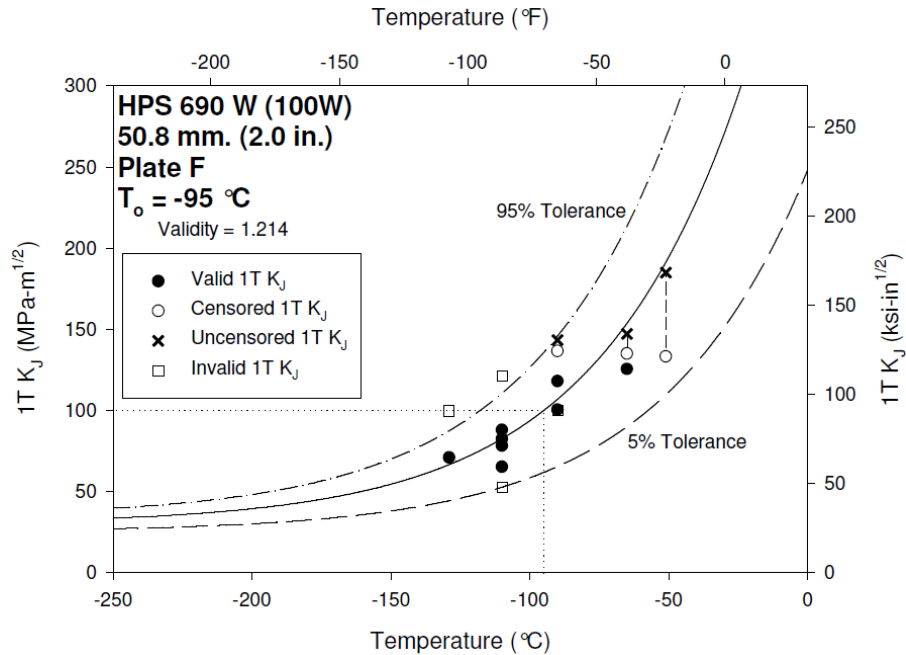


Figure 3-11. Fracture Toughness Data and Master Curve for Plate F, HPS 690W, 50.8 mm

3.3.2 Static Fracture Toughness of HPS 485W (70W)

Master curve evaluation of static fracture toughness data for HPS 485W (70W) yielded extremely low reference temperatures, indicating high toughness at bridge service temperatures. The five plates of HPS 485W (70W) examined yielded 1T reference temperatures ranging from $-134 \text{ }^\circ\text{C}$ ($-209 \text{ }^\circ\text{F}$) for plate J to $-181 \text{ }^\circ\text{C}$ ($-294 \text{ }^\circ\text{F}$) for plate D, with an average value of $-164 \text{ }^\circ\text{C}$ ($-263 \text{ }^\circ\text{F}$). Median fracture toughness values at $-51 \text{ }^\circ\text{C}$ ($-60 \text{ }^\circ\text{F}$) for these reference temperatures range from 369 to 862 MPa $\sqrt{\text{m}}$ (336 to 785 ksi $\sqrt{\text{in}}$). Although ASTM E1921-13 presents no upper bound in the master curve standard, the exponential function is only intended to be representative of fracture behavior on the lower shelf and in the transition region. Therefore, it should be noted materials with extremely low reference temperatures may experience ductile tearing prior to reaching these extremely high median toughness values predicted at much warmer service temperatures. Lower fracture toughness values from tolerance bounds, however, are attainable and can be applied to fracture mechanics problems in design and analysis. The average 1T reference temperature of $-164 \text{ }^\circ\text{C}$ ($-263 \text{ }^\circ\text{F}$) produces 5 and 1 percent fracture toughness values of 339 and 232 MPa $\sqrt{\text{m}}$ (308 and 211 ksi $\sqrt{\text{in}}$), respectively, at $-51 \text{ }^\circ\text{C}$ ($-60 \text{ }^\circ\text{F}$).

Due to an excessive number of specimens fracturing above the master curve censoring limit as well as some invalid tests, plates A and I did not achieve a weighting factor of 1.0. For this reason the reference temperatures of these two plates must be considered conditional, T_{oQ} , and are presented as such. Fracture toughness data of the five HPS 485W (70W) plates, size corrected to 1T, is seen in Figure 3-12 through Figure 3-16, along with the 5 and 95 per cent tolerance bounds. Again, neither invalid data points nor uncensored data violating the size dependent constraint limit were included in the reference temperature calculation.

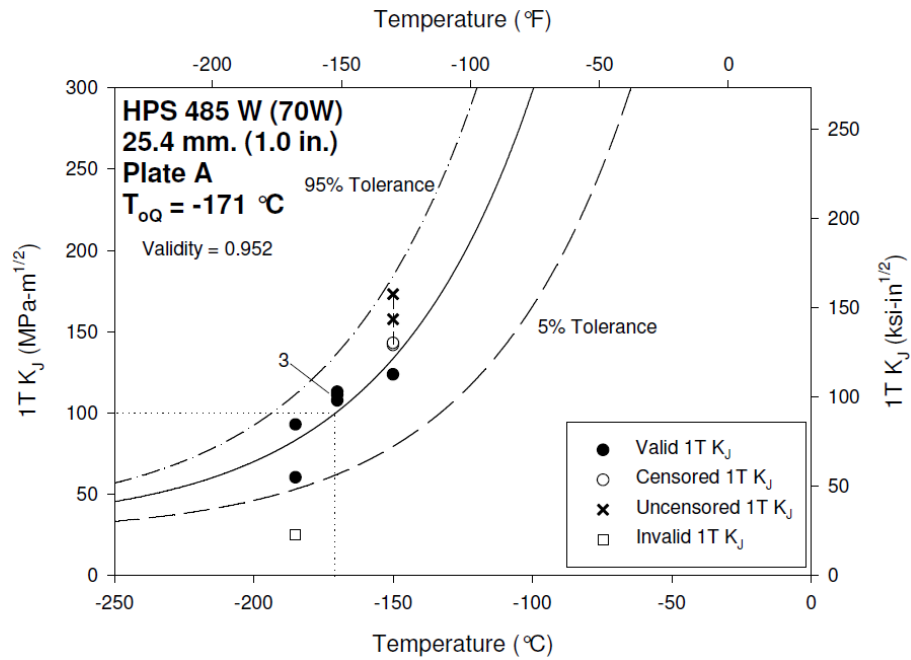


Figure 3-12. Fracture Toughness Data and Master Curve for Plate A, HPS 485W, 25.4 mm

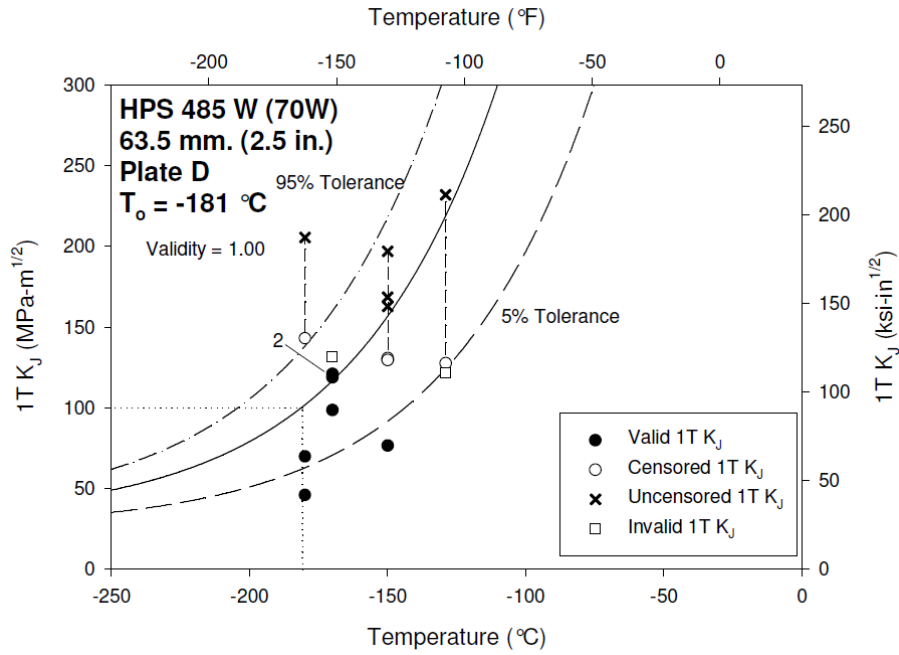


Figure 3-13. Fracture Toughness Data and Master Curve for Plate D, HPS 485W, 63.5 mm

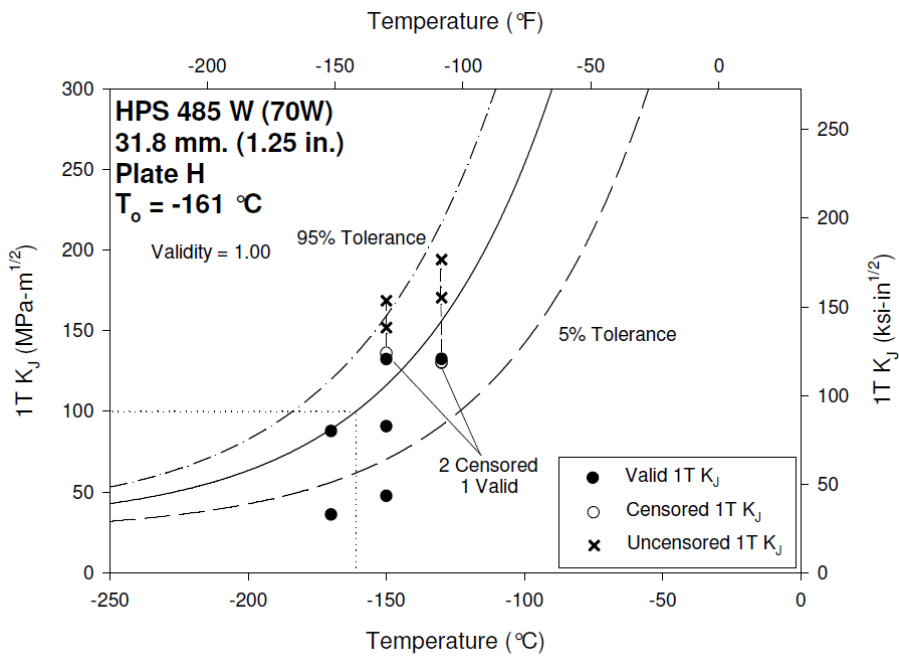


Figure 3-14. Fracture Toughness Data and Master Curve for Plate H, HPS 485W, 31.8 mm

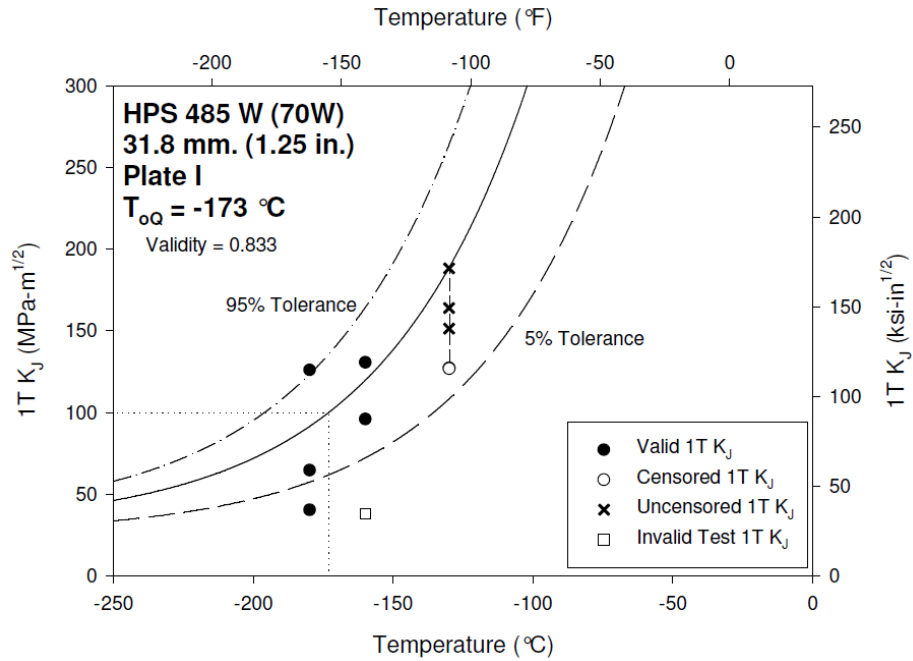


Figure 3-15. Fracture Toughness Data and Master Curve for Plate I, HPS 485W, 31.8 mm

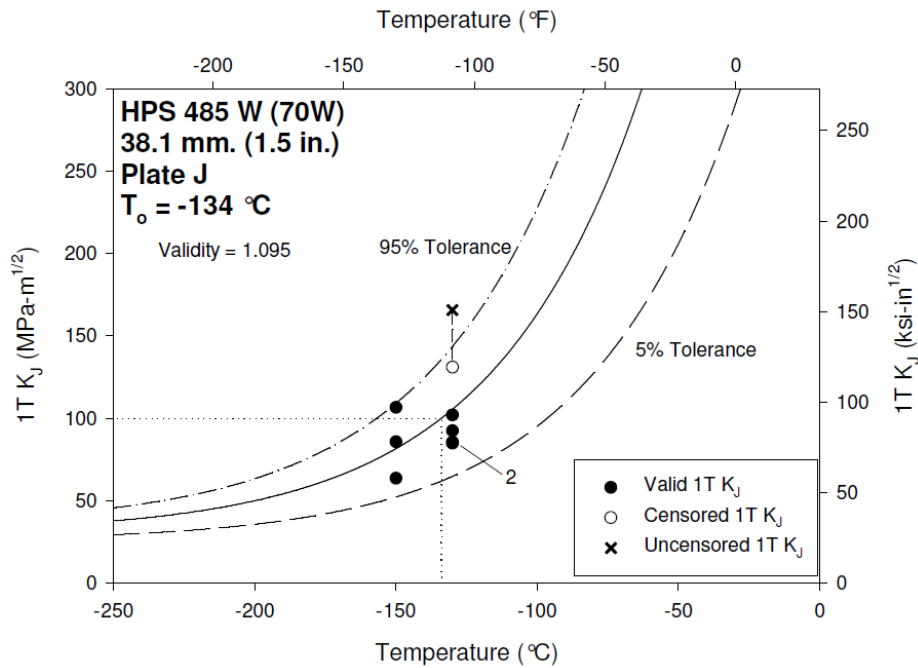


Figure 3-16. Fracture Toughness Data and Master Curve for Plate J, HPS 485W, 38.1 mm

3.4 Dynamic Fracture Toughness Test Results

Following the same procedures used for static fracture toughness testing, all eight plates of HPS 690W (100W) and HPS 485W (70W) were examined at dynamic test rates. Although all dynamic tests were performed at the fastest attainable rate of the servo-hydraulic test frame being used, final stress intensity rate is a function of critical fracture toughness value. In general, higher toughness specimens take longer to break than specimens exhibiting low toughness. Although final stress intensity rates ranged from 1000 to 5000 MPa√m/sec (910 to 4550 ksi√in/sec), all rates are simply designated as dynamic because they are of the same order of magnitude. This grouping of dynamic rates by order of magnitude is addressed in ASTM E1921-13. In this report dynamic reference temperatures are designated by $T_{o,Dyn}$. Dynamic HPS fracture toughness data is tabulated in Appendix C. Test records and fracture surface images for the dynamic fracture toughness testing can be found in the dissertation by Collins (2014).

3.4.1 Dynamic Fracture Toughness of HPS 690W (100W)

The three plates of HPS 690W (100W) have reference dynamic temperatures of -51, -54, and -57 °C, for plates C, E, and F, respectively. The average reference temperature is -54 °C (-65 °F). Examination of the master curve tolerance bounds at service temperatures presents expected toughness values with a provided amount of statistical confidence. Material exhibiting a T_o of -54 °C (-65 °F) has 1T toughness values of 64 and 49 MPa√m (58 and 45 ksi√in) at the 5 and 1 per cent tolerance bounds, respectively.

Presented in Figure 3-17 through Figure 3-19 are the 1T size corrected dynamic fracture toughness datum and resulting master curves and tolerance bounds for Plates C, E, and F. Analysis of all three HPS 690W (100W) data sets resulted in valid reference temperatures with weighting factors greater than 1.0. Although presented in these plots, neither uncensored data exceeding the specimen constraint limit or invalid data were used in the calculation of the reference temperature.

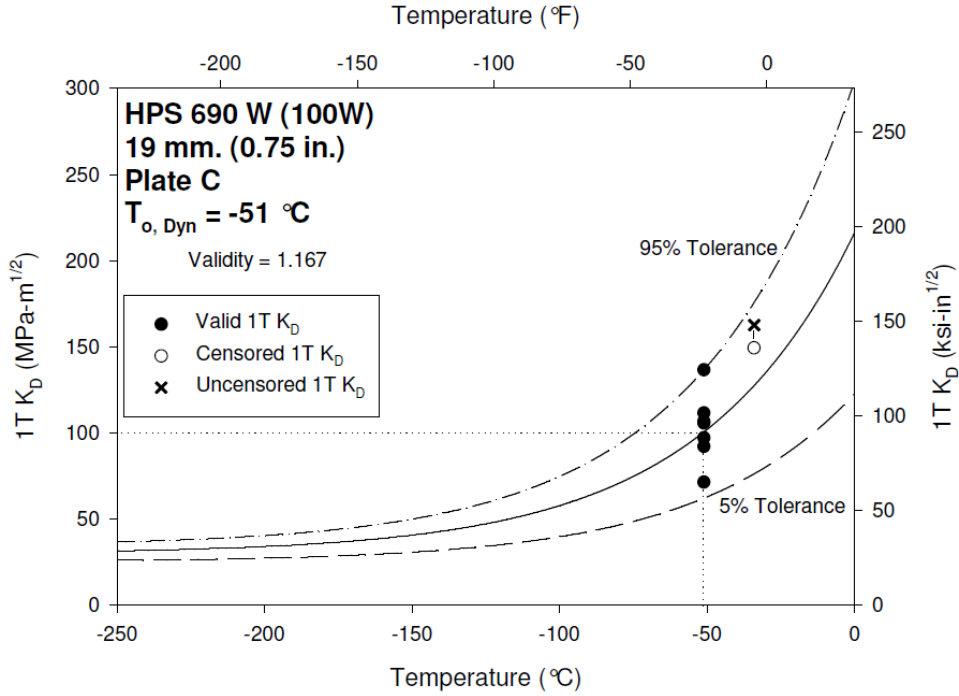


Figure 3-17. Dynamic Fracture Toughness Data and Master Curve for Plate C

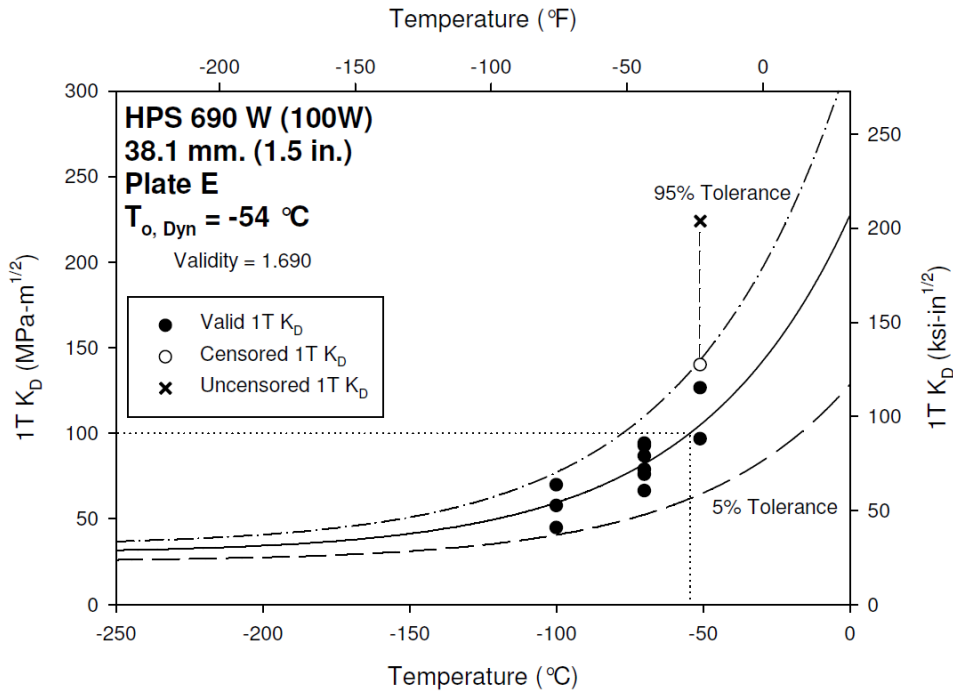


Figure 3-18. Dynamic Fracture Toughness Data and Master Curve for Plate E

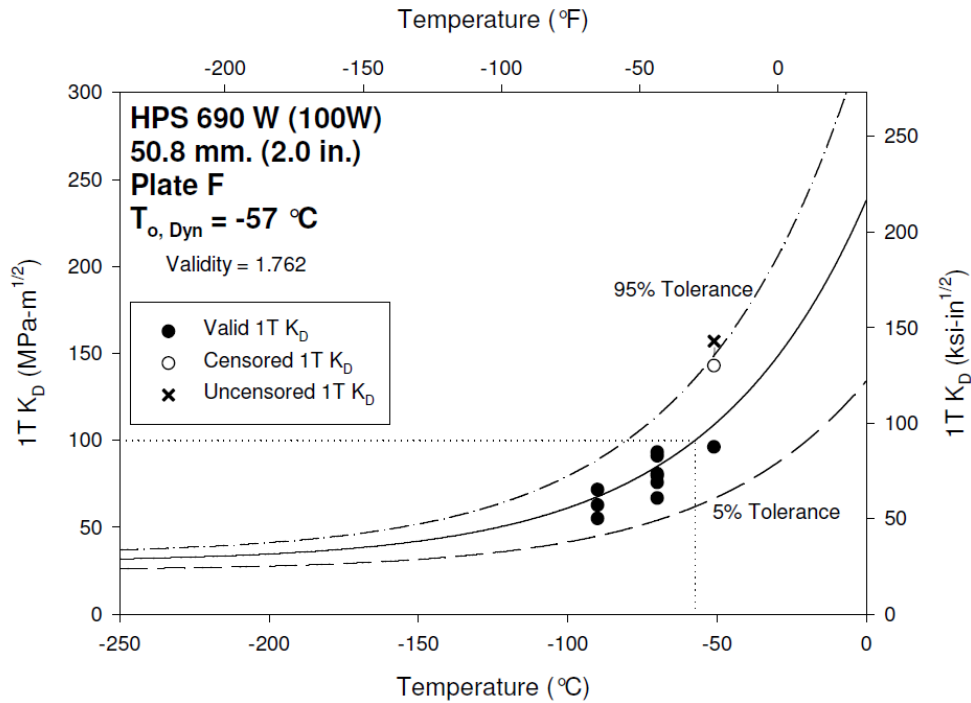


Figure 3-19. Dynamic Fracture Toughness Data and Master Curve for Plate F

3.4.2 Dynamic Fracture Toughness of HPS 485W (70W)

Determination of dynamic reference temperatures for HPS 485W (70W) proved to be difficult. Values of $T_{o, Dyn}$ were not nearly as consistent between plates of HPS 485W (70W) as was seen in the HPS 690W (100W) data. Dynamic 1T reference temperatures varied from -61 to -119 °C (-78 to -182 °F) for the five plates. Difficulty in obtaining valid test results at dynamic rates resulted in invalid reference temperatures, with weighting validity values of less than 1.0. Discrepancies even arose for data with valid reference temperature calculations, seemingly due to limit censored values.

Test specimens machined from HPS 485W (70W) plate A were tested dynamically at temperatures of -100 and -120 °C (-148 and -184 °F). The resulting dynamic reference temperature of the plate was determined to be -113 °C (-171 °F), with a weighting validity factor of 1.50. Figure 3-20 presents the dynamic fracture toughness of plate A, along with the corresponding master curve and 5 and 95 per cent tolerance bounds. Similar to the static analyses, invalid test data are plotted for reference only, and were not used in the calculation of the reference temperature.

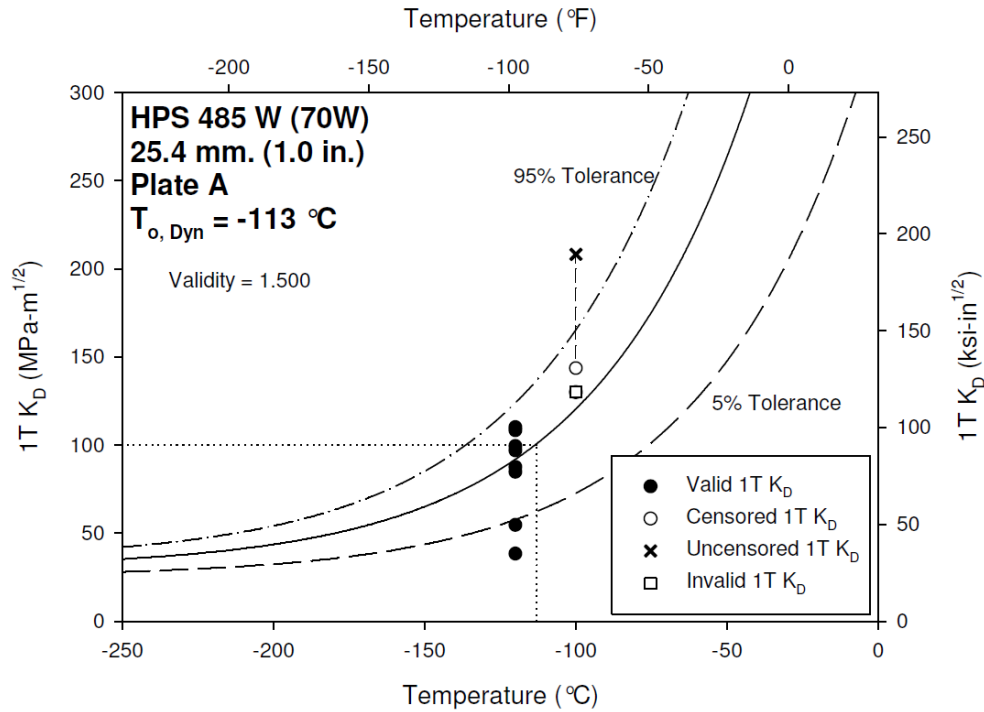


Figure 3-20, Dynamic Fracture Toughness Data and Master Curve for Plate A

Dynamic toughness testing of plate D produced interesting results. Multiple specimens violated the toughness limit resulting in the insertion of censored data. However, in spite of these specimens attaining high toughness values, other tests at the same temperatures resulted in much lower values. Master curve analysis of this data set yielded a dynamic 1T reference temperature of $-111 \text{ } ^\circ\text{C}$ ($-168 \text{ } ^\circ\text{F}$) with a weighting validity factor of 1.619. This would indicate a valid reference temperature. However, visual inspection of the data and master curve, as shown in Figure 3-21, indicates that censored values dominate the determination of $T_{o, Dyn}$, causing the master curve to unconservatively over predict dynamic fracture toughness values.

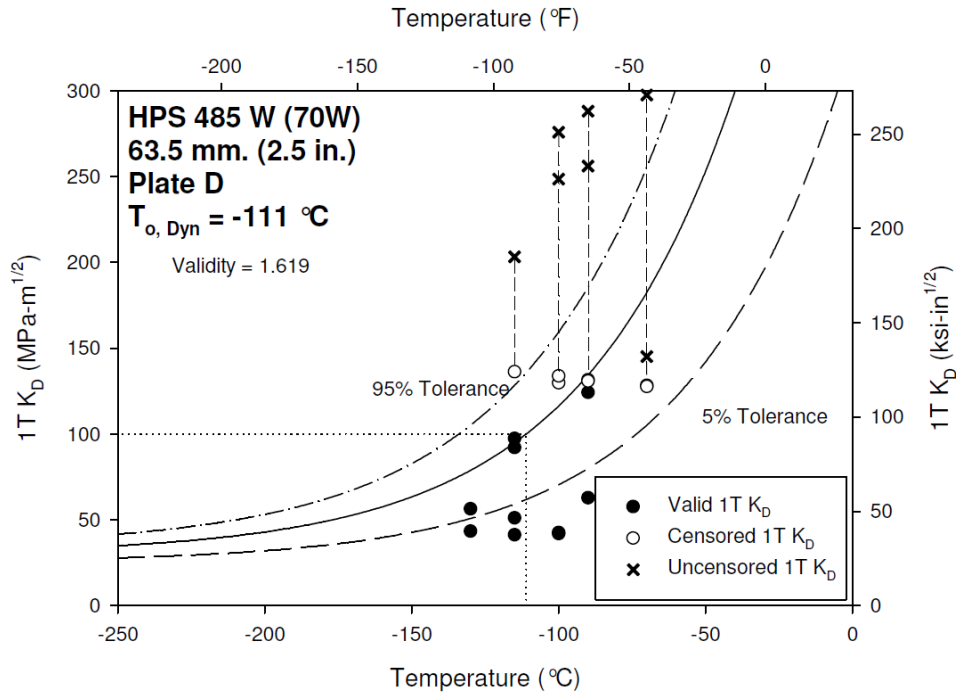


Figure 3-21. Dynamic Fracture Toughness Data and Master Curve for Plate D

If the data set is re-analyzed ignoring the censored values, a new 1T dynamic reference temperature is calculated, which seems to better capture the valid data. This analysis produces a dynamic reference temperature of $-86 \text{ } ^\circ\text{C}$ ($-123 \text{ } ^\circ\text{F}$) and a validity weighting value of 1.440. This analysis, results of which are shown if Figure 3-22, is not in accordance with ASTM E1921-13, although it does seem to better represent fracture behavior than the previous analysis.

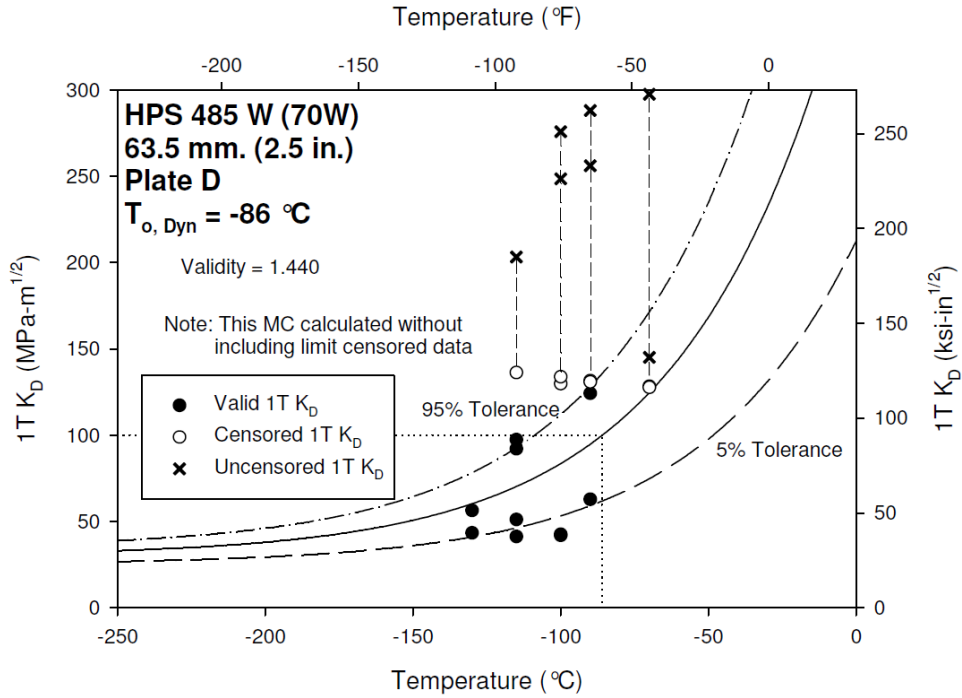


Figure 3-22. Dynamic Fracture Toughness Data and Alternate Master Curve for Plate D

Analysis of dynamic fracture toughness data for both plates H and I resulted in similar scenario to that of plate D. The original analysis of dynamic fracture toughness data for HPS 485W (70W) plate H resulted in a provisional 1T dynamic reference temperature of $-105 \text{ }^\circ\text{C}$ ($-157 \text{ }^\circ\text{F}$), with a validity factor of 0.881. Ignoring censored values in an alternative master curve analysis results in a dynamic reference temperature of $-84 \text{ }^\circ\text{C}$ ($-119 \text{ }^\circ\text{F}$) and a validity factor of 0.857. Test data for plate H and resulting master curves of each analysis method can be seen in Figure 3-23 and Figure 3-24.

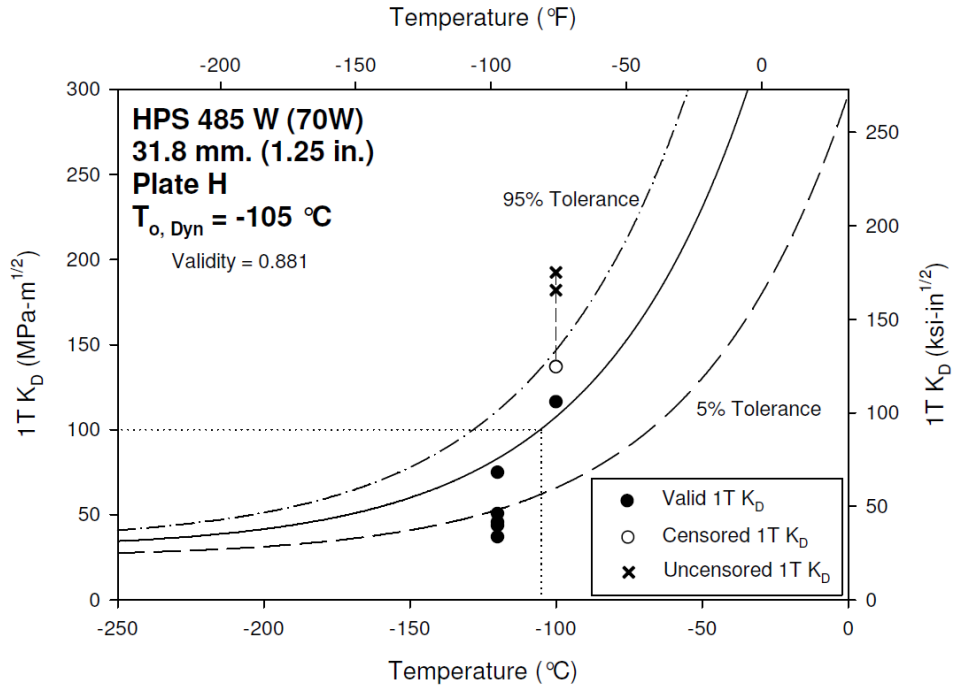


Figure 3-23. Dynamic Fracture Toughness Data and Master Curve for Plate H

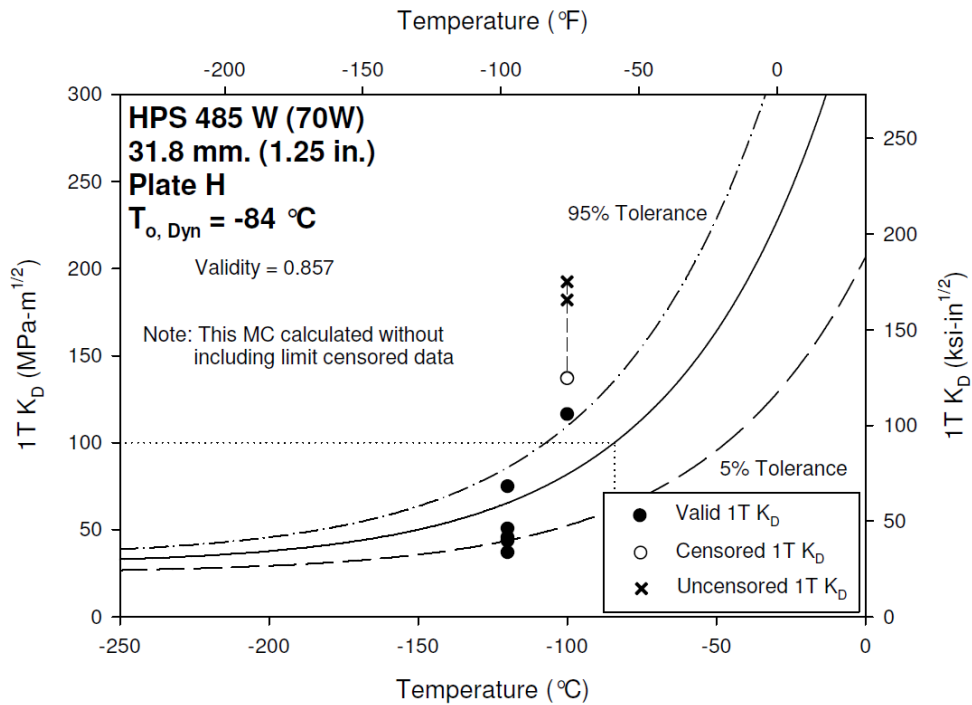


Figure 3-24. Dynamic Fracture Toughness Data and Alternate Master Curve for Plate H

The initial analysis of plate I dynamic fracture toughness data results in a provisional 1T dynamic reference temperature of $-119\text{ }^{\circ}\text{C}$ ($-182\text{ }^{\circ}\text{F}$) with a weighted validity factor of 0.643. An alternate analysis of dynamic reference temperature without using limit censored data results in a $T_{o, \text{Dyn}}$ value of $-69\text{ }^{\circ}\text{C}$ ($-92\text{ }^{\circ}\text{F}$), which visually appears to better represent the valid data than the previous analysis. In this alternate analysis, the weighted validity factor is only 0.286, however, due to the fact that two of the valid tests were performed at temperatures more than $50\text{ }^{\circ}\text{C}$ from the calculated reference temperature. Plate I dynamic fracture toughness data and the two different master curve analyses are presented in Figure 3-25 and Figure 3-26.

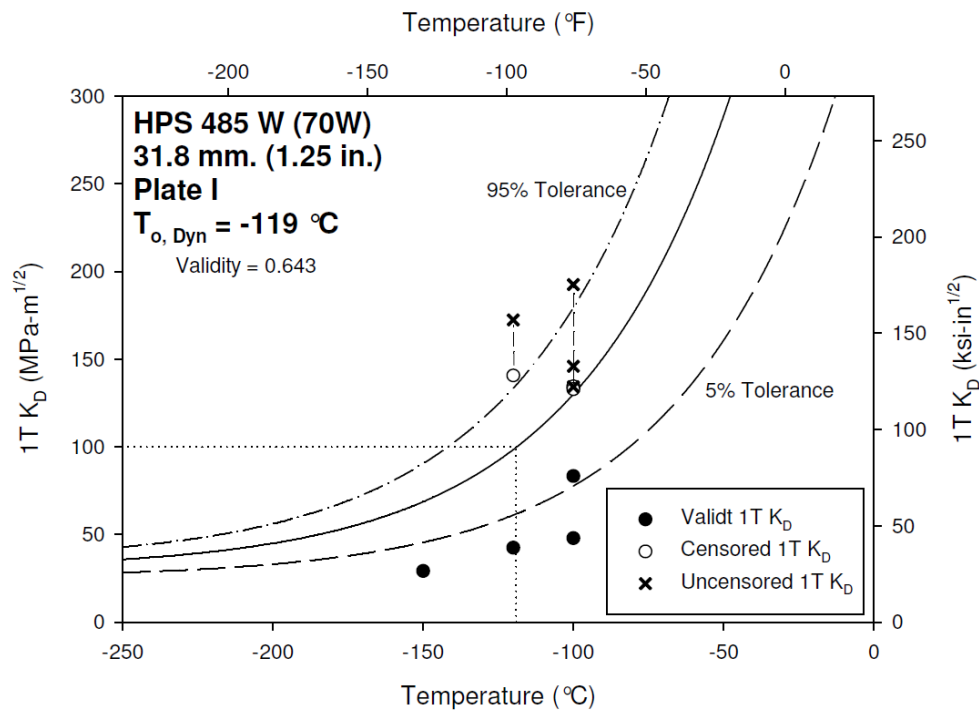


Figure 3-25. Dynamic Fracture Toughness Data and Master Curve for Plate I

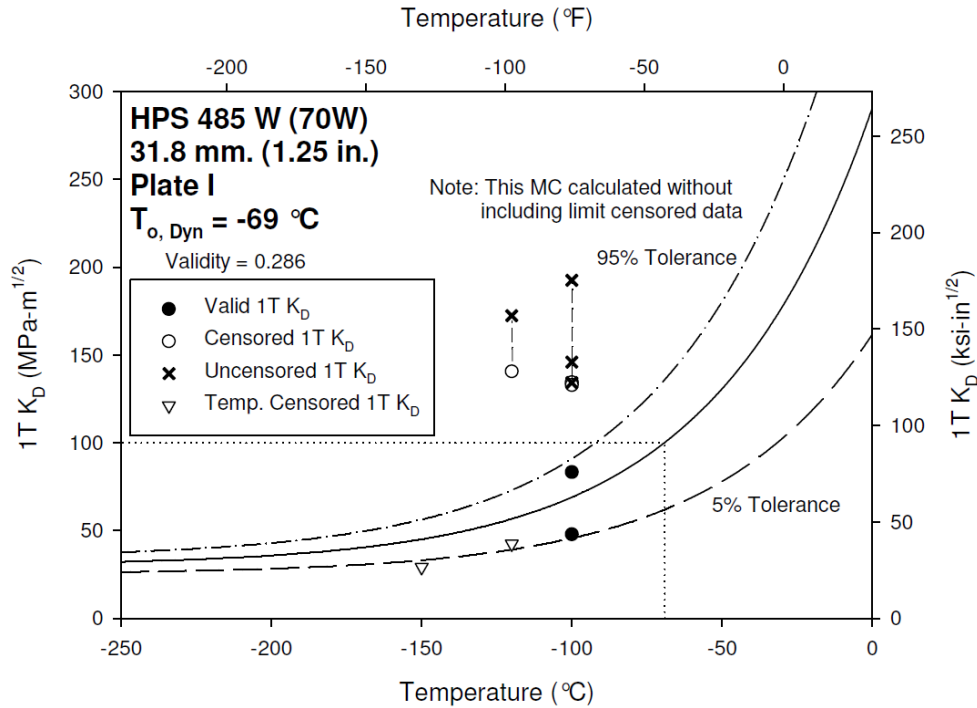


Figure 3-26. Dynamic Fracture Toughness Data and Alternate Master Curve for Plate I

Test specimens from HPS 485W (70W) plate J were tested dynamically over a range of temperatures between -70 and -100 °C (-94 and -148 °F). Fracture toughness values led to the determination of a 1T dynamic reference temperature equal to -61 °C (-78 °F) with a weighted validity value of 1.196. As seen in Figure 3-27, this analysis seems to properly characterize dynamic fracture behavior, with the 5 and 95 per cent tolerance thresholds bounding the data.

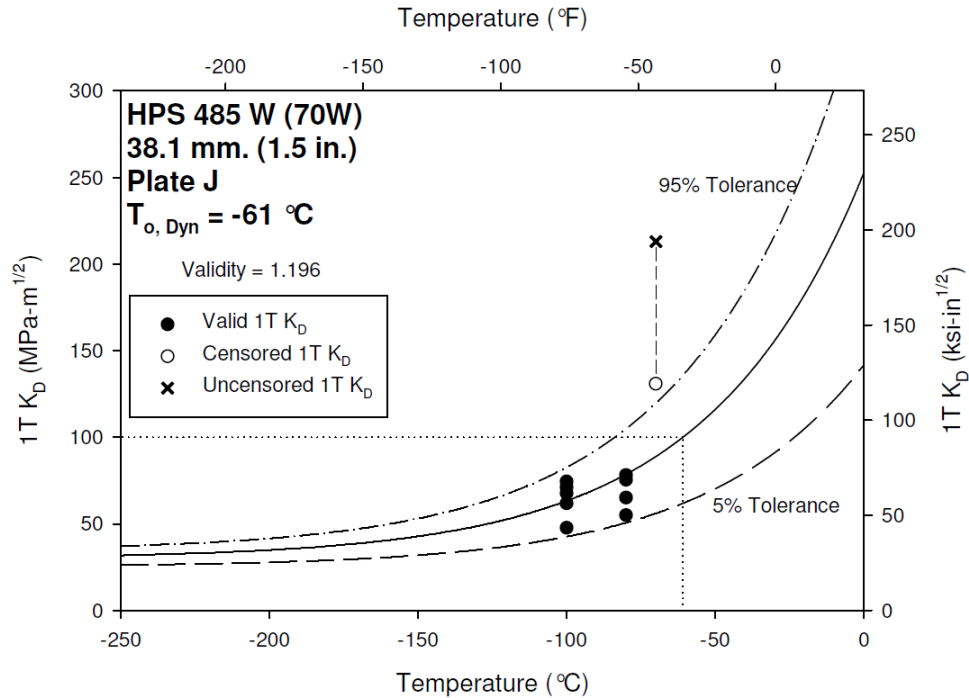


Figure 3-27. Dynamic Fracture Toughness Data and Master Curve for Plate J

3.5 Crack Arrest Toughness Test Results

A total of 55 crack arrest specimens were fabricated from plates D, E, and F. Of these, only 41 specimens fractured during testing, and only 10 of these produced valid crack arrest toughness, K_{Ia} , values. For the majority of specimens for which fracture initiation occurred, the specimen was unable to arrest the propagating crack, leaving only a small remaining ligament intact. Other specimens were able to stop crack propagation, but arrested crack lengths proved to be too long for validity purposes. Unlike invalid fracture initiation toughness, it is difficult to glean any information from invalid arrest tests. This is due to the large amounts of plasticity preceding the crack, reduced crack driving force, and reflective stress waves occurring in the fracturing specimen. The effects of these factors are not currently well understood. For this reason, only data meeting all ASTM E1221-12 validity criteria will be presented herein. Tabulated specimen information for valid tests can be found in Appendix D. Specimen information for invalid test specimens exhibiting some amount of arrest toughness can also be found in Appendix D. Test records and images of specimen fracture surfaces are provided by Collins (2014).

3.5.1 Crack Arrest Toughness of HPS 690W (100W)

For the two plates of HPS 690W (100W), only five crack arrest tests proved to be valid. Plate E produced valid tests at test temperatures of -35 and -50 °C (-31 and -58 °F), while plate F produced two valid tests at -35 °C (-31 °F) and one at -20 °C (-4 °F). Plates E and F produced provisional crack arrest reference temperatures, $T_{K_{IaQ}}$, of -7 and -1 °C (19 and 30 °F), respectively. Clearly neither of these data sets produced a validity weighting factor greater than one. Crack arrest data, along with the provisional master curves, can be seen in Figure 3-28 and Figure 3-29. Unlike tolerance bounds for initiation toughness, which are statistically based off of the master curve itself due to flaw distribution probability, crack arrest tolerance bounds are determined by the scatter of test data. For this reason, and the lack of valid tests, tolerance bounds are not provided for the crack arrest master curves.

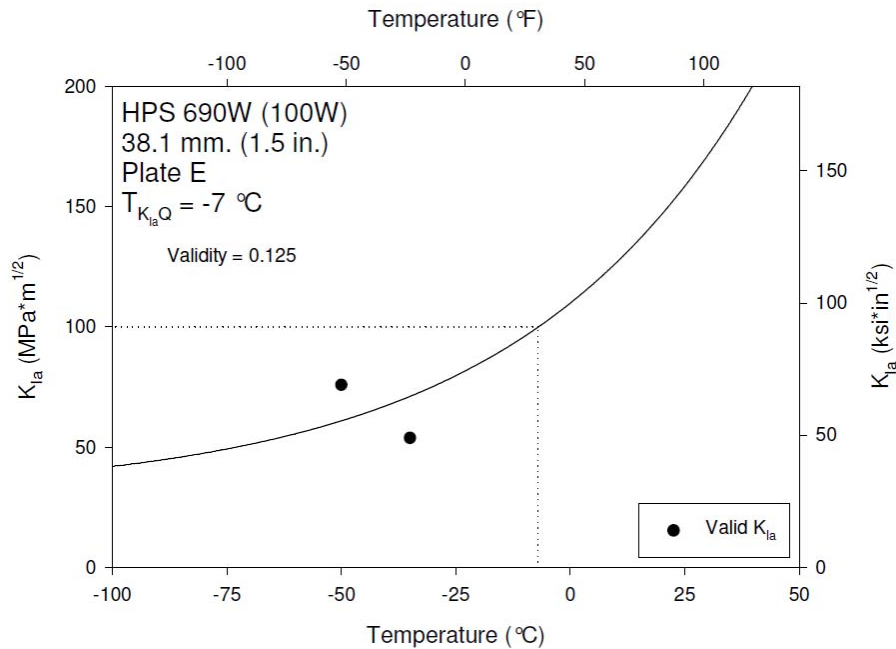


Figure 3-28. Crack Arrest Toughness Data and Master Curve for Plate E

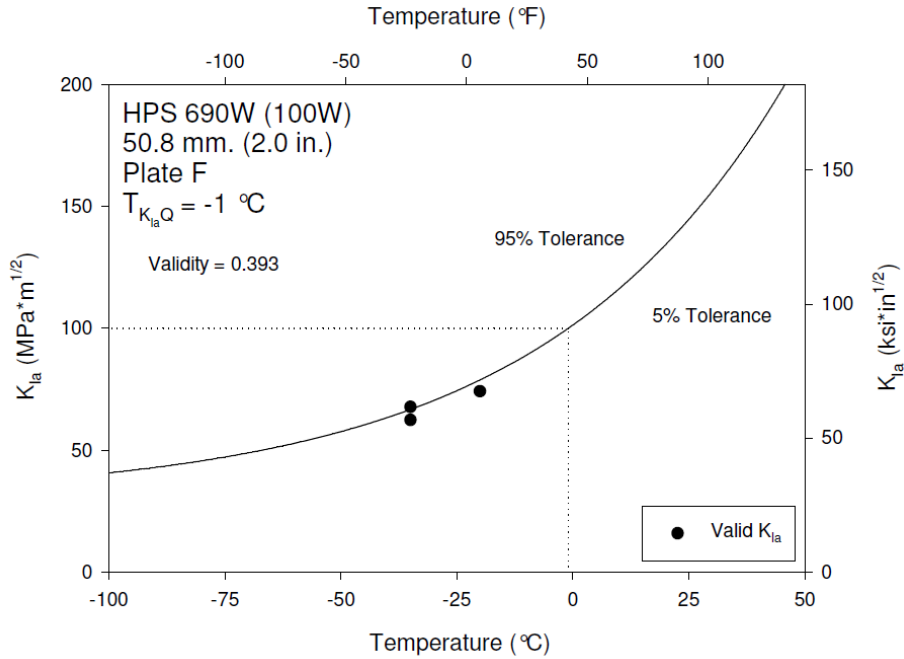


Figure 3-29. Crack Arrest Toughness Data and Master Curve for Plate F

3.5.2 Crack Arrest Toughness of HPS 485W (70W)

HPS 485W (70W) plate D produced five valid crack arrest test values. Two valid tests were performed at a test temperature of -50 °C (-58 °F), while the other three valid tests were performed at -35 °C (-31 °F). These five valid crack arrest tests resulted in a provisional crack arrest reference temperature of -2 °C (28 °F), with a validity factor of 0.557. Plate D crack arrest toughness data and corresponding master curve are presented in Figure 3-30.

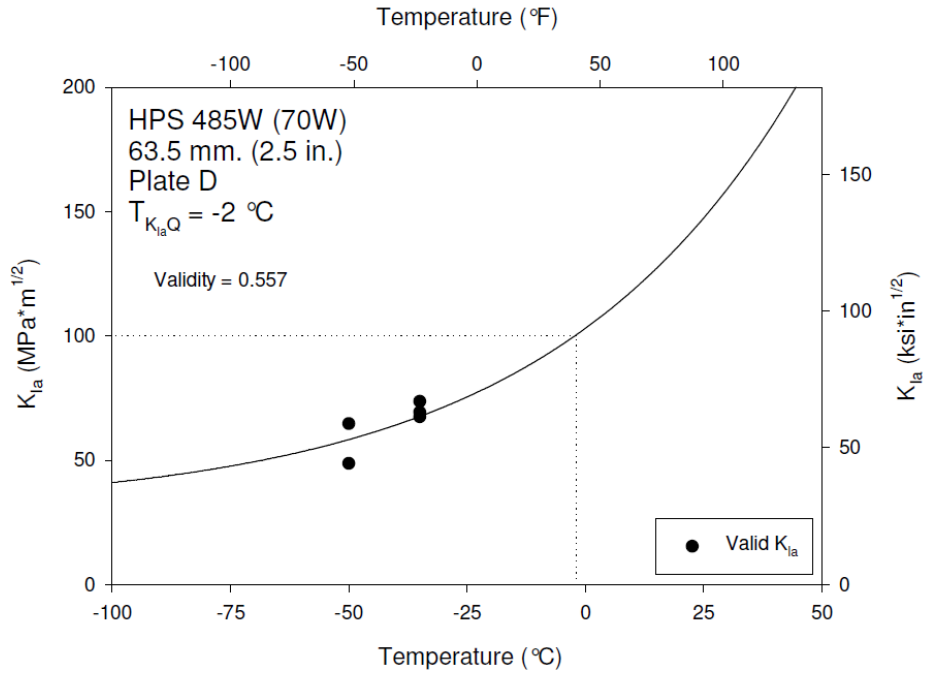


Figure 3-30. Crack Arrest Toughness Data and Master Curve for Plate D

4. SUMMARY AND CONCLUSIONS

Many advances have taken place in the four decades since the inception of AASHTO's original fracture control plan. Specifically, steel production and fabrication have made high performance materials much more economically feasible for the bridge industry. Also, advances in the understanding of elastic-plastic fracture mechanics have made possible the characterization of materials with high toughness and ductility, including structural steel. Consequently, this research has focused on the fracture behavior characterization of modern HPS grade steels. Presented herein is a summary of the findings of this report, as well as conclusions drawn from these findings.

4.1 Summary

Fracture toughness testing was performed on eight different plates A709 HPS 690W (100 W) and 485W (70W). Each plate was characterized with regards to CVN impact energy, static fracture initiation toughness, and dynamic fracture initiation toughness. Additionally, crack arrest toughness testing was performed on three of the plates.

All CVN testing followed ASTM E23-07, and fracture initiation testing, both static and dynamic, was performed in accordance with ASTM E1921-13, while crack arrest toughness testing followed ASTM E1221-12 (ASTM 2007, 2013, 2012). All specimens were oriented in the L-T direction, with fractures propagating perpendicular to plate rolling direction. Specimens were sampled from the plates centered at one-quarter of the thickness. The exception to this was plate C, where thickness of the plate did not allow for this practice, and specimens were sampled centered at one-third of the thickness.

The master curve methodology was used to characterize all fracture toughness data (static, dynamic, and arrest toughness), resulting in 1T reference temperature determinations for each plate. These reference temperature values are summarized in

Table 4-1. It should be noted that there is no distinction made between valid and provisional reference temperatures in this table. Additionally, the plates for which dynamic reference temperature evaluation resulted in multiple values, the more conservative of the two values is presented, again with no distinction between valid and provisional.

Table 4-1. Summary of Static, Dynamic, and Arrest Reference Temperatures

Letter Designation	Grade, MPa (ksi)	T ₀ , °C (°F)	T _{0, Dyn} , °C (°F)	T _{KIa} , °C (°F)
A	485 (70)	-171 (-276)	-113 (-171)	N/A
C	690 (100)	-80 (-112)	-51 (-60)	N/A
D	485 (70)	-181 (-294)	-86 (-123)	-2 (28)
E	690 (100)	-102 (-152)	-54 (-65)	-7 (19)
F	690 (100)	-95 (-139)	-57 (-71)	-1 (30)
H	485 (70)	-161 (-258)	-84 (-119)	N/A
I	485 (70)	-173 (-279)	-69 (-92)	N/A
J	485 (70)	-134 (-209)	-61 (-78)	N/A

4.2 Conclusions

The main conclusions from the findings of this study are presented herein. It should be noted that the results of this testing are only a part of TPF-5(238), and more substantial findings and conclusions will be drawn at the completion of full-scale girder testing. The data presented in this report are meant to complement and be used in conjunction with results of full-scale girder testing currently being conducted at Purdue University.

- Both HPS 690W (100W) and 485W (70W) display CVN impact energies significantly higher than that required in ASTM A709-13 for fracture critical components.
- Although this is a small sample size, it is apparent that HPS is being produced that readily and substantially surpasses current impact energy requirements.
- Static reference temperatures for HPS are extremely low, significantly below bridge service temperatures. Following master curve tolerance bounds, this results in very high fracture initiation toughness, even when low failure probabilities are selected.
- Extremely low reference temperatures require extremely low test temperatures, making testing of HPS to obtain reference temperature determination difficult.
- Additionally, data at such low temperatures forces reliance on extrapolation of the master curve to obtain fracture toughness values at bridge service temperatures. For this reason it is thought that examination of toughness at test temperatures approaching service temperatures may be a more reasonable approach. The high toughness and ductility displayed by HPS indicates that the use of ductile tearing fracture parameters, such as J_{IC} or CTOD, may need to be employed.

- Dynamic reference temperatures for HPS are more difficult to obtain due to loss of specimen constraint at high test rates. However, data indicates that dynamic reference temperature values are still consistently at or below service temperatures for all grades examined.
- The effect of loading rate is clearly evident when examining the results of static and dynamic fracture initiation testing. As seen in the difference in reference temperature values, this effect can be represented by a temperature shift.
- Crack arrest toughness testing proved to be extremely difficult, resulting in very little usable data. Although HPS grade steels may have the ability to arrest running fractures, the state of testing standards and low validity success rate makes more arrest testing unfeasible at this point in time.

REFERENCES

American Society for Testing and Materials (ASTM). (2007), "Standard Specification for Sampling Procedure for Impact Testing of Structural Steel." A673-07, West Conshohocken, Pa.

American Society for Testing and Materials (ASTM). (2013), "Standard Specification for Structural Steel for Bridges" A 709-13, West Conshohocken, Pa.

American Society for Testing and Materials (ASTM). (2007), "Standard Test Methods for Notched Bar Impact Testing of Metallic Materials." E23-07, West Conshohocken, Pa.

American Society for Testing and Materials (ASTM). (2013), "Standard Test Method for Determination of Reference Temperature, T_o , for Ferritic Steels in the Transition Range" E1921-13, West Conshohocken, Pa.

American Society for Testing and Materials (ASTM). (2008), "Standard Test Method for Fracture Toughness" E1820-08, West Conshohocken, Pa.

American Society for Testing and Materials (ASTM). (2008), "Standard Test Methods for Tension Testing of Metallic Materials" E8-08, West Conshohocken, Pa.

American Society for Testing and Materials (ASTM). (2012), "Standard Test Method for Determining Plane-Strain Crack-Arrest Fracture Toughness, K_{Ia} , of Ferritic Steels" E1221-12, West Conshohocken, Pa.

American Society for Testing and Materials (ASTM). (2013), "Standard Test Method for Measurement of Fatigue Crack Growth Rates" E 647-13, West Conshohocken, Pa.

Collins, William N. (2014). "Fracture Behavior Characterization of Conventional and High Performance Steel for Bridge Applications." PhD Dissertation, Virginia Polytechnic Institute and State University, Blacksburg, VA.

Joyce, J. A., and Link, R. E. (2012). *Automated Software for Unloading Compliance Testing*. U.S. Naval Academy. Annapolis, MD.

Madison, R. B., and Irwin, G. R. (1974). "Dynamic K_c Testing of Structural Steel." *J. of the Structural Division*, 100(ST7), 1331-1349.

Wright, W., Candra, H., and Albrecht, P. (unpublished). *Fracture Toughness of A709 HPS Steel*. FHWA Report. Washington, D.C.

Appendix A: Tabulated CVN Data

Table A-1. CVN Data for Plate A, HPS 485W, 25.4 mm

Specimen ID	Orientation	Through-Thickness Location	Test Temperature		CVN Impact Energy	
			°C	°F	J	ft-lbf
A1	L-T	1/4 T	-100	-148	3	2.25
A2	L-T	1/4 T	-100	-148	14	10
A3	L-T	1/4 T	-100	-148	76	56
A4	L-T	1/4 T	-70	-94	127	93.5
A5	L-T	1/4 T	-70	-94	123	91
A6	L-T	1/4 T	-70	-94	141	104
A7	L-T	1/4 T	-30	-22	176	130
A8	L-T	1/4 T	-30	-22	197	145.5
A9	L-T	1/4 T	-30	-22	163	120.5
A10	L-T	1/4 T	-10	14	246	181
A11	L-T	1/4 T	-10	14	244	180
A12	L-T	1/4 T	-10	14	249	183.5
A13	L-T	1/4 T	10	50	256	189
A14	L-T	1/4 T	10	50	247	182
A15	L-T	1/4 T	10	50	256	189
A16	L-T	1/4 T	-80	-112	128	94.5
A17	L-T	1/4 T	-80	-112	106	78.5
A18	L-T	1/4 T	-80	-112	136	100
A19	L-T	1/4 T	-90	-130	118	87
A20	L-T	1/4 T	-90	-130	137	101
A21	L-T	1/4 T	-90	-130	18	13
A22	L-T	1/4 T	-51	-60	153	112.5
A23	L-T	1/4 T	-51	-60	180	133
A24	L-T	1/4 T	-51	-60	152	112
A25	L-T	1/2 T	-51	-60	56	41
A26	L-T	1/2 T	-51	-60	182	134.5
A27	L-T	1/2 T	-51	-60	113	83
A28	T-L	1/4 T	-51	-60	158	116.5
A29	T-L	1/4 T	-51	-60	142	104.5
A30	T-L	1/4 T	-51	-60	138	102

Table A-2. CVN Data for Plate C, HPS 690W, 19 mm

Specimen ID	Orientation	Through-Thickness Location	Test Temperature		CVN Impact Energy	
			°C	°F	J	ft-lbf
C1	L-T	1/3 T	-80	-112	26	19.25
C2	L-T	1/3 T	-80	-112	15	10.75
C3	L-T	1/3 T	-80	-112	13	9.5
C4	L-T	1/3 T	-65	-85	27	19.75
C5	L-T	1/3 T	-65	-85	28	21
C6	L-T	1/3 T	-65	-85	38	28.25
C7	L-T	1/3 T	-30	-22	148	109
C8	L-T	1/3 T	-30	-22	167	123
C9	L-T	1/3 T	-30	-22	157	115.5
C10	L-T	1/3 T	-10	14	176	130
C11	L-T	1/3 T	-10	14	195	144
C12	L-T	1/3 T	-10	14	202	149
C13	L-T	1/3 T	10	50	225	165.5
C14	L-T	1/3 T	10	50	202	149
C15	L-T	1/3 T	10	50	225	165.5
C16	L-T	1/3 T	25	77	212	156
C17	L-T	1/3 T	25	77	209	154
C18	L-T	1/3 T	25	77	225	166
C19	L-T	1/3 T	-100	-148	18	13.25
C20	L-T	1/3 T	-100	-148	31	23
C21	L-T	1/3 T	-100	-148	18	13
C22	L-T	1/3 T	-51	-60	88	65
C23	L-T	1/3 T	-51	-60	54	39.5
C24	L-T	1/3 T	-51	-60	58	43
C25	L-T	1/2 T	-51	-60	86	63.5
C26	L-T	1/2 T	-51	-60	88	64.5
C27	L-T	1/2 T	-51	-60	87	64
C28	T-L	1/3 T	-51	-60	60	44
C29	T-L	1/3 T	-51	-60	50	37
C30	T-L	1/3 T	-51	-60	98	72

Table A-3. CVN Data for Plate D, HPS 485W, 63.5 mm

Specimen ID	Orientation	Through-Thickness Location	Test Temperature		CVN Impact Energy	
			°C	°F	J	ft-lbf
D1	L-T	1/4 T	-80	-112	188	138.5
D2	L-T	1/4 T	-80	-112	171	126
D3	L-T	1/4 T	-80	-112	65	48
D4	L-T	1/4 T	-60	-76	199	146.5
D5	L-T	1/4 T	-60	-76	210	155
D6	L-T	1/4 T	-60	-76	192	141.5
D7	L-T	1/4 T	-40	-40	319	235
D8	L-T	1/4 T	-40	-40	311	229
D9	L-T	1/4 T	-40	-40	235	173
D10	L-T	1/4 T	-51	-60	94	69
D11	L-T	1/4 T	-51	-60	202	149
D12	L-T	1/4 T	-51	-60	210	154.5
D14	L-T	1/4 T	-100	-148	6	4.5
D15	L-T	1/4 T	-100	-148	6	4.25
D16	L-T	1/4 T	-30	-22	239	176
D17	L-T	1/4 T	-30	-22	292	215
D18	L-T	1/4 T	-30	-22	209	154
D19	L-T	1/4 T	-10	14	347	256
D20	L-T	1/4 T	-10	14	304	224
D21	L-T	1/4 T	-10	14	324	239
D22	L-T	1/4 T	-70	-94	206	152
D23	L-T	1/4 T	-70	-94	246	181
D24	L-T	1/4 T	-70	-94	193	142
D25	L-T	1/2 T	-51	-60	351	259
D31	L-T	1/2 T	-51	-60	252	186
D36	L-T	1/2 T	-51	-60	330	243.5
D37	T-L	1/4 T	-51	-60	191	141
D38	T-L	1/4 T	-51	-60	161	118.5
D42	T-L	1/4 T	-51	-60	189	139.5
D49	L-T	1/4 T	-110	-166	10	7.5
D50	L-T	1/4 T	-110	-166	46	34
D51	L-T	1/4 T	-110	-166	9	6.5
D52	L-T	1/4 T	-90	-130	3	2
D53	L-T	1/4 T	-90	-130	16	11.5

Table A-4. CVN Data for Plate E, HPS 690W, 38.1 mm

Specimen ID	Orientation	Through-Thickness Location	Test Temperature		CVN Impact Energy	
			°C	°F	J	ft-lbf
E1	L-T	1/4 T	-80	-112	35	25.75
E2	L-T	1/4 T	-80	-112	30	22
E3	L-T	1/4 T	-80	-112	25	18.25
E4	L-T	1/4 T	-70	-94	47	35
E5	L-T	1/4 T	-70	-94	54	39.5
E6	L-T	1/4 T	-70	-94	45	33.5
E7	L-T	1/4 T	-30	-22	170	125
E8	L-T	1/4 T	-30	-22	155	114.5
E9	L-T	1/4 T	-30	-22	183	135
E10	L-T	1/4 T	-10	14	185	136
E11	L-T	1/4 T	-10	14	196	144.5
E12	L-T	1/4 T	-10	14	208	153
E13	L-T	1/4 T	10	50	229	169
E14	L-T	1/4 T	10	50	212	156.5
E15	L-T	1/4 T	10	50	211	155.5
E16	L-T	1/4 T	-100	-148	6	4.25
E18	L-T	1/4 T	-100	-148	9	6.5
E19	L-T	1/4 T	25	77	247	182
E20	L-T	1/4 T	25	77	231	170
E21	L-T	1/4 T	25	77	248	183
E22	L-T	1/4 T	-51	-60	77	56.5
E23	L-T	1/4 T	-51	-60	109	80
E24	L-T	1/4 T	-51	-60	83	61
E25	L-T	1/2 T	-51	-60	115	84.5
E26	L-T	1/2 T	-51	-60	127	93.5
E27	L-T	1/2 T	-51	-60	79	58
E28	T-L	1/4 T	-51	-60	96	70.5
E29	T-L	1/4 T	-51	-60	103	76
E30	T-L	1/4 T	-51	-60	70	51.5

Table A-5. CVN Data for Plate F, HPS 690W, 50.8 mm

Specimen ID	Orientation	Through-Thickness Location	Test Temperature		CVN Impact Energy	
			°C	°F	J	ft-lbf
F1	L-T	1/4 T	-80	-112	27	20
F2	L-T	1/4 T	-80	-112	28	21
F3	L-T	1/4 T	-80	-112	25	18.75
F4	L-T	1/4 T	-70	-94	60	44.5
F5	L-T	1/4 T	-70	-94	46	34
F6	L-T	1/4 T	-70	-94	57	42
F7	L-T	1/4 T	-30	-22	144	106
F8	L-T	1/4 T	-30	-22	166	122
F9	L-T	1/4 T	-30	-22	149	110
F10	L-T	1/4 T	-10	14	195	144
F11	L-T	1/4 T	-10	14	203	149.5
F12	L-T	1/4 T	-10	14	180	132.5
F13	L-T	1/4 T	10	50	204	150
F14	L-T	1/4 T	10	50	216	159
F15	L-T	1/4 T	10	50	213	157
F16	L-T	1/4 T	-100	-148	4	3.25
F17	L-T	1/4 T	-100	-148	31	22.75
F18	L-T	1/4 T	-100	-148	41	30.5
F19	L-T	1/4 T	25	77	231	170
F20	L-T	1/4 T	25	77	225	166
F21	L-T	1/4 T	25	77	220	162
F22	L-T	1/4 T	-51	-60	96	71
F23	L-T	1/4 T	-51	-60	85	63
F24	L-T	1/4 T	-51	-60	113	83
F25	L-T	1/2 T	-51	-60	49	36
F26	L-T	1/2 T	-51	-60	34	25
F27	L-T	1/2 T	-51	-60	50	37
F28	T-L	1/4 T	-51	-60	100	73.5
F29	T-L	1/4 T	-51	-60	90	66
F30	T-L	1/4 T	-51	-60	69	50.5

Appendix B: Tabulated Static Fracture Toughness

Table B-1. Static Specimen Information for Plate A, HPS 485W, 25.4 mm

Specimen ID	W		a _o		B		B _N	
	mm.	in.	mm.	in.	mm.	in.	mm.	in.
A1'	10.02	0.3945	5.16	0.203	10.01	0.3941	8.00	0.315
A2'	10.01	0.3941	5.16	0.203	10.01	0.3941	8.00	0.315
A3'	10.02	0.3945	5.08	0.200	10.01	0.3941	8.00	0.315
A4'	10.01	0.3941	5.10	0.201	10.02	0.3945	8.00	0.315
A5'	10.00	0.3937	5.10	0.201	10.00	0.3937	8.00	0.315
A6'	10.01	0.3941	5.12	0.202	10.02	0.3945	8.00	0.315
A7'	10.01	0.3941	5.18	0.204	10.01	0.3941	8.00	0.315
A8'	10.01	0.3941	5.14	0.202	10.01	0.3941	8.00	0.315
A9'	10.01	0.3941	5.10	0.201	10.01	0.3941	8.00	0.315

Table B-2. Static Test Information for Plate A, HPS 485W, 25.4 mm

Specimen ID	Test Temperature		Test Result, K _{Jc}		Valid?	Censored?	1T K _{Jc}	
	°C	°F	MPa√m	ksi√in			MPa√m	ksi√in
A1'	-150	-238	150.8	137.2	Yes	No	123.6	112.5
A2'	-150	-238	213.2	194.0	Yes	Yes	141.8	129.1
A3'	-150	-238	193.9	176.4	Yes	Yes	143.1	130.2
A4'	-185	-301	112.0	101.9	Yes	No	92.9	84.6
A5'	-185	-301	71.0	64.6	Yes	No	60.4	55.0
A6'	-185	-301	26.5	24.1	No	No	25.2	22.9
A7'	-170	-274	134.9	122.8	Yes	No	111.0	101.0
A8'	-170	-274	137.4	125.0	Yes	No	113.0	102.8
A9'	-170	-274	130.6	118.8	Yes	No	107.6	97.9

Table B-3. Static Specimen Information for Plate C, HPS 690W, 19 mm

Specimen ID	W		a _o		B		B _N	
	mm.	in.	mm.	in.	mm.	in.	mm.	in.
C1'	10.02	0.3945	5.12	0.202	10.01	0.3941	8.00	0.3152
C2'	10.01	0.3941	5.14	0.202	10.02	0.3945	8.00	0.3152
C3'	10.03	0.3949	5.15	0.203	10.02	0.3945	8.00	0.3152
C4'	10.03	0.3949	5.15	0.203	10.02	0.3945	8.00	0.3152
C5'	10.02	0.3945	5.15	0.203	10.02	0.3945	8.00	0.3152
C6'	No Results- Data File Corrupted							
C7'	10.02	0.3945	5.09	0.200	10.02	0.3945	8.00	0.3152
C8'	10.03	0.3949	5.12	0.202	10.03	0.3949	8.00	0.3152
C9'	10.02	0.3945	5.16	0.203	10.02	0.3945	8.00	0.3152

Table B-4. Static Test Information for Plate C, HPS 690W, 19 mm

Specimen ID	Test Temperature		Test Result, K _{Jc}		Valid?	Censored?	1T K _{Jc}	
	°C	°F	MPa√m	ksi√in			MPa√m	ksi√in
C1'	-110	-166	86.0	78.3	Yes	No	72.3	65.8
C2'	-110	-166	82.3	74.9	Yes	No	69.4	63.1
C3'	-110	-166	64.2	58.4	Yes	No	55.0	50.1
C4'	-70	-94	175.1	159.3	Yes	No	142.9	130.1
C5'	-70	-94	170.0	154.7	Yes	No	138.9	126.4
C6'	No Results- Data File Corrupted							
C7'	-90	-130	128.3	116.8	Yes	No	105.8	96.3
C8'	-90	-130	91.5	83.3	Yes	No	76.7	69.8
C9'	-51	-60	155.9	141.9	Yes	No	127.7	116.2

Table B-5. Static Specimen Information for Plate D, HPS 485W, 63.5 mm

Specimen ID	W		a _o		B		B _N	
	mm.	in.	mm.	in.	mm.	in.	mm.	in.
D3'	10.02	0.394	5.10	0.201	10.00	0.3937	8.00	0.3152
D4'	10.03	0.395	5.33	0.210	10.03	0.3949	8.00	0.3152
D7'	10.02	0.394	5.37	0.211	10.03	0.3949	8.00	0.3152
D8'	10.02	0.394	5.35	0.211	10.03	0.3949	8.00	0.3152
D9'	10.02	0.394	5.31	0.209	10.03	0.3949	8.00	0.3152
D10'	10.02	0.394	5.39	0.212	10.03	0.3949	8.00	0.3152
D13'	10.02	0.394	5.35	0.211	10.03	0.3949	8.00	0.3152
D14'	10.02	0.394	5.33	0.210	10.03	0.3949	8.00	0.3152
D15'	10.02	0.394	5.37	0.211	10.03	0.3949	8.00	0.3152
D16'	10.03	0.395	5.31	0.209	10.02	0.3945	8.00	0.3152
D18'	10.02	0.394	5.38	0.212	10.02	0.3945	8.00	0.3152
D19'	10.03	0.395	5.46	0.215	10.02	0.3945	8.00	0.3152
D20'	10.02	0.394	5.40	0.213	10.02	0.3945	8.00	0.3152

Table B-6. Static Test Information for Plate D, HPS 485W, 63.5 mm

Specimen ID	Test Temperature		Test Result, K _{Jc}		Valid?	Censored?	1T K _{Jc}	
	°C	°F	MPaVm	ksiVin			MPaVm	ksiVin
D3'	-129	-200	287.6	261.7	Yes	Yes	132.0	120.1
D4'	-129	-200	148.4	135.0	No	No	121.8	110.8
D7'	-150	-238	207.4	188.7	No	Yes	129.9	118.2
D8'	-150	-238	91.3	83.1	Yes	No	76.5	69.6
D9'	-150	-238	200.3	182.3	Yes	Yes	130.7	119.0
D10'	-150	-238	243.3	221.4	Yes	Yes	129.7	118.0
D13'	-180	-292	254.1	231.2	Yes	Yes	143.1	130.2
D14'	-180	-292	52.7	48.0	Yes	No	45.9	41.8
D15'	-180	-292	82.8	75.3	Yes	No	69.8	63.5
D16'	-170	-274	161.3	146.8	No	No	132.0	120.1
D18'	-170	-274	144.6	131.6	Yes	No	118.7	108.1
D19'	-170	-274	147.4	134.1	Yes	No	121.0	110.1
D20'	-170	-274	119.1	108.4	Yes	No	98.5	89.7

Table B-7. Static Specimen Information for Plate E, HPS 690W, 38.1 mm

Specimen ID	W		a _o		B		B _N	
	mm.	in.	mm.	in.	mm.	in.	mm.	in.
E1'	10.03	0.395	5.37	0.211	10.01	0.3941	8.00	0.3152
E3'	10.01	0.394	5.34	0.210	10.02	0.3945	8.00	0.3152
E4'	10.02	0.394	5.32	0.209	10.01	0.3941	8.00	0.3152
E5'	10.03	0.395	5.35	0.211	10.02	0.3945	8.00	0.3152
E6'	10.03	0.395	5.48	0.216	10.02	0.3945	8.00	0.3152
E7'	10.02	0.394	5.36	0.211	10.01	0.3941	8.00	0.3152
E8'	10.03	0.395	5.37	0.211	10.04	0.3953	8.00	0.3152
E9'	10.02	0.394	5.45	0.215	10.01	0.3941	8.00	0.3152
E10'	10.03	0.395	5.45	0.215	10.01	0.3941	8.00	0.3152
E11'	10.02	0.394	5.36	0.211	10.02	0.3945	8.00	0.3152
E12'	10.02	0.394	5.36	0.211	10.03	0.3949	8.00	0.3152
E14	10.01	0.394	5.37	0.211	10.02	0.3945	8.00	0.3152
E19'	10.01	0.394	5.38	0.212	10.03	0.3949	8.00	0.3152
E20'	10.03	0.395	5.31	0.209	10.02	0.3945	8.00	0.3152
E21'	10.02	0.394	5.32	0.209	10.03	0.3949	8.00	0.3152

Table B-8. Static Test Information for Plate E, HPS 690W, 38.1 mm

Specimen ID	Test Temperature		Test Result, K _{Jc}		Valid?	Censored?	1T K _{Jc}	
	°C	°F	MPa√m	ksi√in			MPa√m	ksi√in
E1'	-72	-98	133.1	121.1	Yes	No	109.6	99.7
E3'	-129	-200	62.3	56.7	Yes	No	53.5	48.7
E4'	-129	-200	91.5	83.3	No	No	76.7	69.8
E5'	-90	-130	142.5	129.7	No	No	117.1	106.5
E6'	-90	-130	203.3	185.0	Yes	Yes	135.8	123.5
E7'	-90	-130	133.5	121.5	Yes	No	109.9	100.0
E8'	-90	-130	170.3	155.0	Yes	Yes	137.4	125.0
E9'	-110	-166	106.3	96.7	Yes	No	88.4	80.4
E10'	-110	-166	109.4	99.6	Yes	No	90.8	82.7
E11'	-110	-166	99.7	90.7	No	No	83.2	75.7
E12'	-110	-166	91.0	82.8	Yes	No	76.3	69.4
E14	-51	-60	178.1	162.1	Yes	Yes	134.2	122.1
E19'	-110	-166	118.2	107.6	Yes	No	97.8	89.0
E20'	-110	-166	109.7	99.8	Yes	No	91.1	82.9
E21'	-110	-166	135.2	123.0	Yes	No	111.3	101.3

Table B-9. Static Specimen Information for Plate F, HPS 690W, 50.8 mm

Specimen ID	W		a _o		B		B _N	
	mm.	in.	mm.	in.	mm.	in.	mm.	in.
F1'	10.02	0.394	5.31	0.209	10.00	0.3937	8.00	0.3152
F2'	10.01	0.394	5.37	0.211	10.00	0.3937	8.00	0.3152
F3'	10.02	0.394	5.32	0.209	10.00	0.3937	8.00	0.3152
F4'	10.00	0.394	5.36	0.211	10.01	0.3941	8.00	0.3152
F5'	10.02	0.394	5.34	0.210	10.01	0.3941	8.00	0.3152
F6'	10.02	0.394	5.31	0.209	10.03	0.3949	8.00	0.3152
F7'	10.01	0.394	5.34	0.210	10.00	0.3937	8.00	0.3152
F8'	10.02	0.394	5.37	0.211	10.01	0.3941	8.00	0.3152
F9'	10.00	0.394	5.36	0.211	10.01	0.3941	8.00	0.3152
F10'	10.00	0.394	5.33	0.210	10.03	0.3949	8.00	0.3152
F11'	10.02	0.394	5.42	0.213	10	0.3937	8.00	0.3152
F13'	10.01	0.394	5.37	0.211	10.03	0.3949	8.00	0.3152
F18'	10.02	0.394	5.37	0.211	10.02	0.3945	8.00	0.3152
F19'	10.03	0.395	5.33	0.210	10.01	0.3941	8.00	0.3152
F20'	10.02	0.394	5.33	0.210	10.01	0.3941	8.00	0.3152

Table B-10. Static Test Information for Plate F, HPS 690W, 50.8 mm

Specimen ID	Test Temperature		Test Result, K _{Jc}		Valid?	Censored?	1T K _{Jc}	
	°C	°F	MPa√m	ksi√in			MPa√m	ksi√in
F1'	-65	-85	180.7	164.4	Yes	Yes	135.1	122.9
F2'	-65	-85	153.2	139.4	Yes	No	125.5	114.2
F3'	-129	-200	84.4	76.8	Yes	No	71.0	64.6
F4'	-129	-200	120.7	109.8	No	No	99.8	90.8
F5'	-90	-130	121.2	110.3	No	No	100.2	91.2
F6'	-90	-130	121.5	110.6	Yes	No	100.5	91.4
F7'	-90	-130	175.7	159.9	Yes	Yes	136.7	124.4
F8'	-90	-130	143.8	130.9	Yes	No	118.1	107.5
F9'	-110	-166	147.6	134.3	No	No	121.1	110.2
F10'	-110	-166	93.5	85.1	Yes	No	78.3	71.2
F11'	-110	-166	61.3	55.8	No	No	52.7	48.0
F13'	-51	-60	228.1	207.6	Yes	Yes	133.3	121.3
F18'	-110	-166	98.8	89.9	Yes	No	82.5	75.0
F19'	-110	-166	105.8	96.3	Yes	No	88.0	80.1
F20'	-110	-166	77.1	70.2	Yes	No	65.2	59.4

Table B-11. Static Specimen Information for Plate H, HPS 485W, 31.8 mm

Specimen ID	W		a _o		B		B _N	
	mm.	in.	mm.	in.	mm.	in.	mm.	in.
H1'	10.02	0.3945	5.14	0.202	10.02	0.3945	8.00	0.3152
H2'	10.01	0.3941	5.10	0.201	10.02	0.3945	8.00	0.3152
H3'	10.03	0.3949	5.10	0.201	10.01	0.3941	8.00	0.3152
H4'	10.02	0.3945	5.06	0.199	10.01	0.3941	8.00	0.3152
H5'	10.02	0.3945	5.12	0.202	10.01	0.3941	8.00	0.3152
H6'	10.02	0.3945	5.12	0.202	10.03	0.3949	8.00	0.3152
H7'	10.02	0.3945	5.09	0.200	10.01	0.3941	8.00	0.3152
H8'	10.02	0.3945	5.01	0.197	10.02	0.3945	8.00	0.3152
H9'	10.02	0.3945	5.12	0.202	10.02	0.3945	8.00	0.3152
H10'	No Results- Data File Corrupted							
H11'	10.02	0.3945	5.11	0.201	10.03	0.3949	8.00	0.3152

Table B-12. Static Test Information for Plate H, HPS 485W, 31.8 mm

Specimen ID	Test Temperature		Test Result, K _{Jc}		Valid?	Censored?	1T K _{Jc}	
	°C	°F	MPa√m	ksi√in			MPa√m	ksi√in
H1'	-130	-202	239.8	218.2	Yes	Yes	130.1	118.4
H2'	-130	-202	210.0	191.1	Yes	Yes	130.5	118.7
H3'	-130	-202	162.1	147.5	Yes	No	132.6	120.7
H4'	-150	-238	54.8	49.9	Yes	No	47.6	43.3
H5'	-150	-238	186.6	169.8	Yes	Yes	135.8	123.6
H6'	-150	-238	161.9	147.3	Yes	No	132.5	120.6
H7'	-150	-238	207.6	188.9	Yes	Yes	136.2	124.0
H8'	-150	-238	109.4	99.6	Yes	No	90.9	82.7
H9'	-170	-274	40.2	36.6	Yes	No	36.0	32.8
H10'	No Results- Data File Corrupted							
H11'	-170	-274	105.5	96.0	Yes	No	87.8	79.9

Table B-13. Static Specimen Information for Plate I, HPS 485W, 31.8 mm

Specimen ID	W		a _o		B		B _N	
	mm.	in.	mm.	in.	mm.	in.	mm.	in.
I1'	10.03	0.3949	5.16	0.203	10.02	0.3945	8.00	0.3152
I2'	10.02	0.3945	5.16	0.203	10.02	0.3945	8.00	0.3152
I3'	10.01	0.3941	5.18	0.204	10.02	0.3945	8.00	0.3152
I4'	10.02	0.3945	5.18	0.204	10.01	0.3941	8.00	0.3152
I5'	10.03	0.3949	5.12	0.202	10.02	0.3945	8.00	0.3152
I6'	10.02	0.3945	5.20	0.205	10.01	0.3941	8.00	0.3152
I7'	10.02	0.3945	5.13	0.202	10.03	0.3949	8.00	0.3152
I8'	10.02	0.3945	5.06	0.199	10.03	0.3949	8.00	0.3152
I9'	10.02	0.3945	5.10	0.201	10.01	0.3941	8.00	0.3152

Table B-14. Static Test Information for Plate I, HPS 485W, 31.8 mm

Specimen ID	Test Temperature		Test Result, K _{Jc}		Valid?	Censored?	1T K _{Jc}	
	°C	°F	MPaVm	ksiVin			MPaVm	ksiVin
I1'	-130	-202	232.4	211.5	Yes	Yes	127.4	115.9
I2'	-130	-202	185.8	169.1	Yes	Yes	127.3	115.8
I3'	-130	-202	201.8	183.6	Yes	Yes	126.9	115.5
I4'	-180	-292	45.8	41.7	Yes	No	40.4	36.8
I5'	-180	-292	153.9	140.0	Yes	No	126.1	114.8
I6'	-180	-292	76.4	69.5	Yes	No	64.7	58.9
I7'	-160	-256	115.8	105.4	Yes	No	95.9	87.3
I8'	-160	-256	159.7	145.3	Yes	No	130.7	119.0
I9'	-160	-256	42.5	38.7	No	No	37.8	34.4

Table B-15. Static Specimen Information for Plate J, HPS 485W, 38.1 mm

Specimen ID	W		a _o		B		B _N	
	mm.	in.	mm.	in.	mm.	in.	mm.	in.
J1'	10.02	0.3945	5.15	0.203	10.03	0.3949	8.00	0.3152
J2'	10.03	0.3949	5.12	0.202	10.02	0.3945	8.00	0.3152
J3'	Specimen Damaged in Machining							
J4'	10.03	0.3949	5.15	0.203	10.02	0.3945	8.00	0.3152
J6'	10.03	0.3949	5.14	0.202	10.02	0.3945	8.00	0.3152
J7'	10.02	0.3945	5.08	0.200	10.03	0.3949	8.00	0.3152
J8'	10.02	0.3945	5.14	0.202	10.02	0.3945	8.00	0.3152
J9'	10.03	0.3949	5.08	0.200	10.03	0.3949	8.00	0.3152
J10'	10.03	0.3949	5.18	0.204	10.04	0.3953	8.00	0.3152

Table B-16. Static Test Information for Plate J, HPS 485W, 38.1 mm

Specimen ID	Test Temperature		Test Result, K _{Jc}		Valid?	Censored?	1T K _{Jc}	
	°C	°F	MPaVm	ksiVin			MPaVm	ksiVin
J1'	-150	-238	102.8	93.5	Yes	No	85.6	77.9
J2'	-150	-238	129.3	117.7	Yes	No	106.6	97.0
J3'	Specimen Damaged in Machining							
J4'	-150	-238	75.0	68.3	Yes	No	63.6	57.9
J6'	-130	-202	102.6	93.4	Yes	No	85.5	77.8
J7'	-130	-202	203.8	185.5	Yes	Yes	131.1	119.3
J8'	-130	-202	101.8	92.6	Yes	No	84.8	77.2
J9'	-130	-202	111.3	101.3	Yes	No	92.4	84.1
J10'	-130	-202	123.4	112.3	Yes	No	102.0	92.8

Appendix C: Tabulated Dynamic Fracture Toughness

Table C-1. Dynamic Specimen Information for Plate A, HPS 485W, 25.4 mm

Specimen ID	W		a _o		B		B _N	
	mm.	in.	mm.	in.	mm.	in.	mm.	in.
A11'	10.01	0.3941	5.05	0.199	10.02	0.3945	8.00	0.3152
A12'	10.01	0.3941	5.09	0.200	10.01	0.3941	8.00	0.3152
A13'	10.01	0.3941	5.07	0.200	10.01	0.3941	8.00	0.3152
A14'	10.01	0.3941	5.08	0.200	10.01	0.3941	8.00	0.3152
A15'	10.02	0.3945	5.13	0.202	10.01	0.3941	8.00	0.3152
A16'	10.02	0.3945	5.09	0.200	10.01	0.3941	8.00	0.3152
A17'	10.01	0.3941	5.13	0.202	10.01	0.3941	8.00	0.3152
A18'	10.01	0.3941	5.12	0.202	10.01	0.3941	8.00	0.3152
A19'	10.01	0.3941	5.14	0.202	10.01	0.3941	8.00	0.3152
A20'	10.00	0.3937	5.10	0.201	10.01	0.3941	8.00	0.3152
A21'	10.01	0.3941	5.07	0.200	10.01	0.3941	8.00	0.3152

Table C-2. Dynamic Test Information for Plate A, HPS 485W, 25.4 mm

Specimen ID	Test Temperature		Test Result, K _{Jc}		Valid?	Censored?	1T K _{Jc}		Test Rate	
	°C	°F	MPa√m	ksi√in			MPa√m	ksi√in	MPa√m/sec	ksi√in/sec
A11'	-120	-184	131.3	119.5	Yes	No	108.2	98.5	2734	2488
A12'	-120	-184	133.5	121.5	Yes	No	109.9	100.0	2641	2403
A13'	-120	-184	63.5	57.8	Yes	No	54.5	49.6	4326	3937
A14'	-120	-184	101.6	92.5	Yes	No	84.7	77.0	3181	2895
A15'	-120	-184	43.0	39.1	Yes	No	38.2	34.8	5434	4945
A16'	-120	-184	105.1	95.6	Yes	No	87.4	79.6	3177	2891
A17'	-120	-184	116.9	106.4	Yes	No	96.8	88.1	2871	2613
A18'	-120	-184	120.0	109.2	Yes	No	99.2	90.3	2875	2616
A19'	-100	-148	159.0	144.7	No	No	130.1	118.4	2378	2164
A20'	-100	-148	257.5	234.3	Yes	Yes	143.5	130.6	1398	1272
A21'	-100	-148	158.7	144.4	Yes	No	129.9	118.2	2307	2099

Table C-3. Dynamic Specimen Information for Plate C, HPS 690W, 19 mm

Specimen ID	W		a _o		B		B _N	
	mm.	in.	mm.	in.	mm.	in.	mm.	in.
C11'	10.02	0.3945	5.11	0.201	10.03	0.3949	8.00	0.3152
C12'	10.02	0.3945	5.12	0.202	10.03	0.3949	8.00	0.3152
C13'	10.03	0.3949	5.08	0.200	10.03	0.3949	8.00	0.3152
C14'	10.01	0.3941	5.08	0.200	10.02	0.3945	8.00	0.3152
C15'	10.02	0.3945	5.10	0.201	10.02	0.3945	8.00	0.3152
C16'	10.02	0.3945	5.09	0.200	10.03	0.3949	8.00	0.3152
C17'	10.01	0.3941	5.08	0.200	10.02	0.3945	8.00	0.3152
C19'	10.02	0.3945	5.10	0.201	10.01	0.3941	8.00	0.3152

Table C-4. Dynamic Test Information for Plate C, HPS 690W, 19 mm

Specimen ID	Test Temperature		Test Result, K _{Jc}		Valid?	Censored?	1T K _{Jc}		Test Rate	
	°C	°F	MPa√m	ksi√in			MPa√m	ksi√in	MPa√m/sec	ksi√in/sec
C11'	-34	-29	200.0	182.0	Yes	Yes	149.3	135.9	1973	1795
C12'	-51	-60	128.1	116.6	Yes	No	105.7	96.2	2724	2479
C13'	-51	-60	84.9	77.3	Yes	No	71.4	65.0	3649	3321
C14'	-51	-60	129.3	117.7	Yes	No	106.6	97.0	2701	2458
C15'	-51	-60	117.4	106.8	Yes	No	97.2	88.4	2913	2651
C16'	-51	-60	110.9	100.9	Yes	No	92.1	83.8	2980	2712
C17'	-51	-60	135.5	123.3	Yes	No	111.5	101.5	2616	2381
C19'	-51	-60	167	152.2	Yes	No	136.7	124.4	2196	1998

Table C-5. Dynamic Specimen Information for Plate D, HPS 485W, 63.5 mm

Specimen ID	W		a _o		B		B _N	
	mm.	in.	mm.	in.	mm.	in.	mm.	in.
D21'	10.01	0.394	5.36	0.211	10.02	0.3945	8.00	0.3152
D22'	10.03	0.395	5.38	0.212	10.02	0.3945	8.00	0.3152
D23'	10.01	0.394	5.06	0.199	10.00	0.3937	8.00	0.3152
D24'	10.00	0.394	5.05	0.199	10.01	0.3941	8.00	0.3152
D25'	10.00	0.394	5.10	0.201	10.01	0.3941	8.00	0.3152
D26'	Specimen Did Not Fracture- No Test							
D27'	10.00	0.394	5.11	0.201	10.02	0.3945	8.00	0.3152
D28'	10.00	0.394	5.07	0.200	10.01	0.3941	8.00	0.3152
D29'	10.02	0.394	5.14	0.202	10.01	0.3941	8.00	0.3152
D30'	10.01	0.394	5.07	0.200	10.00	0.3937	8.00	0.3152
D31'	10.01	0.394	5.05	0.199	10.00	0.3937	8.00	0.3152
D32'	10.01	0.394	5.10	0.201	10.01	0.3941	8.00	0.3152
D33'	10.01	0.394	5.11	0.201	10.01	0.3941	8.00	0.3152
D34'	10.01	0.394	5.06	0.199	10.00	0.3937	8.00	0.3152
D35'	10.02	0.394	5.08	0.200	10.00	0.3937	8.00	0.3152
D36'	10.01	0.394	5.08	0.200	10.01	0.3941	8.00	0.3152
D37'	10.02	0.394	5.09	0.200	10.00	0.3937	8.00	0.3152
D38'	10.02	0.394	5.07	0.200	10.01	0.3941	8.00	0.3152

Table C-6. Dynamic Test Information for Plate D, HPS 485W, 63.5 mm

Specimen ID	Test Temperature		Test Result, K_{Jc}		Valid?	Censored?	1T K_{Jc}		Test Rate	
	°C	°F	MPaVm	ksiVin			MPaVm	ksiVin	MPaVm/sec	ksiVin/sec
D21'	-100	-148	308.4	280.6	Yes	Yes	129.8	118.1	941	856
D22'	-100	-148	48.5	44.1	Yes	No	42.6	38.8	5100	4641
D23'	-100	-148	47.6	43.3	Yes	No	41.9	38.1	5034	4581
D24'	-70	-94	178.0	162.0	Yes	Yes	128.4	116.8	1893	1723
D25'	-70	-94	370.4	337.1	Yes	Yes	127.7	116.2	318	289
D26'	Specimen Did Not Fracture- No Test									
D27'	-90	-130	151.5	137.9	Yes	No	124.2	113.0	2294	2088
D28'	-90	-130	318.1	289.5	Yes	Yes	131.6	119.7	940	855
D29'	-90	-130	358.5	326.2	Yes	Yes	130.9	119.1	722	657
D30'	-90	-130	74.0	67.3	Yes	No	62.8	57.1	3984	3625
D31'	-100	-148	343.0	312.1	Yes	Yes	133.9	121.8	766	697
D32'	-115	-175	110.9	100.9	Yes	No	92.0	83.7	2950	2685
D33'	-115	-175	251.3	228.7	Yes	Yes	136.3	124.0	1348	1227
D34'	-115	-175	59.3	54.0	Yes	No	51.1	46.5	4495	4090
D35'	-115	-175	46.9	42.7	Yes	No	41.3	37.6	5231	4760
D36'	-115	-175	117.6	107.0	Yes	No	97.3	88.6	2824	2570
D37'	-130	-202	49.5	45.0	Yes	No	43.4	39.5	4918	4475
D38'	-130	-202	65.9	60.0	Yes	No	56.4	51.3	4260	3877

Table C-7. Dynamic Specimen Information for Plate E, HPS 690W, 38.1 mm

Specimen ID	W		a _o		B		B _N	
	mm.	in.	mm.	in.	mm.	in.	mm.	in.
E22'	Specimen Reserved							
E23'	Specimen Used to Check Dynamic Test Method							
E24'	10.03	0.395	5.34	0.210	10.03	0.3949	8.00	0.3152
E25'	10.02	0.394	5.23	0.206	10.03	0.3949	8.00	0.3152
E26'	10.02	0.394	5.30	0.209	10.03	0.3949	8.00	0.3152
E27'	10.03	0.395	5.31	0.209	10.03	0.3949	8.00	0.3152
E28'	10.03	0.395	5.32	0.209	10.02	0.3945	8.00	0.3152
E29'	10.02	0.394	5.32	0.209	10.01	0.3941	8.00	0.3152
E30'	10.02	0.394	5.29	0.208	10.02	0.3945	8.00	0.3152
E31'	10.03	0.395	5.28	0.208	10.02	0.3945	8.00	0.3152
E32'	10.03	0.395	5.25	0.207	10.03	0.3949	8.00	0.3152
E33'	10.03	0.395	5.28	0.208	10.01	0.3941	8.00	0.3152
E34'	10.03	0.395	5.28	0.208	10.03	0.3949	8.00	0.3152
E35'	Specimen Used to Check Pre-Crack Procedure							
E36'	10.03	0.395	5.09	0.200	10.03	0.3949	8.00	0.3152
E37'	10.03	0.395	5.12	0.202	10.02	0.3945	8.00	0.3152

Table C-8. Dynamic Test Information for Plate E, HPS 690W, 38.1 mm

Specimen ID	Test Temperature		Test Result, K _{Jc}		Valid?	Censored?	1T K _{Jc}		Test Rate	
	°C	°F	MPa√m	ksi√in			MPa√m	ksi√in	MPa√m/sec	ksi√in/sec
E22'	Specimen Reserved									
E23'	Specimen Used to Check Dynamic Test Method									
E24'	-100	-148	71.8	65.3	Yes	No	61.1	55.6	3838	3493
E25'	-100	-148	67.7	61.6	Yes	No	57.8	52.6	3998	3638
E26'	-100	-148	82.9	75.4	Yes	No	69.9	63.6	3790	3449
E27'	-100	-148	51.4	46.8	Yes	No	44.9	40.9	4737	4311
E28'	-51	-60	154.4	140.5	Yes	No	126.5	115.1	2345	2134
E29'	-51	-60	277.4	252.4	Yes	Yes	140.1	127.5	1241	1129
E30'	-51	-60	116.9	106.4	Yes	No	96.8	88.1	2806	2553
E31'	-70	-94	90.7	82.5	Yes	No	76.0	69.2	3742	3405
E32'	-70	-94	94.3	85.8	Yes	No	78.9	71.8	3302	3005
E33'	-70	-94	111.9	101.8	Yes	No	92.8	84.5	2939	2674
E34'	-70	-94	113.7	103.5	Yes	No	94.3	85.8	2976	2708
E35'	Specimen Used to Check Pre-Crack Procedure									
E36'	-70	-94	78.6	71.5	Yes	No	66.5	60.5	3642	3314
E37'	-70	-94	104.2	94.8	Yes	No	86.7	78.9	3210	2921

Table C-9. Dynamic Specimen Information for Plate F, HPS 690W, 50.8 mm

Specimen ID	W		a _o		B		B _N	
	mm.	in.	mm.	in.	mm.	in.	mm.	in.
F21'	10.03	0.395	5.35	0.211	10.03	0.3949	8.00	0.3152
F22'	10.03	0.395	5.38	0.212	10.03	0.3949	8.00	0.3152
F23'	Specimen Used to Check Pre-Crack Procedure							
F24'	10.03	0.395	5.14	0.202	10.03	0.3949	8.00	0.3152
F25'	10.01	0.394	5.08	0.200	10.00	0.3937	8.00	0.3152
F26'	10.01	0.394	5.20	0.205	10.01	0.3941	8.00	0.3152
F27'	10.02	0.394	5.18	0.204	10.00	0.3937	8.00	0.3152
F28'	10.02	0.394	5.15	0.203	10.00	0.3937	8.00	0.3152
F29'	10.00	0.394	5.10	0.201	10.00	0.3937	8.00	0.3152
F30'	10.00	0.394	5.16	0.203	10.00	0.3937	8.00	0.3152
F31'	10.00	0.394	5.19	0.204	10.02	0.3945	8.00	0.3152
F32'	Specimen Damaged in Machining							
F33'	10.00	0.394	5.07	0.200	10.02	0.3945	8.00	0.3152
F34'	10.00	0.394	5.09	0.200	10.02	0.3945	8.00	0.3152

Table C-10. Dynamic Test Information for Plate F, HPS 690W, 50.8 mm

Specimen ID	Test Temperature		Test Result, K _{Jc}		Valid?	Censored?	1T K _{Jc}		Test Rate	
	°C	°F	MPa√m	ksi√in			MPa√m	ksi√in	MPa√m/sec	ksi√in/sec
F21'	-51	-60	154.5	140.6	Yes	No	126.6	115.2	2294	2088
F22'	-51	-60	192.9	175.5	Yes	Yes	143.0	130.1	1942	1767
F23'	Specimen Used to Check Pre-Crack Procedure									
F24'	-51	-60	116.0	105.6	Yes	No	96.1	87.5	2875	2616
F25'	-70	-94	112.3	102.2	Yes	No	93.1	84.7	2986	2717
F26'	-70	-94	95.2	86.6	Yes	No	79.6	72.4	3599	3275
F27'	-70	-94	79.0	71.9	Yes	No	66.7	60.7	3558	3238
F28'	-70	-94	96.6	87.9	Yes	No	80.7	73.4	3245	2953
F29'	-70	-94	90.4	82.3	Yes	No	75.8	68.9	3474	3161
F30'	-70	-94	109.6	99.7	Yes	No	91.0	82.8	2929	2665
F31'	-90	-130	64.1	58.3	Yes	No	55.0	50.0	4353	3961
F32'	Specimen Damaged in Machining									
F33'	-90	-130	85.1	77.4	Yes	No	71.6	65.1	3640	3312
F34'	-90	-130	73.9	67.2	Yes	No	62.7	57.1	3857	3510

Table C-11. Dynamic Specimen Information for Plate H, HPS 485W, 31.8 mm

Specimen ID	W		a _o		B		B _N	
	mm.	in.	mm.	in.	mm.	in.	mm.	in.
H13'	10.02	0.3945	5.09	0.200	10.02	0.3945	8.00	0.3152
H14'	10.02	0.3945	5.10	0.201	10.03	0.3949	8.00	0.3152
H15'	Specimen Did Not Fracture- No Test							
H16'	Specimen Damaged in Machining							
H17'	10.02	0.3945	5.11	0.201	10.02	0.3945	8.00	0.3152
H18'	10.02	0.3945	5.12	0.202	10.02	0.3945	8.00	0.3152
H19'	10.02	0.3945	5.07	0.200	10.02	0.3945	8.00	0.3152
H20'	10.01	0.3941	5.12	0.202	10.02	0.3945	8.00	0.3152
H21'	10.02	0.3945	5.10	0.201	10.02	0.3945	8.00	0.3152
H22'	10.02	0.3945	5.10	0.201	10.01	0.3941	8.00	0.3152

Table C-12. Dynamic Test Information for Plate H, HPS 485W, 31.8 mm

Specimen ID	Test Temperature		Test Result, K _{Jc}		Valid?	Censored?	1T K _{Jc}		Test Rate	
	°C	°F	MPa√m	ksi√in			MPa√m	ksi√in	MPa√m/sec	ksi√in/sec
H13'	-120	-184	49.9	45.4	Yes	No	43.7	39.8	4647	4229
H14'	-120	-184	41.4	37.7	Yes	No	37.0	33.6	5334	4854
H15'	Specimen Did Not Fracture- No Test									
H16'	Specimen Damaged in Machining									
H17'	-100	-148	141.6	128.9	Yes	No	116.4	105.9	2480	2257
H18'	-100	-148	237.5	216.1	Yes	Yes	137.1	124.7	1463	1331
H19'	-120	-184	52.4	47.7	Yes	No	45.7	41.6	4742	4315
H20'	-100	-148	224.3	204.1	Yes	Yes	136.9	124.6	1603	1459
H21'	-120	-184	89.2	81.2	Yes	No	74.8	68.1	3483	3170
H22'	-120	-184	58.7	53.4	Yes	No	50.7	46.1	4559	4149

Table C-13. Dynamic Specimen Information for Plate I, HPS 485W, 31.8 mm

Specimen ID	W		a _o		B		B _N	
	mm.	in.	mm.	in.	mm.	in.	mm.	in.
I11'	10.03	0.3949	5.05	0.199	10.02	0.3945	8.00	0.3152
I12'	10.02	0.3945	5.06	0.199	10.02	0.3945	8.00	0.3152
I13'	10.02	0.3945	5.11	0.201	10.04	0.3953	8.00	0.3152
I14'	10.02	0.3945	5.15	0.203	10.03	0.3949	8.00	0.3152
I15'	10.01	0.3941	5.12	0.202	10.03	0.3949	8.00	0.3152
I16'	10.02	0.3945	5.10	0.201	10.03	0.3949	8.00	0.3152
I17'	10.02	0.3945	5.12	0.202	10.03	0.3949	8.00	0.3152
I18'	10.01	0.3941	5.23	0.206	10.03	0.3949	8.00	0.3152

Table C-14. Dynamic Test Information for Plate I, HPS 485W, 31.8 mm

Specimen ID	Test Temperature		Test Result, K _{Jc}		Valid?	Censored?	1T K _{Jc}		Test Rate	
	°C	°F	MPaVm	ksiVin			MPaVm	ksiVin	MPaVm/sec	ksiVin/sec
I11'	-120	-184	212.4	193.3	Yes	Yes	140.7	128.0	1637	1490
I12'	-150	-238	31.5	28.7	Yes	No	29.1	26.5	6625	6029
I13'	-120	-184	48.2	43.9	Yes	No	42.4	38.5	5223	4753
I14'	-100	-148	179.1	163.0	Yes	Yes	134.1	122.0	1922	1749
I15'	-100	-148	99.8	90.8	Yes	No	83.3	75.8	3167	2882
I16'	-100	-148	55.2	50.2	Yes	No	47.9	43.6	4642	4224
I17'	-100	-148	237.8	216.4	Yes	Yes	134.5	122.4	1446	1316
I18'	-100	-148	164.1	149.3	Yes	Yes	132.9	120.9	2135	1943

Table C-15. Dynamic Specimen Information for Plate J, HPS 485W, 38.1 mm

Specimen ID	W		a _o		B		B _N	
	mm.	in.	mm.	in.	mm.	in.	mm.	in.
J12'	10.03	0.3949	5.14	0.202	10.02	0.3945	8.00	0.3152
J13'	Specimen Damaged in Machining							
J14'	10.03	0.3949	5.13	0.202	10.03	0.3949	8.00	0.3152
J15'	10.03	0.3949	5.10	0.201	10.03	0.3949	8.00	0.3152
J16'	10.04	0.3953	5.14	0.202	10.03	0.3949	8.00	0.3152
J17'	10.03	0.3949	5.14	0.202	10.03	0.3949	8.00	0.3152
J18'	10.03	0.3949	5.13	0.202	10.04	0.3953	8.00	0.3152
J19'	10.03	0.3949	5.12	0.202	10.02	0.3945	8.00	0.3152
J20'	10.03	0.3949	5.13	0.202	10.03	0.3949	8.00	0.3152
J21'	10.03	0.3949	5.13	0.202	10.03	0.3949	8.00	0.3152
J22'	10.03	0.3949	5.07	0.200	10.02	0.3945	8.00	0.3152

Table C-16. Dynamic Test Information for Plate J, HPS 485W, 38.1 mm

Specimen ID	Test Temperature		Test Result, K _{JC}		Valid?	Censored?	1T K _{JC}		Test Rate	
	°C	°F	MPaVm	ksiVin			MPaVm	ksiVin	MPaVm/sec	ksiVin/sec
J12'	-70	-94	263.6	239.9	Yes	Yes	131.0	119.2	1285	1169
J13'	Specimen Damaged in Machining									
J14'	-100	-148	84.5	76.9	Yes	No	71.1	64.7	3681	3350
J15'	-100	-148	80.1	72.9	Yes	No	67.6	61.6	3859	3512
J16'	-100	-148	72.8	66.2	Yes	No	61.9	56.3	4470	4068
J17'	-100	-148	55.0	50.1	Yes	No	47.7	43.4	4632	4215
J18'	-80	-112	89.9	81.8	Yes	No	75.4	68.6	3526	3209
J19'	-80	-112	93.5	85.1	Yes	No	78.3	71.2	3384	3079
J20'	-80	-112	77.0	70.1	Yes	No	65.2	59.3	3849	3503
J21'	-80	-112	64.2	58.4	Yes	No	55.0	50.1	4389	3994
J22'	-100	-148	88.7	80.7	Yes	No	74.4	67.7	3452	3141

Appendix D: Tabulated Crack Arrest Toughness

Table D-1. Valid Arrest Specimen Information

Specimen ID	Test Temperature		W		a _o		B		B _N		a _a		N	
	°C	°F	mm.	in.	mm.	in.	mm.	in.	mm.	in.	mm.	in.	mm.	in.
D1a	-35	-31	101.63	4.001	27.84	1.0961	50.90	2.004	39.00	1.535	74.88	2.9481	9.86	0.388
D2a	-35	-31	101.60	4.000	28.07	1.1053	50.83	2.001	38.90	1.532	74.35	2.9273	10.03	0.395
D4a	-50	-58	101.79	4.007	27.97	1.1010	50.88	2.003	39.03	1.537	75.44	2.9700	10.01	0.394
D5a	-50	-58	101.63	4.001	28.06	1.1049	50.90	2.004	38.88	1.531	65.97	2.5972	10.11	0.398
D9a	-35	-31	101.62	4.001	27.76	1.0928	50.95	2.006	38.99	1.535	77.96	3.0694	10.01	0.394
E1a	-35	-31	101.13	3.982	32.64	1.2849	37.47	1.475	29.05	1.144	84.72	3.3354	10.85	0.427
E19a	-50	-58	102.06	4.018	27.94	1.1001	36.98	1.456	28.45	1.120	83.52	3.2880	10.11	0.398
F4a	-35	-31	102.40	4.032	28.44	1.1195	50.14	1.974	38.33	1.509	80.89	3.1847	9.88	0.389
F5a	-35	-31	101.93	4.013	27.76	1.0930	50.32	1.981	38.89	1.531	79.38	3.1251	10.08	0.397
F9a	-20	-4	101.32	3.989	27.72	1.0913	49.99	1.968	38.77	1.527	79.75	3.1396	10.08	0.397

Table D-2. Valid Arrest Test Record Information

Specimen ID	δ_o		δ_a		δ_{R1}		δ_{R-last}		K_o		K_{Ia}	
	mm.	in.	mm.	in.	mm.	in.	mm.	in.	MPa√m	ksi√in	MPa√m	ksi√in
D1a	0.7795	0.03069	0.8806	0.03467	0.0025	0.0001	0.0892	0.0035	155.9	141.9	69.1	62.9
D2a	0.7584	0.02986	0.8402	0.03308	0.0033	0.0001	0.0881	0.0035	150.7	137.1	67.4	61.3
D4a	0.5093	0.02005	0.6101	0.02402	-0.0010	0.0000	0.0069	0.0003	113.1	102.9	48.6	44.2
D5a	0.5987	0.02357	0.6650	0.02618	-0.0025	-0.0001	0.0411	0.0016	125.4	114.1	64.6	58.8
D9a	0.9378	0.03692	1.0282	0.04048	0.0005	0.0000	0.1709	0.0067	173.8	158.2	73.6	67.0
E1a	0.7625	0.03002	0.8865	0.03490	0.0015	0.0001	0.0198	0.0008	147.3	134.0	53.7	48.9
E19a	1.046	0.04118	1.1466	0.04514	-0.0061	-0.0002	0.0503	0.0020	224.2	204.0	75.7	68.9
F4a	0.8207	0.03231	0.9784	0.03852	-0.0046	-0.0002	0.0452	0.0018	173.1	157.5	67.7	61.6
F5a	0.7125	0.02805	0.8717	0.03432	0.0000	0.00000	0.0094	0.00037	158.7	144.4	62.3	56.7
F9a	0.8954	0.03525	1.0284	0.04049	-0.0069	-0.00027	0.0175	0.00069	197.7	179.9	74.1	67.4

Table D-3. Invalid Arrest Specimen Information

Specimen ID	Test Temperature		W		a _o		B		B _N		a _a		N	
	°C	°F	mm.	in.	mm.	in.	mm.	in.	mm.	in.	mm.	in.	mm.	in.
D3a	-35	-31	101.17	3.983	37.84	1.4898	50.90	2.004	39.01	1.536	87.90	3.4605	10.03	0.395
D6a	-20	-4	101.51	3.996	27.92	1.0990	50.93	2.005	38.96	1.534	82.21	3.2365	10.16	0.400
D7a	-35	-31	101.60	4.000	32.80	1.2913	50.93	2.005	38.71	1.524	76.93	3.0287	9.96	0.392
D16a	-35	-31	101.65	4.002	27.77	1.0935	50.83	2.001	38.48	1.515	82.39	3.2438	10.03	0.395
D18a	-50	-58	101.71	4.005	27.81	1.0950	50.42	1.985	38.51	1.516	85.72	3.3749	10.08	0.397
E9a	-10	14	101.49	3.996	27.71	1.0910	37.36	1.471	28.66	1.128	87.47	3.4436	10.52	0.414
E16a	-20	-4	102.20	4.024	27.80	1.0943	37.19	1.464	28.45	1.120	84.69	3.3344	10.21	0.402
E21a	-20	-4	102.05	4.018	27.59	1.0864	37.01	1.457	28.50	1.122	88.74	3.4936	10.21	0.402

Table D-4. Invalid Arrest Test Record Information

Specimen ID	δ _o		δ _a		δ _{R1}		δ _{R-last}		K _o		K _{ia}	
	mm.	in.	mm.	in.	mm.	in.	mm.	in.	MPa√m	ksi√in	MPa√m	ksi√in
D3a	1.6002	0.06300	1.6990	0.06689	-0.0127	-0.0005	0.2047	0.0081	246.5	224.3	91.1	82.9
D6a	1.2271	0.04831	1.3185	0.05191	-0.0185	-0.0007	0.3759	0.0148	192.1	174.8	79.7	72.5
D7a	1.1816	0.04652	1.2581	0.04953	-0.0094	-0.0004	0.1417	0.0056	207.8	189.1	97.5	88.7
D16a	1.5019	0.05913	1.5565	0.06128	-0.0056	-0.0002	0.3470	0.0137	263.1	239.4	99.2	90.3
D18a	1.4475	0.05699	1.5235	0.05998	0.0010	0.0000	0.2911	0.0115	262.0	238.4	87.3	79.4
E9a	1.3658	0.05377	1.4803	0.05828	0.0020	0.0001	0.1689	0.0067	271.2	246.8	80.8	73.5
E16a	1.5761	0.06205	1.6970	0.06681	-0.0023	-0.0001	0.2283	0.0090	305.6	278.1	104.1	94.7
E21a	1.6436	0.06471	1.7556	0.06912	0.0018	0.0001	0.3790	0.0149	287.3	261.4	87.7	79.8